

Control-Oriented System Identification: Classical, Learning, and Physics-Informed Approaches

S. Sivarajanji^{a,1,*}, Yuanyuan Shi^{b,1,*}, Nikolay Atanasov^{b,1,*}, Thai Duong^{c,2}, Jie Feng^{b,2}, Tim Martin^{d,2}, Yuezhu Xu^{a,2}, Vijay Gupta^e, Frank Allgöwer^d

^a*Edwardson School of Industrial Engineering, Purdue University, West Lafayette, IN, 47907, USA*

^b*Electrical and Computer Engineering, University of California San Diego, La Jolla, CA, 92093, USA*

^c*Department of Computer Science, Rice University, Houston, TX, 77005, USA*

^d*University of Stuttgart, Institute for Systems Theory and Automatic Control, Stuttgart, Germany*

^e*Elmore Family School of Electrical and Computer Engineering, Purdue University, West Lafayette, IN, 47907, USA*

Abstract

This article surveys classical, machine learning, and data-driven system identification approaches to learn control-relevant and physics-informed models of dynamical systems. In recent years, machine learning approaches have enabled system identification from noisy, high-dimensional, and complex data. However, their utility in control applications is limited by their ability to provide provable guarantees on control-relevant properties. Meanwhile, traditional control theory has identified several properties of physical systems that are useful in analysis and control synthesis, such as dissipativity, monotonicity, energy conservation, and symmetry-preserving structures. In this paper, we postulate that merging system identification algorithms with such control-relevant or physics-informed properties can provide useful inductive bias, enhance explainability, enable control synthesis with provable guarantees, and improve sample complexity. We formulate system identification as an optimization problem where control-relevant properties can be enforced in three ways, namely, direct parameterization (constraining the model structure to satisfy a desired property by construction), soft constraints (encouraging control-relevant properties through regularization or penalty terms), and hard constraints (imposing control-relevant properties as constraints in the optimization problem). Through this lens, we survey methods to learn physics-informed and control-relevant models spanning classical linear and nonlinear system identification techniques, machine learning-based approaches, as well as direct identification through data-driven and behavioral representations. Throughout the paper, we provide several expository examples that are accompanied by code and brief tutorials on a public Github repository. We also describe several challenging directions for future research in this area, including identification in networked, switched, and time-varying systems, experiment design, and bridging the gaps between data-driven, learning-based, and control-oriented system identification.

Keywords: System identification, machine learning, identification for control, physics-informed learning, data-driven control, control-oriented system identification, learning for control

1. Introduction

Machine learning, at its core, is learning from data. Since control theory also seeks to utilize data to identify system models and estimate and regulate their states, it is natural to ask if the resurgent interest in machine learning can translate to new algorithms and guarantees useful in control. This survey focuses on techniques for system identification as a precursor to model-based control. System identification is a fundamental and widely studied topic in both the automatic control and signal processing communities. The basic problem considers a system that is excited using some ‘input’ data and generates measurements or ‘output’ data. Using the inputs and the outputs, we seek to generate a model of the system that not only

explains the data that were used to generate it, but also generalizes to other unseen input data (Ljung et al., 2020). One could interpret this as a function approximation problem, which is exactly the problem that machine learning seeks to solve with the potential ability to consider arbitrary noise distributions, high dimensional data, and complex loss functions. However, the central premise of this survey is that while machine learning can indeed yield exciting new algorithms for system identification, to realize this promise fully, ‘vanilla’ machine learning algorithms will not do — we need physics-informed and control-oriented learning algorithms that guarantee properties in the learned models useful for the subsequent control design.

What do we mean by control-oriented learning algorithms? Traditional control theory has identified several properties of dynamical system that are useful for analyzing dynamical systems or synthesizing control laws. These properties typically arise from first principles underlying the system physics or dynamics, e.g., symmetries or energy dissipation properties, and

*sseetha@purdue.edu, yyshi@ucsd.edu, natanasov@ucsd.edu

¹These authors contributed equally to this work.

²These authors contributed equally and are ordered alphabetically by last name.

are useful for designing controllers to achieve desired closed-loop responses. By merging such physics-based or control-relevant properties with learning algorithms, we hope to identify system models that provide the best of both philosophies.

The first reason to insist on such properties when learning a model is that they may provide a useful inductive bias to the learning algorithm. The possible choices of a model that can explain the given (or training) input-output data are many; the only test for utility among such models is the ability to generalize to unseen (or test) data. Constraining the learned model to display properties that we know hold from physics or system structure is potentially a strong and useful inductive bias to the learning algorithm. Even if the learned model yields some ground on the error criterion over the training data, a physics-constrained model will likely have better generalization ability.

The second reason for ensuring that such properties are satisfied by the learned model is that several decades of developments in control synthesis explicitly utilize these properties to provide provable guarantees. In control engineering applications, the aim is typically not to just learn an *open-loop* model using the input-output data, but rather to utilize this model for control design with desired *closed-loop* characteristics. Many methods for controller design utilize properties such as dissipativity and monotonicity to obtain guarantees on closed-loop system behavior. For instance, compositionality properties of dissipative and monotone systems have been widely leveraged for scalable control designs in networked systems. If the learned model also displays such properties that we expect to be satisfied from physics, similar controller synthesis procedures can be used and strong guarantees on the closed-loop system behavior can be obtained.

Another reason to incorporate a priori information about physics is to obtain explainable system models. It is well-known that the outputs, and consequently the failure modes, of black-box models such as neural networks utilized in learning-based control cannot be readily intuited. Therefore, when control designs that utilize these models do not perform as intended, the root cause is often unclear, resulting in the designer having to resort to trial-and-error to achieve acceptable performance. Instead, if black-box system models like neural networks can be imbued with key physics properties, such as conservation laws, symmetries, or energy dissipation, their outputs or failure modes can be explained in terms of measures defined on these properties (e.g., dissipativity indices) or violation of these properties (e.g., violation of symmetries). Then, desired input-output behaviors can be translated into specifications on these properties and shaped by explainable control designs.

Finally, we also expect that enforcing such properties could improve the sample complexity of the learning algorithms. The intuition here is that these properties constrain the degrees of the freedom for the learned model and hence the model can be learned in a more efficient fashion. Some empirical evidence for this can be observed in [Miller et al. \(2020\)](#); [Cuomo et al. \(2022\)](#); [Son et al. \(2023\)](#), where physics-informed neural networks achieve similar prediction accuracy as unstructured neural networks with significantly less training data.

Due to these reasons, extending the powerful methods de-

veloped in the learning literature to identify dynamical system models that are physics-informed and control-oriented has emerged as a key direction of work in multiple research communities. It has the potential to move the identification methods in automatic control and signal processing beyond the limiting assumptions classically made, while at the same time, making the learning algorithms more relevant for analysis and control of physical systems. The purpose of this survey is to provide students, researchers, and practitioners with an overview of this field. We aim to categorize the types of methods that have been proposed so that the reader obtains a map of the area, given the often bewildering mix of modeling philosophies and approaches that have been proposed. We also identify how classical system identification techniques rooted in the control literature form an important pillar in this area and must be mastered by anybody seeking to make meaningful contributions in this domain. At the same time, we present the reader with a succinct understanding of where these methods can be complemented and extended by newer approaches and tools from learning, as well as new ideas in data-driven representations stemming from notions like behavioral systems theory.

While there are many excellent surveys on various facets at the intersection of learning and control, our aim and presentation differ from them. Specifically considering the problem of system modeling and identification, there are two lines of research closely aligned with the focus of this paper. The first is *physics-informed or scientific machine learning*, surveyed in works such as [Wang and Yu \(2021\)](#); [Chen et al. \(2021b\)](#); [Karniadakis et al. \(2021\)](#); [Cuomo et al. \(2022\)](#); [Willard et al. \(2020\)](#); [Yu and Wang \(2024\)](#), where the idea is to leverage prior knowledge of system physics to enhance the generalizability and interpretability of deep learning models, with applications to a wide array of problems including forecasting, inference, and solution of ordinary or partial differential equations. However, these works do not typically focus on control-relevant models, with the exception of recent tutorials ([Nghiem et al., 2023](#); [Drgona et al., 2025](#)), some parts of which discuss physics-informed learning for system identification for specific model classes and structural priors. The second closely related line of research is *identification for control*, which has a long rich history, surveyed in works such as [Gevers \(2005\)](#), which typically focus on classical system identification tools. An exception here is [Pillonetto et al. \(2025\)](#) that focuses on deep learning architectures for system identification, primarily from the viewpoint of optimization algorithms and kernel-based methods. The renewed interest in data-driven control ([van Waarde et al., 2025](#)) in recent years has also led to surveys on data-driven system representations based on behavioral systems theory ([Markovsky and Dörfler, 2021](#)) and operator dynamical models such as Koopman operators ([Bevanda et al., 2021](#)). Even within these domains, there are no comprehensive surveys focusing on the problem of learning representations or models capturing specific control-relevant properties or physics-based constraints. This paper bridges the gap between these two lines of research and existing review papers, surveying both *classical and learning-based approaches to address the specific problem of identifying physics-constrained and control-relevant models*

for dynamical systems and control synthesis.

This paper is organized as follows. In Section 2, we begin by introducing system modeling techniques and describing the control-relevant properties considered in this work, namely, dissipativity, monotonicity, and symmetry-preserving structures (such as Lagrangian and Hamiltonian dynamics). We, then, formally pose the problem of identifying a model satisfying these properties as a constrained optimization problem, and outline various perspectives on how to solve this problem in Section 3. Then, we survey classical (Section 4) and deep-learning (Section 5) system identification techniques capturing control-relevant properties, as well as direct data-driven identification of these properties through, e.g., behavioral representations (Section 6). The code for all the numerical examples in this paper is available in our Github repository.³ We conclude by providing several directions for future exploration in Section 7.

Notation: Throughout the manuscript, scalars and vectors are denoted by lower-case letters. The set of real numbers is denoted by \mathbb{R} , and the set of n -dimensional real vectors by \mathbb{R}^n . For a vector $x \in \mathbb{R}^n$, $\|x\|$ denotes its Euclidean norm. The operator ∇_x denotes the gradient with respect to the variable x . For a function $t \mapsto x(t)$, the notation \dot{x} and \ddot{x} denotes the first and second time derivatives of $x(t)$, respectively. The set of complex numbers is denoted by \mathbb{C} . The variable $s \in \mathbb{C}$ denotes the Laplace variable (complex frequency), and $\omega \in \mathbb{R}$ denotes the real frequency, with $s = i\omega$ in the Fourier domain. Matrices are denoted by upper-case letters. For a matrix A , its transpose is denoted by A^\top , and its inverse (if it exists) is denoted by A^{-1} . Inequalities between matrices are defined in the standard positive (semi)definite sense: $A > 0$ indicates that A is positive definite, while $A \geq 0$ indicates positive semidefiniteness. Similarly, $A < 0$ and $A \leq 0$ denote negative definite and negative semidefinite matrices, respectively.

2. Control-Related Properties and Constraints

2.1. System Modeling

Continuous-time dynamical systems are commonly modeled using ordinary differential equations (ODEs):

$$\frac{d^n}{dt^n}y(t) = \phi\left(y(t), \frac{d}{dt}y(t), \dots, \frac{d^{n-1}}{dt^{n-1}}y(t), u(t)\right), \quad (1)$$

where $u(t)$ is the system input at time t , $y(t)$ is the system output, and ϕ is a function capturing the relationship among the system input and the time-derivatives of its output. A state-space model converts the n -th order ODE in (1) to a system of n first-order ODEs by defining state variables $x(t) = (x_1(t), \dots, x_n(t))$ corresponding to the output time derivatives:

$$x_1(t) = y(t), \quad x_2(t) = \frac{d}{dt}y(t), \quad \dots, \quad x_n(t) = \frac{d^{n-1}}{dt^{n-1}}y(t) \quad (2)$$

and observing that one can write $\dot{x}_1(t) = x_2(t)$, $\dot{x}_2(t) = x_3(t)$, \dots , $\dot{x}_{n-1}(t) = x_n(t)$, and $\dot{x}_n(t) = \phi(x_1(t), \dots, x_n(t), u(t))$, is shorthand notation for the first time derivative of state x_i .

In general, a state-space model describes a continuous-time dynamical system as:

$$\begin{aligned} \dot{x}(t) &= f(x(t), u(t)), \\ y(t) &= h(x(t), u(t)), \end{aligned} \quad (3)$$

where $x(t) \in \mathcal{X} \subseteq \mathbb{R}^{n_x}$ is the state, $u(t) \in \mathcal{U} \subseteq \mathbb{R}^{n_u}$ is the input, $y(t) \in \mathcal{Y} \subseteq \mathbb{R}^{n_y}$ is the output, $f : \mathbb{R}^{n_x} \times \mathbb{R}^{n_u} \rightarrow \mathbb{R}^{n_x}$ is the system dynamics model, $h : \mathbb{R}^{n_x} \times \mathbb{R}^{n_u} \rightarrow \mathbb{R}^{n_y}$ is the output model, and the initial condition $x(0)$ is given.

It is often sufficient from a system modeling perspective and beneficial from a control design perspective to consider models that are affine in the control input $u(t)$:

$$\begin{aligned} \dot{x}(t) &= A(x(t)) + B(x(t))u(t), \\ y(t) &= C(x(t)) + D(x(t))u(t), \end{aligned} \quad (4)$$

or even in both the state $x(t)$ and the input $u(t)$:

$$\begin{aligned} \dot{x}(t) &= Ax(t) + Bu(t), \\ y(t) &= Cx(t) + Du(t). \end{aligned} \quad (5)$$

The Laplace transform converts a linear time-invariant (LTI) system from a linear ODE in the time domain, given by (5), to a linear algebraic equation in the complex domain. The input-output relationship of an LTI system in the complex domain with zero initial conditions is described by its transfer function $G : \mathbb{C} \mapsto \mathbb{C}^{n_y \times n_u}$:

$$Y(s) = G(s)U(s) = (C(sI - A)^{-1}B + D)U(s), \quad (6)$$

where $U(s)$ and $Y(s)$ are the Laplace transforms of the input $u(t)$ and output $y(t)$, respectively. In the time domain, the relationship in (6) shows that, with zero initial conditions, the system output is the result of convolution:

$$y(t) = g(t) * u(t) = \int_0^t g(t-\tau)u(\tau)d\tau \quad (7)$$

of the system impulse response $g(t) = Ce^{At}B + D\delta(t)$ (inverse Laplace transform of $G(s)$) with the input signal $u(t)$.

A *control law*, also referred to as *control policy*, is a function $\pi : \mathcal{X} \times [0, \infty) \rightarrow \mathcal{U}$ that determines an input $u(t) = \pi(x(t), t)$ for a dynamical system based on the system's current state $x(t)$, time t , and desired behavior. The composition of the system dynamics model f in (3) with a control policy π creates a *closed-loop system* with dynamics model:

$$\dot{x}(t) = F(x(t), t) := f(x(t), \pi(x(t), t)). \quad (8)$$

To guarantee existence and uniqueness of solutions of the ODE in (8), the function F needs to be Lipschitz continuous in x and continuous in t (Khalil, 2002, Thm. 3.1). A special case of (8) arises when F does not explicitly depend on t ; that is

$$\dot{x} = F(x), \quad (9)$$

³https://github.com/ExistentialRobotics/physics_based_sysid

in which case the closed-loop system is said to be *autonomous*.

If the system state $x(t)$ is not available to the control policy, the input $u(t)$ must be determined by an *output-feedback* control policy, relying on the output $y(t)$ instead of $x(t)$. In this case, the closed-loop dynamics F is obtained by the composition of the open-loop dynamics model f , the control policy π , and the output model h in (3).

Instead of representing a system using a state-space model (3) or transfer function (6), behavioral system theory (Markovsky and Dörfler, 2021; Willems, 1986a) considers a representation-free perspective, viewing a system as a set of trajectories:

$$\{\omega : [0, \infty) \rightarrow \mathbb{R}^q\}. \quad (10)$$

A trajectory $\omega(t)$ may be related to an input-output representation via a permutation matrix $\Pi \in \mathbb{R}^{q \times q}$ with $q = n_u + n_y$ and $\omega(t) = \Pi \begin{bmatrix} u(t) \\ y(t) \end{bmatrix}$. The behavioral framework describes a system as the span of all possible input-output trajectories generated by its dynamics. The complexity of a system is defined by its structure indices (Willems, 1986a): the number of inputs n_u , the order n_x , and the lag ℓ (the smallest integer ℓ for which the matrix $[C \ C A \ \dots \ CA^{\ell-1}]$ has rank n_x).

The system models described so far can also be formulated in discrete time $k \in \mathbb{N}$ with input $u_k \in \mathbb{R}^{n_u}$, state $x_k \in \mathbb{R}^{n_x}$, and output $y_k \in \mathbb{R}^{n_y}$. Discrete-time versions of the nonlinear model in (3), control-affine model in (4), and LTI model in (5) are defined using difference equations with equivalent notation. Specifically, a discrete-time nonlinear system can be written as:

$$\begin{aligned} x_{k+1} &= f(x_k, u_k), \\ y_k &= h(x_k, u_k), \end{aligned} \quad (11)$$

and a discrete-time LTI model can be formulated as:

$$\begin{aligned} x_{k+1} &= Ax_k + Bu_k, \\ y_k &= Cx_k + Du_k, \end{aligned} \quad (12)$$

with given initial conditions x_0 . Instead of using the Laplace transform, discrete-time LTI systems are converted to the complex domain using the Z transform and are associated with a discrete-time transfer function $G(z)$ such that $Y(z) = G(z)U(z)$, where $U(z)$ and $Y(z)$ are the Z transforms of the input u_k and output y_k .

In the discrete-time setting⁴, within the behavioral framework, Willems' fundamental lemma (Willems et al., 2005a) provides a representation of LTI system using a single sufficiently informative and long trajectory. Consider a trajectory $\{\tilde{u}_k, \tilde{y}_k\}_{k=0}^{N-1}$ from an LTI system (12) that satisfies a condition called persistent excitation. Then, we can verify whether any arbitrary trajectory $\{u_k, y_k\}_{k=0}^{L-1}$ of shorter length L comes from the same LTI system as long as $N \geq (n_u + 1)(n_x + L) - 1$. In detail, let $\tilde{\mathbf{u}} = [\tilde{u}_0^\top \ \dots \ \tilde{u}_{N-1}^\top]^\top$, $\tilde{\mathbf{y}} = [\tilde{y}_0^\top \ \dots \ \tilde{y}_{N-1}^\top]^\top$, $\mathbf{u} = [u_0^\top \ \dots \ u_{L-1}^\top]^\top$, and $\mathbf{y} = [y_0^\top \ \dots \ y_{L-1}^\top]^\top$. The input sequence $\tilde{\mathbf{u}}$ is persistently exciting of order $k \in [1, N]$ if the

Hankel matrix $\mathcal{H}_k(\tilde{\mathbf{u}})$ of depth k constructed from $\tilde{\mathbf{u}}$ has full row rank (Willems et al., 2005a). If $\tilde{\mathbf{u}}$ is persistently exciting of order $n_x + L$, then \mathbf{u}, \mathbf{y} is a trajectory of (12) if there exists a vector $\alpha \in \mathbb{R}^{N-L+1}$ such that

$$\begin{bmatrix} \mathcal{H}_L(\tilde{\mathbf{u}}) \\ \mathcal{H}_L(\tilde{\mathbf{y}}) \end{bmatrix} \alpha = \begin{bmatrix} \mathbf{u} \\ \mathbf{y} \end{bmatrix}. \quad (13)$$

Intuitively, the algebraic condition (13) states that any trajectory of a discrete-time LTI system with finite length is a linear combination of one sufficiently informative and long trajectory.

2.2. System Identification

Given a set $\mathcal{W} = \{(u_i(t), y_i(t))\}_i$ of input-output trajectories from a continuous-time dynamical system, *system identification* is the problem of constructing a model of the system. This involves choosing a model order (state dimension n_x) and mathematical structure (e.g., nonlinear, control-affine, or linear state-space model), and specifying associated model parameters (e.g., matrices A, B, C, D for the linear state-space model in (5), parametrization of the nonlinear functions f, h in (3), or parameterization of the transfer function $G(s)$ in (6)). The parameters of the chosen model are determined by minimizing a suitably chosen difference between the predicted model output and the actual system output observed in the data \mathcal{W} . For example, considering a nonlinear state-space model with dynamics f_θ and output model h_θ , the model parameters θ may be obtained from an optimization problem:

$$\begin{aligned} \min_{\theta} \quad & c(\theta; \mathcal{W}) := \sum_i \int_t \|y_i(t) - \hat{y}_i(t)\|^2 dt \\ \text{s.t.} \quad & \dot{\hat{x}}_i(t) = f_\theta(\hat{x}_i(t), u_i(t)), \\ & \hat{y}_i(t) = h_\theta(\hat{x}_i(t), u_i(t)), \end{aligned} \quad (14)$$

where $\{(\hat{x}_i(t), \hat{y}_i(t))\}_i$ are state and output trajectories predicted by the model f_θ, h_θ . The above formulation (14) focuses on parametric system identification, where f_θ, h_θ are the models to be identified. Motivated by Willems's work (Willems, 1986a,b, 1987), system identification can also be carried out using non-parametric techniques, such as total least-squares (Rooda and Heij, 1995), deterministic subspace (Van Overschee and De Moor, 1996), and structured low-rank approximation (Markovsky, 2014) approaches.

After the identification of a system model, model validation and model analysis are crucial next steps to guarantee the usefulness of the model for prediction, optimization, and control design. Model validation refers to assessing the accuracy of the identified model by comparing its predictions with additional (validation) data that was not used during the parameter estimation phase. This helps to verify that the model's performance on the validation data and the training data are comparable, i.e., the model is not overfitting. Model analysis refers to asserting that the identified model satisfies properties and performance characteristics expected to be true for the considered system. This is essential to ensure that the model accurately represents the real-world system, facilitating reliable prediction, robust control design, and safe operation.

⁴Continuous time analogues of Willems' fundamental lemma have also been recently proposed (Lopez and Müller, 2022).

2.3. System Properties

Real-world dynamical systems display important properties. From a control perspective, desirable properties that may be considered include stability, dissipativity, monotonicity, symmetries, to name a few. Ensuring that, when a system satisfies these properties, they are reflected in the system model is important for model accuracy and control design. Capturing these properties in the system model can often lead to simplified mathematical treatment, accurate reflection of a real system's behavior, and convenient control design.

2.3.1. Lyapunov Stability

Lyapunov stability is a fundamental concept for understanding the behavior of a dynamical system. Stable systems behave predictably in the sense that they return to an equilibrium (or a set of equilibria) after a disturbance and do not exhibit unbounded behavior. Suppose $x_e \in D$, $D \subset \mathbb{R}^n$, is an equilibrium of the closed-loop autonomous system (9), that is $F(x_e) = 0$. For convenience, we state all definitions and theorems in this section for the case when the equilibrium point is at the origin of \mathbb{R}^n , that is $x_e = 0$. There is no loss of generality in doing so because any equilibrium point can be shifted to the origin via a change of variables (Khalil, 2002).

Theorem 2.1 (Lyapunov Stability). *Let $x = 0$ be an equilibrium point for the closed-loop autonomous system in (9) and $D \subset \mathbb{R}^n$ be a domain containing $x = 0$. Let $V : D \rightarrow \mathbb{R}$ be a continuously differentiable function such that*

$$V(0) = 0 \text{ and } V(x) > 0, \forall x \in D \setminus \{0\},$$

$$\dot{V}(x) := \frac{\partial V}{\partial x} F(x) \leq 0, \forall x \in D.$$

Then, $x = 0$ is stable. Moreover, if

$$\dot{V}(x) < 0, \forall x \in D \setminus \{0\},$$

then $x = 0$ is asymptotically stable.

The condition that $\dot{V}(x)$ is negative in Thm. 2.1 suggests that for any initial condition $x(0) \in D$, the system trajectories $x(t)$ move to smaller and smaller values of $V(x)$, eventually approach or converge to $x = 0$.

LaSalle's invariance principle (Khalil, 2002, Theorem 4.4) generalizes the above notion of stability from an equilibrium point to stability with respect to a set. To state LaSalle's invariance theorem, we need to introduce a few definitions. A set M is said to be an invariant set with respect to the closed-loop autonomous system (9) if $x(0) \in M \Rightarrow x(t) \in M, \forall t \in \mathbb{R}$. That is, if a solution belongs to M at some time instant, then it belongs to M for all future and past time. A set M is said to be a positively invariant set with respect to the closed-loop autonomous system (9) if $x(0) \in M \Rightarrow x(t) \in M, \forall t \geq 0$.

Theorem 2.2 (LaSalle's Invariance Principle). *Let $\Omega \subset D$ be a compact set that is positively invariant with respect to (9) and $D \subset \mathbb{R}^n$ be a domain containing $x = 0$. Let $V : D \rightarrow \mathbb{R}$ be a continuously differentiable function such that $\dot{V}(x) \leq 0$ in Ω .*

Let E be the set of all points in Ω where $\dot{V} = 0$. Let M be the largest invariant set in E . Then every solution starting in Ω approaches M as t approaches infinity. That is, for any $\epsilon > 0$, there exists a $T > 0$ such that $\text{dist}(x(t), M) < \epsilon$ for all $t > T$, where $\text{dist}(x(t), M) = \inf_{p \in M} \|x(t) - p\|$.

In Lyapunov stability analysis and its generalization via the LaSalle's invariance principle, one first needs to identify a candidate Lyapunov function $V(x)$. However, finding a Lyapunov function for a nonlinear system is challenging, especially when the system dynamics are unknown. For dynamical systems with a special structure, such as networked systems or mechanical systems, there are some natural choices of Lyapunov or generalized energy functions, which we will introduce in the following subsections.

2.3.2. Dissipativity and Passivity

Dissipativity extends the concept of passive circuit elements from circuit theory to a generalized notion of energy (not necessarily corresponding to a physical quantity) that is applicable to nonlinear dynamical systems. Dissipativity theory offers a powerful framework for analyzing dynamical systems and designing controllers, as it can be used to establish crucial properties such as stability, passivity, and sector-boundedness (see Definition 2.4). One of the key advantages of dissipativity is its preservation across various network interconnection structures, making it particularly valuable for compositional and distributed control synthesis (Antsaklis et al., 2013; Agarwal et al., 2021, 2020, 2019; Vidyasagar, 1979). Owing to these attractive properties, dissipativity has been widely studied in the control literature, and finds application in several domains including, but not limited to, robotics (Hatanaka et al., 2015), electromechanical systems (Ortega et al., 2013), aerospace systems (Forbes, 2011), process control (Bao and Lee, 2007), and power and energy systems (Sivarajani et al., 2020a,b). Concretely, we define dissipativity for a nonlinear system as follows.

Definition 2.3 (Dissipativity). *The dynamical system (3) is said to be dissipative with respect to a supply rate $s : \mathcal{U} \times \mathcal{Y} \rightarrow \mathbb{R}$, where $\int_0^T |s(u, y)| dt < \infty, \forall 0, T \in \mathbb{R}_+$, if there exists a positive definite function $V : X \rightarrow \mathbb{R}_+$, such that, $\forall t \in [0, T], x(0) \in X$, and $y \in \mathcal{Y}$,*

$$\int_0^T s(u, y) dt \geq V(x(T)) - V(x(0)), \quad (15)$$

where $x(T)$ is the state of the dynamical system (3) at time T , resulting from the initial condition $x(0)$ and input $u(\cdot)$.

For nonlinear systems, dissipativity from Definition 2.3 often holds only in the neighbourhood of an equilibrium. Incremental dissipativity (Forni et al., 2013; Verhoek et al., 2023b) extends this notion by considering the relationship between two arbitrary system trajectories. In general, incremental dissipativity implies dissipativity but not vice versa. For linear systems, incremental and non-incremental properties are equivalent. The analysis of incremental dissipativity can be particularly useful when operating a system in a transient mode,

between operating points, or in a reference tracking scenario where stability and performance with respect to a certain trajectory are desired. Specifically, incremental dissipativity can be obtained by replacing the supply rate $s(u, y)$ in Definition 2.3 by $s(u_1 - u_2, y_1 - y_2), u_1, u_2 \in \mathcal{U}, y_1, y_2 \in \mathcal{Y}$, and the storage functions by $V(x_1(\cdot), x_2(\cdot))$. Analogous discrete-time notions of dissipativity and incremental dissipativity can also be appropriately defined, but are omitted here for brevity of exposition.

A particularly useful special case of dissipativity is the property of quadratic dissipativity, commonly referred to as *QSR*-dissipativity, defined as follows.

Definition 2.4 (QSR-Dissipativity). *The nonlinear system (3) is said to be QSR-dissipative with dissipativity matrices $Q = Q^\top$, S and $R = R^\top$ of appropriate dimensions, if $\forall x \in X$ and control inputs $u \in \mathcal{U}$, Definition 2.3 holds with $s(u, y) = y^\top Qy + u^\top Ru + 2y^\top Su$. By selecting appropriate dissipativity matrices Q, S , and R , this formalism can capture several control-theoretic properties of importance, including but not limited to:*

- (i) passivity, with $Q = 0, S = \frac{1}{2}I$ and $R = 0$,
- (ii) strict passivity, with $Q = -aI, S = \frac{1}{2}I$ and $R = -bI$, where $a, b \in \mathbb{R}^+ \setminus \{0\}$,
- (iii) \mathcal{L}_2 stability, with $Q = -\frac{1}{\gamma}I, S = 0$ and $R = \gamma I$ where $\gamma \in \mathbb{R}^+$ is an \mathcal{L}_2 gain of the system,
- (iv) conicity, with $Q = -I, S = cI$ and $R = (r^2 - c^2)I$, where $c \in \mathbb{R}$ and $r \in \mathbb{R}^+ \setminus \{0\}$, and,
- (v) sector-boundedness, with $Q = -I, S = (a + b)I$ and $R = -abI$, where $a, b \in \mathbb{R}$.

Note that the same choices of supply rates can also be used in the appropriate definitions to establish discrete-time or incremental counterparts of these properties.

For LTI systems, dissipativity is guaranteed if there exists matrix $P > 0$ satisfying the linear matrix inequality (LMI)

$$\begin{bmatrix} A^\top P + PA - C^\top QC & PB - C^\top S - C^\top QD \\ (PB - C^\top S - C^\top QD)^\top & -D^\top QD - (D^\top S + S^\top D) - R \end{bmatrix} \leq 0, \quad (16)$$

where appropriate choices of the Q, S , and R matrices can be made to reflect special cases like passivity, as described in Definition 2.4.

For transfer function models $G_\theta(s)$, where the parameters θ represent the coefficients of the numerator and denominator polynomials of the transfer function, properties like passivity, positive realness, and bounded realness, which are special cases of dissipativity, can be directly imposed by enforcing their corresponding frequency domain conditions. For example, strict passivity (positive realness) can be enforced by ensuring that $G_\theta(s)$ is stable, while satisfying the hard constraint

$$g(\theta) = -G_\theta(i\omega) - G_\theta(-i\omega) < 0, \forall \omega \in \mathbb{R}. \quad (17)$$

Similarly, bounded realness can be enforced by requiring that $G_\theta(s)$ is stable and satisfies the hard constraint

$$g(\theta) = -I + G_\theta^\top(-i\omega)G_\theta(i\omega) < 0, \forall \omega \in \mathbb{R}. \quad (18)$$

Analogous definitions of these properties for discrete-time models and LMI conditions for state-space models (similar to (16)) are also available (Kottenstette and Antsaklis, 2010).

There are also related properties such as differential dissipativity (Forni et al., 2013; van der Schaft, 2013) and equilibrium-independent dissipativity (Simpson-Porco, 2018; Hines et al., 2011); however, these notions have not yet been explored as much in the context of system identification. Similarly, integral quadratic constraints (IQC) establish an attractive framework to achieve tighter descriptions of input-output properties, with a number of uncertainties that can be characterized by IQCs in Megretski and Rantzer (1997). However, in the context of physics-constrained system identification, IQCs have not been explored much thus far.

2.3.3. Monotonicity

Monotone systems have outputs that change in a consistent direction in response to changes in inputs. Similar to dissipativity, this property simplifies the model analysis and control design by providing guarantees about the direction of the system responses. A special case of monotonicity is positivity of the dynamics, where the state variables are constrained to be positive. This corresponds to the physics of several systems such as reaction networks where the concentration of a chemical species cannot be negative.

Monotone systems feature in several control applications of interest, including chemical reaction networks (Leenheer et al., 2007), biological systems (Angeli, 2021), epidemiological processes (Brauer et al., 2012), and traffic flow networks (Lovisari et al., 2014; Coogan and Arcak, 2015). In fact, most compartmental flow networks, which describe the flow of a commodity (such as traffic or a reactant) from one compartment to another under a conservation law, follow monotone dynamics (Haddad et al., 2010). Cooperation and competition dynamics in populations and teams can also be modeled using monotone systems (Hirsch and Smith, 2005; Smith, 2017). From a control standpoint, monotonicity is an important property that can be exploited for distributed stability analysis (Coogan, 2019), reachability analysis (Althoff et al., 2021), and control design (Shiroimoto et al., 2018; Rantzer and Bernhardsson, 2014; Cui et al., 2024) in large-scale networks. This is due to the fact that linear monotone systems admit Lyapunov functions that are separable in terms of the Lyapunov functions corresponding to individual state variables, allowing for compositional stability verification (Haddad et al., 2010). These compositional properties also extend to certain classes of nonlinear monotone systems (Dirr et al., 2015). Mathematically, monotonicity of dynamical systems is defined below, following Angeli and Sontag (2003).

Definition 2.5 (Monotone Systems). *Consider a controlled dynamical system f as defined in (3) $\dot{x} = f(x, u)$. Assume that solution $x(t) = \phi(t, x_0, u)$ with initial condition $x(0) = x_0$. The dynamics f is said to be monotone if the following implication holds for all $t \geq 0$:*

$$u_1 \geq u_2, x_1 \geq x_2 \Rightarrow \phi(t, x_1, u_1) \geq \phi(t, x_2, u_2),$$

for a suitably defined ordering \geq . The typical case for the ordering $y \geq z$ for $y, z \in \mathbb{R}^n$ means each coordinate of y is bigger or equal than the corresponding coordinate of z . However, other orderings could be induced by choosing other orthants in \mathbb{R}^n other than the positive orthants $K = \mathbb{R}_{\geq 0}^n$.

2.3.4. Symmetries of Physical Systems

Symmetric systems have responses that are invariant to certain continuous transformations. System models that capture symmetries reduce the model complexity and improve the computational efficiency and accuracy of system dynamics prediction. A continuous transformation $\gamma \in \Gamma$ is typically described by the action of a compact Lie group Γ on the state space X of the system.

Definition 2.6 (Group Action). *Let Γ be a group with operation \cdot and identity element e . An action of Γ on set X is a function $\rho : \Gamma \times X \rightarrow X$ that satisfies an identity property, $\rho(e, x) = x$, and a compatibility property, $\rho(a, \rho(b, x)) = \rho(a \cdot b, x)$ for $a, b \in \Gamma$. The notation is commonly simplified as $\gamma x := \rho(\gamma, x)$.*

A group element $\gamma \in \Gamma$ is a *symmetry* of the dynamics F of a closed-loop system (8) if, for every solution $x(t)$, $\gamma x(t)$ is also a solution. This leads to a useful condition for γ to be a symmetry of F (Golubitsky and Stewart, 2002).

Definition 2.7 (Equivariant System). *A system $\dot{x} = F(x, t)$ with $x \in X$ is equivariant under an action of group Γ on X if $F(\gamma x, t) = \gamma F(x, t)$ for all t , $\gamma \in \Gamma$, $x \in X$.*

Symmetry in physical systems (Marsden and Ratiu, 2013) has been widely studied in physics, from Lagrangian and Hamiltonian mechanics (Lurie, 2002; Holm, 2008) to quantum mechanics (Greiner and Müller, 2012). One of the most well-known results is Noether's theorem (Noether, 1983), which states that there is a conservation law for every continuous symmetry of a system. The dynamics of a physical system can be described using a Lagrangian function \mathcal{L} . The action of the system, defined as the integral over time of the Lagrangian, governs the system behavior via the principle of least action (Holm, 2008). If the Lagrangian is invariant under a group of transformations Γ , i.e., $\mathcal{L}(\gamma x) = \mathcal{L}(x)$, $\forall \gamma \in \Gamma$, Noether's theorem guarantees the existence of conserved quantities associated with the generators of that group. For example, time-invariant Lagrangians, i.e., $\mathcal{L}(t + \delta t) = \mathcal{L}(t)$, lead to the conservation of the total energy of the system. Translation-invariant Lagrangians, i.e., $\mathcal{L}(x + \delta x) = \mathcal{L}(x)$, lead to the conservation of linear momentum, while rotational invariant Lagrangians, i.e., $\mathcal{L}(Rx) = \mathcal{L}(x)$ where R is a rotation matrix, lead to the conservation of angular momentum.

In reality, the assumption on conservative forces rarely holds as there are often external non-conservative forces, such as frictions or resistance, applied on the system. Such forces dissipate energy from the system and require a generalization of the mechanics model to account for energy dissipation. For example, a port-Hamiltonian model (Van Der Schaft and Jeltsema, 2014) combines concepts from Hamiltonian mechanics (which uses energy to describe motion) with port-based modeling (which views systems as interconnected elements exchanging power).

3. Physics-Informed System Identification: Motivation, Problem, and Approaches

3.1. Why Preserve Control-Relevant Properties?

In general, preserving control-relevant and other physics-informed system properties, such as those described in Section 2.3, provides several advantages. Firstly, incorporating a priori information regarding system physics often improves the sample efficiency of the identification algorithms and generalizability of the identified models. Secondly, control-relevant properties such as dissipativity and monotonicity can be exploited to facilitate scalable and distributed control designs with provable guarantees. Finally, capturing physics-based properties such as symmetries allows for explainability of the identified model, which is crucial when utilized in high-stake control applications. Here, we demonstrate through two concrete examples how control-relevant and physics-informed properties can directly aid in control design.

We start by considering the example of conservation laws - specifically, energy conservation. Energy conservation, if preserved in the dynamics model, has been shown to be beneficial for data efficiency, control design and stability analysis (Greydanus et al., 2019; Zhong et al., 2019; Wang et al., 2020; Duong and Atanasov, 2021). While the law of energy conservation universally holds for physical systems, a black-box machine learning model may struggle to learn this knowledge, even from a large amount of data. By enforcing the law of energy conservation in the machine learning model, e.g., using Lagrangian or Hamiltonian formulations of physical systems, energy conservation is guaranteed by design, thus improving data efficiency and prediction accuracy (Miller et al., 2020). Preserving the law of energy conservation also facilitates control design with the learned model from an energy perspective. Given a desired state x^* , the total energy of the system is generally not minimized at x^* , i.e., x^* is not an equilibrium point of the system. By decomposing the system into energy storing and dissipating elements in a Hamiltonian formulation, one can inject energy through the control input to shape the total energy of the system to a desired total energy function, minimized at x^* , and thus, move the equilibrium point to x^* (Van Der Schaft and Jeltsema, 2014). We now illustrate how preserving the Hamiltonian structure in neural dynamical models can help to achieve superior training performance compared to black box models.

Example 3.1 (Hamiltonian neural ODE). *Consider a pendulum system with dynamics:*

$$\ddot{\varphi} = -\frac{g}{l} \sin \varphi + u, \quad (19)$$

where φ is the angle of the pendulum with respect to its downward position, u is a scalar control input, g is the gravitational acceleration and l is the length of the pendulum. As a physical system, the pendulum dynamics can be formulated using Hamiltonian formulation, either on \mathbb{R}^n , i.e., using the angle φ as the state (Zhong et al., 2019), or on a Lie group, i.e. using the rotation matrix, generated from the Euler angle $[0, 0, \varphi]$, as

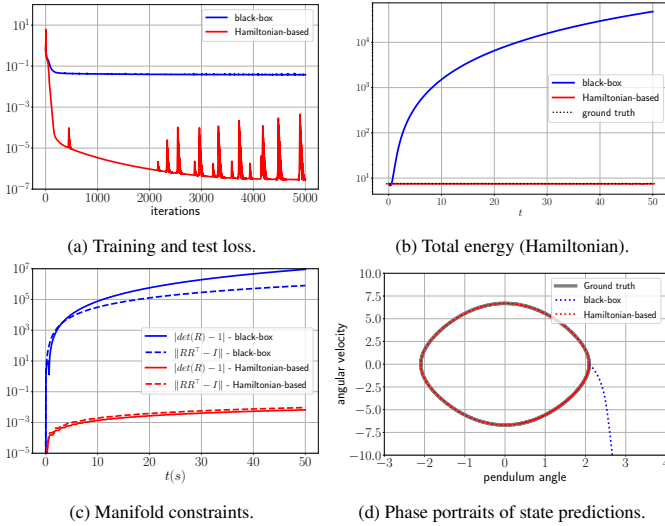


Figure 1: Pendulum dynamics identification using an $SO(3)$ port-Hamiltonian neural ODE network (Duong et al., 2024a).

a state R on the $SO(3)$ manifold:

$$R = \begin{bmatrix} \cos \varphi & -\sin \varphi & 0 \\ \sin \varphi & \cos \varphi & 0 \\ 0 & 0 & 1 \end{bmatrix}. \quad (20)$$

The matrix R satisfies the $SO(3)$ constraints: $R^T R = I$, $\det(R) = 1$. The control input u is randomly sampled and applied to the pendulum to collect a dataset of state-control trajectories. This dataset trains a $SO(3)$ Hamiltonian-based neural ODE network (Duong et al., 2024a), which encodes both energy conservation and $SO(3)$ constraints via a Hamiltonian formulation. We discuss such physics-informed architectures in Section 5. The dataset is also used to train a black-box neural ODE network for comparison, where the dynamics function f in (3) is represented by a multilayer perceptron network. Fig. 1a shows that enforcing physics constraints improves training with faster convergence. Figs. 1b and 1c show the learned model preserves energy and $SO(3)$ constraints when rolled out from an initial angle $\varphi = \frac{2\pi}{3}$ without control. The predicted angle and velocity also follow the pendulum's phase portraits (Fig. 1d).

The above example demonstrates how properties such as energy conservation can be leveraged to fit models with better sample efficiency and interpretability. Incorporating properties like dissipativity can also facilitate scalable analysis and control in large-scale networked systems (Arcak et al., 2016; Arcak, 2022; Agarwal et al., 2021, 2020; Jena et al., 2021; Sivaranjani et al., 2020a). We provide an additional example demonstrating how dissipativity can be leveraged for distributed synthesis of controllers in our Github repository. Overall, these benefits motivate the idea of preserving control-relevant properties in system identification.

3.2. Does Classical System Identification Preserve Control-relevant Properties?

Since it is desirable to preserve properties such as energy conservation and dissipativity that can inform or simplify control designs for complex systems, a natural question is: *If we are able to identify models that approximate the dynamics very closely, will these system properties be naturally inherited in the identified model?* Unfortunately, this is not the case, as we illustrate with a simple counter-example. We show that even for a linear system, there is no guarantee that a learned model that approximates the system very closely will preserve the dissipativity property possessed by the original system.

Example 3.2 (Linear system counter-example). *We consider a linear system as follows.*

$$\begin{aligned} \dot{x}(t) &= Ax(t) + Bu(t) \\ y(t) &= Cx(t) + Du(t), \end{aligned}$$

where

$$A = \begin{bmatrix} -2 & -3 & -4 \\ 1 & 0 & 0 \\ 0 & 1 & 0 \end{bmatrix}, \quad B = \begin{bmatrix} 1 \\ 0 \\ 0 \end{bmatrix}, \quad C = \begin{bmatrix} -1 & 0 & 2 \end{bmatrix}, \quad D = 1.$$

This system possesses the property of passivity, that is, it is dissipative with $Q = 0, S = \frac{1}{2}, R = 0$, which we can verify, e.g., using the MATLAB `isPassive` function. For system identification, we generate training data using the input $u(t) = te^{-5t}$. We show that even if we can measure the exact output, which is the most desirable case, and identify a linear model that closely approximates the system behavior, we still lose the passivity property in the identified model.

In Fig. 2, we compare the trajectory of the ground truth and the one generated by the identified linear model using the MATLAB System Identification Toolbox. The identified learned model has matrices

$$A_{id} = \begin{bmatrix} -0.033 & -1.325 & -0.001 \\ 1.176 & -0.146 & -1.693 \\ -0.5 & 0.654 & -1.842 \end{bmatrix}, \quad B_{id} = \begin{bmatrix} -4.68 \\ 14.2 \\ -6.28 \end{bmatrix},$$

$C_{id} = [3.368 \quad -0.023 \quad 0]$ and $D_{id} = 0$. We can observe that the model manages to approximate the input-output behavior of the system extremely well, as seen from the validation/test data, with goodness of fit being 99.6%. However, when we test the passivity of the identified model ($A_{id}, B_{id}, C_{id}, D_{id}$) using the MATLAB function `isPassive`, we find that this model is, in fact, not passive! This demonstrates that system identification does not guarantee to preserve the underlying dynamical system properties, even when the identified model behavior is extremely close to the system input-output behavior.

One intuition behind this observation is that there are an infinite number of models that can achieve a desired level of fit for a set of system input-output trajectories. These models may differ significantly in their parameters (such as the (A, B, C, D) matrices in the above example), but be close in terms of overall

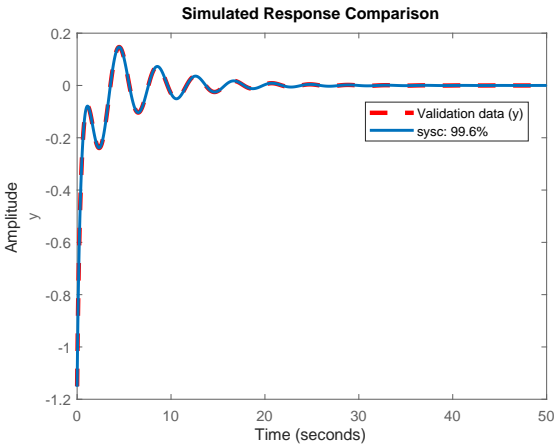


Figure 2: Linear system vs model trajectories for Example 3.2. The model closely approximates the system test data (with a fit of 99.6% in this case) but does not preserve the passivity of the system.

input-output behavior in the region of the state-space in which they are trained to approximate the unknown system dynamics.

From the preceding discussion, given that system properties like passivity are not inherited in system identification even for linear models, it is clear that we cannot provide any guarantees on more complex models like neural network models—even if the model accurately approximates the system behavior. Therefore, it necessitates specific approaches to impose control-relevant properties during identification.

3.3. Physics-Informed Identification as an Optimization Problem: Parametrization, Constraints, or Regularization?

Considering the identification problem for a nonlinear system (3), there are, in general, three ways of imposing structure on the obtained system model: *direct parameterization*, *hard constraints*, and *soft constraints*. In direct parametrization, we may use a particular parametrization of f_θ and h_θ to impose system properties, such as assuming linear structure and identifying A, B, C, D matrices rather than a general neural network parameterized dynamics f_θ, h_θ . Alternately, we may impose hard constraints on the parameters θ in the optimization problem in (14), such as dissipativity imposed as an LMI (Martin and Allgöwer, 2022a). Finally, we may impose a soft constraint on θ in the form of a regularization term in the cost function in (14), which promotes a property of interest such as stability (Lechner et al., 2020) and energy conservation (Greydanus et al., 2019). These three ways of imposing model structure are summarized in Fig. 3. They can be introduced in the general system identification optimization in (14) as:

$$\begin{aligned} \min_{\theta} c(\theta; \mathcal{W}) &:= \sum_i \int_t \|y_i(t) - \hat{y}_i(t)\|^2 dt + r(\theta) \\ \text{s.t. } \dot{\hat{x}}_i(t) &= f_\theta(\hat{x}_i(t), u_i(t)), \\ \hat{y}_i(t) &= h_\theta(\hat{x}_i(t), u_i(t)), \\ g(\theta) &\leq 0, \end{aligned} \quad (21)$$

where $\mathcal{W} = \{(u_i(t), y_i(t))\}_i$ represents the set of input-output trajectories from a continuous-time dynamical system, f_θ, h_θ

encode model structure through their parametrization, $g(\theta)$ captures hard constraints on the model parameters θ , and $r(\theta)$ is a regularization term capturing soft constraints.

We provide concise illustrations of each method. An example of imposing structure through *direct parameterization* is a Lagrangian neural network (Cranmer et al., 2020), which imposes the Euler-Lagrange equation in the design of f_θ as a physics prior. Given a physical system with state $x = (q, \dot{q})$, consisting of the system configuration q and velocity \dot{q} , and torque input u , the Euler-Lagrange equation describes the system's motion as:

$$\frac{d}{dt} \nabla_{\dot{q}} L(t, q, \dot{q}) - \nabla_q L(t, q, \dot{q}) = u \quad (22)$$

where L is the Lagrangian. Using the chain rule to expand the time derivative through the gradient of the Lagrangian and a neural network to parameterize L_θ leads to a parametric model of the system dynamics that encodes the Lagrangian structure:

$$\begin{bmatrix} \dot{q} \\ \ddot{q} \end{bmatrix} = f_\theta(q, \dot{q}, u) \quad (23)$$

$$= \begin{bmatrix} 0 & 1 \\ 0 & -(\nabla_{\dot{q}} \nabla_{\dot{q}}^\top L_\theta)^{-1} \nabla_q \nabla_{\dot{q}}^\top L_\theta \end{bmatrix} \begin{bmatrix} q \\ \dot{q} \end{bmatrix} + \begin{bmatrix} 0 \\ (\nabla_{\dot{q}} \nabla_{\dot{q}}^\top L_\theta)^{-1} \end{bmatrix} (\nabla_q L_\theta + u).$$

As an example of imposing a *hard constraint* on the model parameters θ , we consider requiring that the identified system model is internally stable in the Lyapunov sense. Gaby et al. (2022) propose a candidate Lyapunov function of the form:

$$V_\theta(x) = \|\phi_\theta(x) - \phi_\theta(0)\|^2 + \alpha \|x\|^2, \quad (24)$$

where $\alpha > 0$ and $\phi_\theta(x)$ is a fully connected neural network with parameters θ and tanh activations. This construction ensures that $V_\theta(0) = 0$ and $V_\theta(x) \geq \alpha \|x\|^2 > 0$ for $x \neq 0$ as required by Theorem 2.1. The last condition in that result for $V_\theta(x)$ to be a valid Lyapunov function can be ensured by imposing a hard constraint in (21) of the form:

$$g(\theta) = \int \max\{\dot{V}_\theta(x) + \gamma \|x\|, 0\} dx \leq 0, \quad (25)$$

where $\gamma > 0$ and the time derivative of $V_\theta(x)$ is computed along the system trajectory. In practice, the integral in (25) is approximated with a finite number of samples.

Finally, an example of imposing structure through *soft constraints (parameter regularization)* is the use of Gershgorin circle theorem (Lechner et al., 2020) to encourage the eigenvalues of A_θ in a linear system model (5) to be negative. This can be achieved by adding a regularization term $r(\theta)$ to the cost function in (21) of the form:

$$r(\theta) = \sum_{i=1}^n \max\{0, [A_\theta]_{i,i} + \sum_{j \neq i} |[A_\theta]_{i,j}| + \epsilon\}, \quad (26)$$

where $\epsilon > 0$ is a small constant.

With the above formulation in hand, we can now survey and classify approaches for imposing control-relevant and physics-informed structures into system identification proposed in the literature, in the context of both classical system identification and learning-based methods.

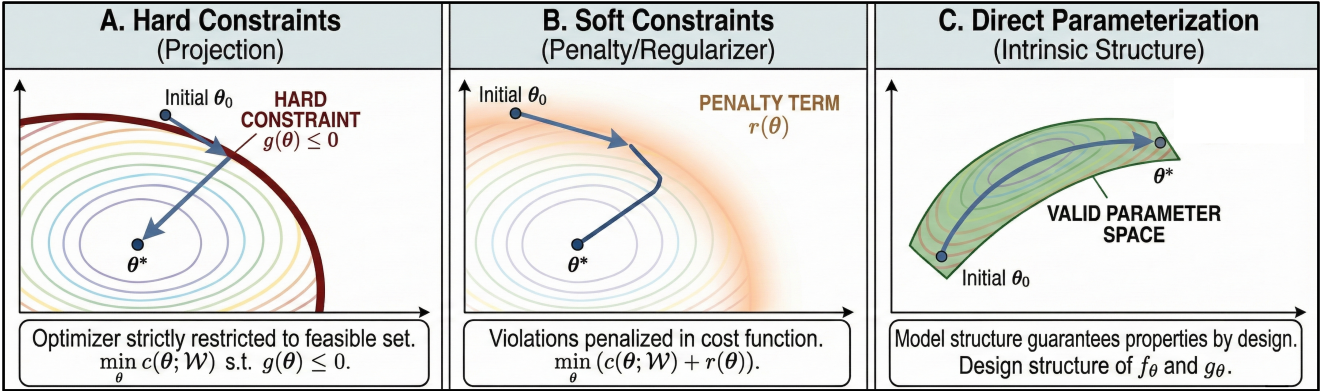


Figure 3: Approaches to impose control-oriented properties in optimization-based formulation of system identification.

4. Classical System Identification

We now focus on imposing physics-informed and control-relevant properties in classical system identification for linear and nonlinear dynamical systems.

4.1. Linear System Identification

Linear system identification techniques are concerned with learning either time-domain representations in the form of state space models like (5), frequency domain representations like transfer function models (6), or their discrete-time counterparts. Typical approaches for unconstrained identification such as least squares regression and subspace methods are surveyed in classic texts such as [Ljung et al. \(1987\)](#).

4.1.1. Stable System Identification

First, consider the fundamental property of stability. In linear system identification, stability can be imposed using any of the three approaches described in Section 3.3. For example, in subspace identification of state-space models of the form (5) or (12) parameterized by $\theta = (A, B, C, D)$, stability can be imposed through suitable choice of the structure of the A matrix as in [Maciejowski \(1995\)](#). Alternatively, the Lyapunov equation can be introduced as a hard constraint as in [Lacy and Bernstein \(2003\)](#); for example, we have the constraint $g(\theta) = A^\top P A - P$ with $P > 0$ to enforce stability in the discrete-time model (12). Another approach is to impose stability through soft constraints as in [Van Gestel et al. \(2001\)](#), by introducing a regularization term $r(\theta) = Tr(AWA^\top)$ with positive semi-definite weighting matrix $W \geq 0$, where the magnitude of the regularization is determined by solving a generalized eigenvalue problem.

Similarly, in identifying stable frequency domain models, stable parameterizations of transfer functions including certain canonical forms can be chosen; alternatively, hard or soft constraints on the pole locations can be imposed to ensure stability. Since stability-preserving system identification is a vast and well-studied topic, we direct the reader to pedagogical resources such as [Pintelon and Schoukens \(2012\)](#); [Verhaegen and Verdult \(2007\)](#); [Van Overschee and De Moor \(2012\)](#). The remainder of this section will then focus on identification approaches (direct parameterization, hard constraint, and soft

constraint based) to preserve other control-relevant properties like dissipativity, monotonicity, and symmetries, following the framework described in Section 3.3.

4.1.2. Hard Constraints

Consider the problem of identifying a linear system (5) with parameters (A, B, C, D) . Convex formulations of constraints for special cases like positive real systems and passive systems as defined in Section 2.3.2 are considered in works such as [Hoagg et al. \(2004\)](#); [Coelho et al. \(2004\)](#). For example, (16) can be directly imposed as hard constraints while minimizing traditional identification objectives such as error between the actual system outputs and the predicted outputs from the identified model.

However, directly imposing hard constraints during identification is often not desirable since it may introduce uncontrollable model bias ([Pintelon and Schoukens, 2012](#)). To understand this, consider the identification problem posed in (14). This problem can be viewed as filtering out the noise in the observed input-output data to obtain the best model fit. Thus, the cost function should ideally be weighted by the inverse of the noise variance. Adding hard constraints to this problem introduces a fundamental tradeoff since it does not hold a priori that model achieving the best noise variance will satisfy these hard constraints. For example, in the frequency domain, the model errors corresponding to this constraint and those corresponding to noise filtering may be distributed in different ranges in the frequency spectrum. In order to address this challenge, hard constraints such as dissipativity are often imposed through a two-stage identification process. First, the unconstrained optimization problem (14) is solved to identify a model that achieves the best fit to the observed system behavior. Then, a small perturbation is introduced in the parameters to ensure that the perturbed values satisfy the hard constraints while minimizing deviation from the original model. Let $\hat{\theta}$ be the solution to the unconstrained problem (14), and let $G_{\theta_p}(s)$ be the perturbed model with parameter values θ_p that satisfy the desired constraints. Then, in frequency domain identification, the constrained optimization problem in (21) is modified to minimize the cost function $c(\theta, \mathcal{W}) = \|G_\theta(s) - G_{\theta_p}(s)\|_F^2$ where $\|\cdot\|_F$ denotes the Frobenius norm, with hard constraints $g(\theta_p)$ on model $G_{\theta_p}(s)$ corresponding to the desired property, such as (17) or

(18). In essence, this approach attempts to find the minimal deviation from the best unconstrained model that satisfies the desired hard constraints. A similar perturbation approach can be employed in the state space setting to enforce hard constraints corresponding to the desired property, such as the dissipativity constraint in (16). Here, we demonstrate through an example how passivity constraints can be enforced through such a perturbation approach.

Example 4.1 (Passive linear model identification for an RLC circuit). We consider a RLC circuit where resistor, inductor and capacitor are in series. We set the state variable $x_1(t)$ to be the current in the circuit and $x_2(t)$ to be the voltage of the capacitor. We let input $u(t)$ to be source voltage and output $y(t)$ to be current (i.e. $x_1(t)$). With $R = L = C = 1$, we write the linear state-space model as

$$\begin{aligned} \begin{bmatrix} \dot{x}_1(t) \\ \dot{x}_2(t) \end{bmatrix} &= \begin{bmatrix} -1 & -1 \\ 1 & 0 \end{bmatrix} \begin{bmatrix} x_1(t) \\ x_2(t) \end{bmatrix} + \begin{bmatrix} 1 \\ 0 \end{bmatrix} u(t) \\ y(t) &= \begin{bmatrix} 1 & 0 \end{bmatrix} \begin{bmatrix} x_1(t) \\ x_2(t) \end{bmatrix} \end{aligned} \quad (27)$$

In other words, the real coefficient matrices are $A = \begin{bmatrix} -1 & -1 \\ 1 & 0 \end{bmatrix}$, $B = \begin{bmatrix} 1 \\ 0 \end{bmatrix}$, $C = \begin{bmatrix} 1 & 0 \end{bmatrix}$, and $D = 0$. Let $P = I_2 > 0$. Then we have

$$\begin{bmatrix} A^\top P + PA & PB - C^\top \\ B^\top P - C & -(D + D^\top) \end{bmatrix} = \begin{bmatrix} -2 & 0 & 0 \\ 0 & 0 & 0 \\ 0 & 0 & 0 \end{bmatrix} \leq 0.$$

According to the Positive Real Lemma, the real system is passive. Now we generate trajectory data for input $u(t) = e^{-0.1t} \sin(\pi t)$ with initial state being $[0.1, 0.2]^\top$. We also add additional Gaussian noise $\sim N(0, 0.005^2)$ to make it more realistic. With the data, we use function `ssest` from the System Identification Toolbox in MATLAB and identify a baseline system model where the fit goodness reaches 95.81%. The identified model has coefficients $A_{id} = \begin{bmatrix} -0.6661 & -0.2035 \\ 3.7286 & -0.2876 \end{bmatrix}$, $B_{id} = \begin{bmatrix} -4.3142 \\ -1.7815 \end{bmatrix}$, $C_{id} = \begin{bmatrix} -0.2338 & 0.0144 \end{bmatrix}$, and $D_{id} = 0$. However, the following problem is not feasible,

$$P_1 \geq 0 \quad \begin{bmatrix} A_{id}^\top P_1 + P_1 A_{id} & P_1 B_{id} - C_{id}^\top \\ B_{id}^\top P_1 - C_{id} & -(D_{id} + D_{id}^\top) \end{bmatrix} \leq 0, \quad (28)$$

where P_1 is a symmetric matrix of size 2, which indicates that the identified model is not passive. Now we will design a perturbation ΔC , where the perturbed $C_p = C_{id} + \Delta C$ is as small as possible to impose passivity. This is formulated as an optimization problem as below, where P_2 is a symmetric matrix of size 2 and the objective is the Frobenius norm of the perturbation ΔC .

$$\begin{aligned} \min \quad & \|\Delta C\|_F \\ \text{s.t.} \quad & P_2 \geq 0 \quad \begin{bmatrix} A_{id}^\top P_2 + P_2 A_{id} & P_2 B_{id} - C_p^\top \\ B_{id}^\top P_2 - C_p & -(D_{id} + D_{id}^\top) \end{bmatrix} \leq 0 \end{aligned} \quad (29)$$

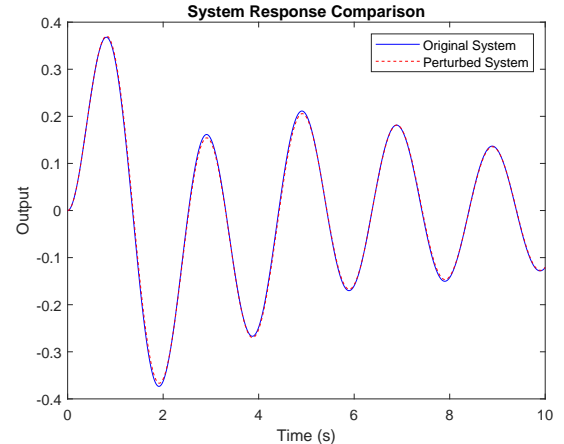


Figure 4: Passive linear model vs system trajectories for Example 4.1. The model closely approximates the system test data and is certified to be passive.

We have the resulting $\Delta C = \begin{bmatrix} -0.0001 & -0.0025 \end{bmatrix}$ with $P_2 = \begin{bmatrix} 0.0559 & -0.0042 \\ -0.0042 & 0.0119 \end{bmatrix} \geq 0$. The corresponding $C_p = \begin{bmatrix} -0.2339 & -0.0119 \end{bmatrix}$. Finally, we obtain a linear model with system matrices to be $A_p = A_{id}$, $B_p = B_{id}$, $C_p = C_{id} + \Delta C$, $D_p = D_{id}$ that is passive. We demonstrate the fit of the perturbed system, which is certified to be passive in Fig. 4. The goodness of fit score is still high (95.23%) and we can see that the final model closely matches the ground-truth.

There are multiple choices for deciding which parameters to perturb. Perturbing the system matrix A is generally avoided, as it contains key dynamical features like dominant modes or eigenvalues. Alternatively, perturbation of the feedthrough matrix D can be leveraged in cases where $D > 0$ is necessary to enforce strict dissipativity or other similar properties though it only affects direct input-output coupling, not internal dynamics. From a transfer function view, this is an asymptotic perturbation affecting behavior as $s \rightarrow \infty$. Since passivity is an input-output property, perturbing the input matrix B or output matrix C is also natural, as in Example 4.1. Such approaches for identifying dissipative (including QSR -dissipative) models have been explored in Sivarajani et al. (2022); Bradde et al. (2020).

Another approach for passivity enforcement in identified models is to consider the Hamiltonian matrix. Consider a parameterized state-space realization (A, B, C, D) of order n with corresponding transfer function $G(s)$. The associated Hamiltonian matrix $M_H \in \mathbb{R}^{2n \times 2n}$ is defined as:

$$M_H = \begin{bmatrix} A - BR_1^{-1}D^\top C & -BR_1^{-1}B^\top \\ C^\top S_1^{-1}C & -A^\top + C^\top DR_1^{-1}B^\top \end{bmatrix} \quad (30)$$

where $R_1 = I - D^\top D$, and $S_1 = I - DD^\top$. Assuming that $\|D\| = \sigma_{max}(D) < 1$, passivity violations occur when M has purely imaginary eigenvalues $\mu_k = j\omega_k$, or correspondingly, at frequencies where the largest singular value of $G(j\omega)$ exceeds unity. When only the C matrix of the system is perturbed to $C + \Delta C$ as discussed above, the corresponding perturbation on the

Hamiltonian can be written using the first-order approximation:

$$\Delta M_H \approx \begin{bmatrix} BR_1^{-1}D^\top \Delta C & 0 \\ -C^\top S_1^{-1}\Delta C - \Delta C^\top S_1^{-1}C & -\Delta C^\top DR_1^{-1}B^\top \end{bmatrix} \quad (31)$$

The perturbation affects the eigenvalues of the Hamiltonian matrix according to

$$\Delta \lambda_i = \frac{v_i^H \Delta M_H w_i}{v_i^H w_i} \quad (32)$$

where v_i and w_i are the left and right eigenvectors corresponding to the imaginary eigenvalues of the original Hamiltonian.

Using this property, a general passivity enforcement approach can be developed as follows. The eigenvalues of M_H are computed for the baseline (unperturbed) model to identify frequencies where $\sigma_{\max}(G(j\omega)) > 1$. Then, the singular value decomposition is computed at these violation frequencies to obtain left and right singular vectors u_i, v_i of M_H corresponding to the imaginary eigenvalues that represent the directions of passivity violation in the frequency response. Finally, the optimization problem to determine the minimal passivity-enforcing perturbation is formulated as:

$$\begin{aligned} \min \quad & \|\Delta C\|_F \\ \text{s.t.} \quad & \Delta \lambda_i < 0, \quad \operatorname{Re}\{u_i^H \Delta G(j\omega_k) v_i\} < 0. \end{aligned} \quad (33)$$

Such Hamiltonian perturbation approaches were originally proposed in Grivet-Talocia (2004), with subsequent works extending this approach to large-scale systems (Grivet-Talocia and Ubolli, 2006), descriptor systems where $D + D^\top$ is singular (Wang et al., 2010), negative imaginary systems (Mabrok et al., 2011), and proposing improved algorithms to decrease the dispersion of the perturbed model from the original dynamics (Gustavsen, 2008). We further direct the reader to the monograph by Grivet-Talocia and Gustavsen (2015) for an in-depth discussion of these approaches.

In the frequency domain, baseline rational transfer function models are often obtained through vector fitting approaches (Gustavsen and Semlyen, 1999). When the resulting models do not satisfy desired dissipativity properties, iterative pole-residue perturbation of the identified transfer function is employed to correct for violations at specific frequency ranges through heuristic or linear and quadratic programming approaches Gustavsen and Semlyen (2001); Gustavsen (2007); Saraswat et al. (2005, 2004); Chen and Fang (2003). Here, LMIs directly corresponding to properties like dissipativity or tools the Hamiltonian matrix in (30) may be employed for property verification.

4.1.3. Soft Constraints

In several system identification problems, hard constraints as described in Section 4.1.2, while desirable in terms of provably guaranteeing control-relevant properties, are challenging to impose. For instance, efficiently solving such formulations requires convex parameterizations of the constraints which may not be possible. Even if such parameterizations are available, direct imposition during learning is rarely adopted, and a two-stage perturbation or projection approach is often employed

(Pintelon and Schoukens, 2012) due to issue of model bias as described in Section 4.1.2.

Instead, it may be easier to obtain system models satisfying desired properties like stability or passivity by imposing soft constraints in the form of regularization terms as in the identification problem (21). While such approaches may not possess theoretical guarantees of yielding an identified model that satisfies the desired property, they nonetheless often yield property-preserving models in practice. These soft constraint based identification approaches may be particularly attractive in online system identification applications, where minimal violations of desired properties may be tolerated in favor of decreased computational complexity. As an example of such an approach, we now illustrate how soft constraints can help to enforce dissipativity-type properties in system identification.

Consider the problem of identifying a positive real discrete-time linear state-space model of the form (12). Then, as described in Goethals et al. (2003), the cost function in (21) can be modified to obtain a positive real model parameterized by $\theta = (A, C)$ as

$$c(\theta, \mathcal{W}) = c_1(\theta) + r(\theta).$$

Here, the term

$$c_1(\theta) = \left\| \begin{bmatrix} \hat{X}_{k+1} \\ Y_k \end{bmatrix} - \begin{bmatrix} A \\ C \end{bmatrix} \hat{X}_k \right\|_F^2 \quad (34)$$

is employed to minimize model error with respect to the input-output data. Additionally, the regularization term

$$r(\theta) = \operatorname{Tr} \left(\begin{bmatrix} A \\ C \end{bmatrix}^\top W \begin{bmatrix} A \\ C \end{bmatrix} \right), \quad W > 0 \quad (35)$$

is employed to promote positive realness of the identified model. Note that Goethals et al. (2003) considers identification with noise in the system dynamics and outputs, and additional constraints on W are imposed based on the covariance matrices obtained from data. Similar regularization approaches have been employed in Peternell (1995) and Vaccaro and Vukina (1993) where the output covariance matrix is regularized to ensure positive realness. However, such soft constraint based approaches as a whole have received limited attention in classical system identification. This is in stark contrast to machine learning based approaches where soft constraint based approaches are, in fact, dominant. We will describe such learning-based models in Section 5.4.

4.1.4. Direct Parameterization

Considering the identification problem in (21), one approach to imposing physics-informed or control-relevant properties is to directly parameterize the functions f_θ and g_θ , representing the system dynamics, to preserve the desired property of interest, while choosing a parameterization that facilitates tractable solutions of (21). For example, consider the property of positive realness. Given a continuous-time SISO transfer function structure

$$H(s) = d + \frac{c(s)}{a(s)}, \quad a(s) = s^n + a_1 s^{n-1} + \cdots + a_n,$$

where $a(s)$ is monic and Hurwitz, following Dumitrescu (2002), every positive-real $H(s)$ can be parameterized using a single symmetric positive semidefinite matrix $Z \in \mathbb{R}^{n \times n}$ as follows:

$$d = \text{tr}(\Lambda_0 Z), \quad c_k = \text{tr}(\Lambda_k Z) \quad (k = 1, \dots, n),$$

where $\{\Lambda_k\}_{k=0}^n$ are constant symmetric matrices computed as explicit linear functions of (a_1, \dots, a_n) . This construction guarantees positive realness of $H(s)$ for all $Z \geq 0$. Parameterizations of the numerator polynomial of the transfer function have also been developed to capture properties like passivity and positive realness (Marquez and Damaren, 1995).

Similarly, in discrete-time, any stable LTI system $G(z)$ can be uniquely represented as a series expansion $G(z) = \sum_{i=1}^{\infty} \theta_i \psi_i(z^{-1})$, where $\{\psi_i(z^{-1})\}_{i=1}^{\infty}$ is a prechosen orthonormal basis (e.g., Laguerre or Kautz) and $\theta_i = \langle G, \psi_i \rangle_{\mathcal{H}_2}$ are model parameters. In practice, we can obtain an approximate finite-dimensional representation:

$$G_N(z) = \sum_{i=1}^N \theta_i \psi_i(z^{-1}),$$

where hard constraints can be enforced via linear inequalities on θ similar to Section 4.1.2 to enforce properties like positive realness, passivity, or dissipativity. For example, Prakash et al. (2022) formulate a convex optimization problem

$$\begin{aligned} \min_{\theta \in \mathbb{R}^N} \quad & \sum_{k=1}^p \left| Y(e^{j\omega_k}) - \sum_{i=1}^N \theta_i \psi_i(e^{-j\omega_k}) \right|^2, \\ \text{s.t.} \quad & \Re \left\{ \sum_{i=1}^N \theta_i \psi_i(e^{-j\omega_k}) \right\} \geq \epsilon > 0, \quad k = 1, \dots, p, \end{aligned} \quad (36)$$

where $Y(e^{j\omega_k})$ are measured frequency-response samples on the grid of frequencies $\{\omega_k\}$, the constraint enforces strict positive-realness. In multivariable settings, balanced state-space realizations (with equal and diagonal reachability and observability Gramians) can be utilized to develop stable minimal parameterizations capturing a variety of useful properties including minimum phase and positive realness (Chou and Maciejowski, 1997). Such parameterizations have the advantage of providing injective mappings from the parameter space to input–output behavior, thus ensuring the existence of a unique parameter vector corresponding to each transfer function. Further, contraction mappings have been leveraged to preserve positive realness under reduction with explicit \mathcal{L}_{∞} bounds (Opdenacker and Jonckheere, 1988), and reproducing kernel Hilbert space (RKHS) methods have been adopted to identify nonnegative input–output operators that preserve passivity by solving semidefinite programs (SDPs) (Shali and van Waarde, 2024). In summary, some control-relevant properties such as stability and passivity can be directly embedded through parameterization of transfer functions or state-space models. However, capturing more complex physics-informed or control-relevant properties through identifiable parameterizations remains an open challenge. We will further discuss this in the context of learning-based models in Section 5.

4.2. Nonlinear System Identification

Nonlinear system identification, focused on learning representations of the form (3), is a classical topic (Sjöberg et al., 1995; Schön et al., 2011; Ljung, 2010), with special cases like the identification of linearized models and Lure-type systems receiving especially significant attention (Schoukens and Tiels, 2017). However, identification in the nonlinear systems context remains a challenging problem due to local minima in model fitting, high long-term prediction errors, and difficulty in selecting stable model classes or parameterizations that adequately capture the rich and complex spectrum of dynamical behavior that such systems can exhibit. We will now describe specific model classes that have been extensively utilized in preserving physics-informed and control-relevant properties during nonlinear system identification.

4.2.1. Implicit Representations

Implicit representations of nonlinear systems that allow for a convex parameterization of all stable models have been introduced to facilitate robust nonlinear system identification minimizing simulation or prediction errors (Megretski, 2008; Toubenkin et al., 2010; Manchester et al., 2012; Umenberger and Manchester, 2018). For example, considering an implicit representation of the form

$$e(x_{k+1}) = f(x_k, u_k), \quad y_k = g(x_k, u_k), \quad (37)$$

where e, f, g are drawn from a linearly parameterized polynomial basis with parameters ρ , stability can be enforced through the convex inequalities

$$\begin{aligned} F(x, u) P^{-1} F(x, u)^T - E(x) P^{-1} E(x)^T + \mu I + G(x, u) P^{-1} G(x, u)^T > 0, \\ P > 0, \quad \mu > 0, \end{aligned} \quad (38)$$

where $E(x) = \nabla_x e(x)$, $F(x, u) = \nabla_x f(x, u)$, $G(x, u) = \nabla_x g(x, u)$, which can be solved using sum-of-squares relaxations (Umenberger and Manchester, 2018). Such implicit representations have also been extended to obtain convex parametrizations guaranteeing monotonicity, positivity, and contraction properties (Revay et al., 2021).

4.2.2. Koopman Operator Models

The Koopman operator provides an approach to model nonlinear dynamical systems by approximating them through high-dimensional linear models. This is accomplished by introducing a lifting map Φ that stacks scalar-valued functions of the system states and inputs, termed as *observables*. On this observable space, the time evolution is linear under the typically infinite-dimensional Koopman operator, which acts by composition with the system dynamics. In practical implementations, this infinite-dimensional operator is approximated using a finite set of basis functions, yielding a high-dimensional albeit linear representation of the nonlinear dynamics.

Specifically, considering a nonlinear dynamical system in continuous-time as in (3) or discrete-time as in (11), denote \mathbb{F} to be the forward state-input nonlinear operator such that $\mathbb{F}(x, u) \triangleq \begin{bmatrix} f(x, u) \\ S(u) \end{bmatrix}$, where S is the forward time-shift forward

operator. The infinite dimensional lifting function is expressed as $\Phi_{\text{inf}}(x, u) = [\phi_{1,\text{inf}}(x, u), \phi_{2,\text{inf}}(x, u), \dots]^T$. The Koopman operator \mathcal{K} is then defined as

$$\mathcal{K}[\Phi_{\text{inf}}(x, u)] \triangleq \Phi_{\text{inf}}(\mathbb{F}(x, u)), \quad (39)$$

that is, \mathcal{K} takes Φ_{inf} as the input and produces a new function whose value at (x, u) equals the value of the original observable evaluated at the state-input pair obtained by evolving (x, u) forward in time.

In practice, finite-dimensional approximations of the Koopman operator, as defined below, are often employed. Consider the class of lifting functions defined as

$$\phi_i(x, u) \triangleq \begin{bmatrix} \phi_i(x) \\ u \end{bmatrix} \quad i = 1, 2, \dots, n_z, \quad (40)$$

where each $\phi_i(x)$ is a scalar function of the state, and u is included in its original form to preserve control-affine structure. Typical examples of $\phi_i(x)$ include monomials (for polynomial lifting), radial basis functions, Fourier modes, or features learned by a neural network. Then, the high-dimensional observable is defined as $z \triangleq \Phi(x) \triangleq [\phi_1(x), \phi_2(x), \dots, \phi_{n_z}(x)]^T \in \mathbb{R}^{n_z}$, and the Koopman linear model of the nonlinear dynamics (3) can be written as

$$z^+ = Az + Bu \quad y = Cz + Du. \quad (41)$$

In discrete time, z^+ denotes the lifted state at the next time step, z_{k+1} , while in continuous time it denotes the time derivative \dot{z} .

Given trajectory data, data-driven methods such as Dynamic Mode Decomposition (DMD) (Rowley et al., 2009), Extended DMD (EDMD) (Williams et al., 2015), and Sparse Identification of Nonlinear Dynamics (SINDy) (Brunton et al., 2016) are commonly used to learn the Koopman operators and to design controllers Korda and Mezić (2018). Mauroy and Goncalves (2016); Haseli and Cortés (2023) improve the methods addressing accuracy and efficiency issues and Strässer et al. (2025) provides closed-loop guarantees. Neural networks can also be employed to learn the lifting functions in the Koopman operator framework (Yeung et al., 2019; Zinage and Bakolas, 2023; Hao et al., 2024).

While Koopman operator models can be trained to accurately approximate system behavior, control-relevant properties are not inherently guaranteed. To address this, efforts have been made to impose physics-informed and control-relevant constraints on Koopman operator models. Stability in learning the Koopman operator can be achieved by limiting the parameterization to Hurwitz matrices (Bevanda et al., 2022), or by establishing an equivalence between stability conditions on the Koopman model and contraction criteria, which can be embedded into constrained optimal control formulations (Fan et al., 2022, 2024; Wang et al., 2024). Alternatively, stability can be enforced by applying a suitable control barrier function or control Lyapunov function-based gradient descent during the iterative learning process (Mitjans et al., 2024; Huang et al., 2018).

Other control-relevant properties, such as quadratic dissipativity (Hara et al., 2020) and special structures like negative

imaginary properties (Mabrok et al., 2023), are typically embedded by deriving convex matrix inequality constraints that can be imposed during the Koopman identification. For example, consider identifying a nonlinear discrete-time dissipative system with no direct relationship between the lifted states and outputs (i.e., $D = 0$). Define the input, output, and lifted states sampled from dynamical trajectory data as

$$\begin{aligned} U_k &\triangleq [u(k), u(k+1), \dots, u(k+M-1)] \in \mathbb{R}^{n_u \times M} \\ Y_k &\triangleq [y(k), y(k+1), \dots, y(k+M-1)] \in \mathbb{R}^{n_y \times M} \\ Z_k &\triangleq [z(k), z(k+1), \dots, z(k+M-1)] \in \mathbb{R}^{n_z \times M} \\ Z_{k+1} &\triangleq [z(k+1), z(k+2), \dots, z(k+M)] \in \mathbb{R}^{n_z \times M}, \end{aligned} \quad (42)$$

where $n_u = n_y$ under the quadratic dissipativity constraints. In order to identify a Koopman operator model (41) parameterized by $\theta = (A, B, C, D)$, the cost function in (21) takes the form

$$c(\theta, \mathcal{W}) = c_1(A, B) + c_2(C),$$

where

$$c_1(A, B) \triangleq \left\| Z_{k+1} - [A \ B] \begin{bmatrix} Z_k \\ U_k \end{bmatrix} \right\|_F^2, \quad c_2(C) \triangleq \|Y_k - CZ_k\|_F^2. \quad (43)$$

Further, we can ensure that this model preserves dissipativity by solving (21) with hard constraints

$$g_1(\theta) = P > 0, \quad (44)$$

$$g_2(\theta) = \begin{bmatrix} A & B \\ I & 0 \end{bmatrix}^T \begin{bmatrix} P & 0 \\ 0 & -P \end{bmatrix} \begin{bmatrix} A & B \\ I & 0 \end{bmatrix} + \Theta < 0, \quad (45)$$

where

$$\Theta = \begin{bmatrix} C & 0 \\ 0 & I \end{bmatrix}^T \Xi \begin{bmatrix} C & 0 \\ 0 & I \end{bmatrix}, \quad \Xi = \begin{bmatrix} Q & S \\ S^\top & R \end{bmatrix}, \quad (46)$$

and Q, S, R are the dissipativity indices as in Definition 2.4. This approach of imposing hard constraints to preserve properties like dissipativity is similar to the methods described in Section 4.1.2. Another common practice is to use a soft constraint that penalizes the violation of the constraints as a part of the objective. We demonstrate such a soft-constraint based approach to enforce stability in Koopman operator identification in the following example.

Example 4.2 (Stable Koopman linear model identification for Duffing oscillator). Consider a Duffing oscillator with state $x(t) = [x_1(t), x_2(t)]^T \in \mathbb{R}^2$, input $u(t) \in \mathbb{R}$, and dynamics:

$$\dot{x}(t) = \begin{bmatrix} x_2(t) \\ -2x_2(t) - x_1(t) \cos(x_1(t) + x_2(t)) + u(t) \end{bmatrix}. \quad (47)$$

While the Duffing oscillator is defined in continuous time, we identify the Koopman model from data sampled every $\Delta t = 0.01$ s under zero-order hold on $u(t)$. The exact flow map is approximated using a fourth-order Runge–Kutta step. To build

a Koopman model, we define a lifting function $\psi : \mathbb{R}^2 \rightarrow \mathbb{R}^{2+N_{rbf}}$ and observables as follows:

$$z \triangleq \psi(x) = \begin{bmatrix} x \\ \phi(x) \end{bmatrix}, \quad \phi_j(x) = \text{rbf}(x, c_j), \quad j = 1, \dots, N_{rbf}, \quad (48)$$

where rbf is the thin-plate kernel with $\{c_j\}$ being centers randomly chosen from $[-1, 1]^2$. Here, we choose $N_{rbf} = 8$. With the discretized system, we generate N_{traj} trajectories of length M each, with initial states $x_0 \sim \mathcal{U}([-1, 1]^2)$ and control inputs $u_k \sim \mathcal{U}([-1, 1])$. Then we calculate the lifted states according to (48) to form U_k , Z_k and Z_{k+1} as in (42). With the Koopman model structure in (41), we define the reconstruction error to be $\|\mathcal{R}\|_F^2$, where \mathcal{R} is the long stacked vector of all \mathcal{R}_k from every time step k along each trajectory, with all trajectories concatenated, that is, there are $N_{traj}(M - 1)$ of \mathcal{R}_k in total. Each \mathcal{R}_k is formed from the quadruple (Z_k, U_k, Z_{k+1}, Y_k) at time step k as

$$\mathcal{R}_k = \begin{bmatrix} Z_{k+1} \\ Y_k \\ CZ_k + DU_k \end{bmatrix} - \begin{bmatrix} AZ_k + BU_k \\ CZ_k + DU_k \end{bmatrix}. \quad (49)$$

To enforce stability of the learned model, we desire the spectral radius of A to be smaller than 1. However, directly penalizing the spectral radius $\rho(A)$ yields a non-smooth, non-convex objective. As a practical convex surrogate for the upper bounds of $\rho(A)$, we instead impose a penalty on the operator 2-norm $\|A\|_2$. We enforce this penalty in the form of a soft constraint by solving the unconstrained optimization problem

$$\min_{A,B,C,D} c(\theta, \mathcal{W}) := \|\mathcal{R}\|_F^2 + \lambda \|A\|_2^2, \quad (50)$$

where $\lambda > 0$ is a hyper-parameter that balances model accuracy and stability. To make the problem more computationally tractable, we introduce slack variables τ and γ to transform the problem into a convex problem

$$(A_1^*, B_1^*, C_1^*, D_1^*, \gamma^*, \tau^*) = \underset{\text{argmin}_{A,B,C,D,\gamma,\tau}}{\text{argmin}} \|\mathcal{R}\|_F^2 + \lambda \tau^2, \\ \text{s.t. } \begin{bmatrix} \gamma I & A \\ A^\top & \gamma I \end{bmatrix} \geq 0, \quad \tau \geq \gamma, \quad \tau \geq 0, \quad (51)$$

We choose $\lambda = 200$ and solve (51) using the Mosek solver ([MOSEK ApS, 2025](#)). For comparison, we also obtain the Koopman model without soft constraints, we solve the problem

$$(A_2^*, B_2^*, C_2^*, D_2^*) = \underset{\text{argmin}_{A,B,C,D}}{\text{argmin}} \|\mathcal{R}\|_F^2 \quad (52)$$

To assess the performance of the identified Koopman model, we simulate the system dynamics and that of the learned model with initial condition $[-0.6, 1.4]^\top$ on the horizon $T = [0, 10]$ with time step $\Delta t = 0.01$ s (that is, total number of steps $M = 1000$). We set the test input to be

$$u(k) = 0.8 \sin(0.2 k), \quad k = 0, \dots, M - 1. \quad (53)$$

From Fig. 5, we can observe that the Koopman model with soft constraints is stable and closely approximates the true system trajectory, with the optimal solution $\rho(A_1^*) = 0.9958$, satisfying the stability condition. On the other hand, it is obvious that the Koopman model learned without the soft constraints diverges from the true dynamics and is in fact unstable with $\rho(A_2^*) = 1.0035$.

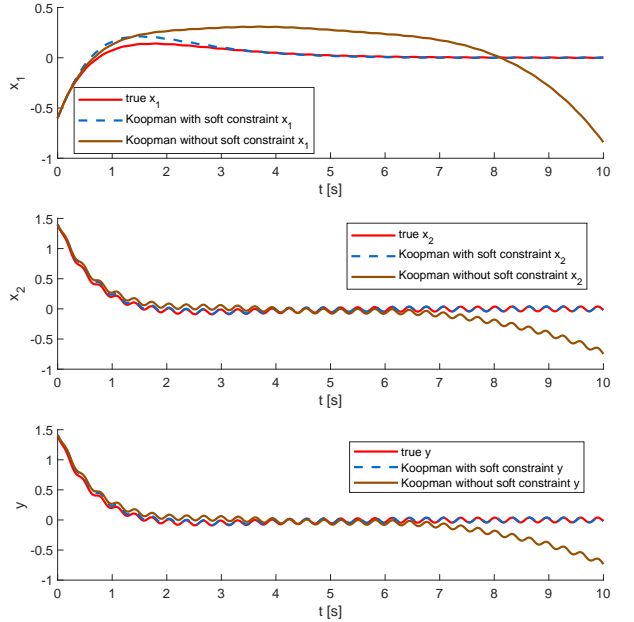


Figure 5: Koopman operator model with soft constraints vs Koopman Model without soft constraints vs ground truth for Example 4.2.

4.2.3. Sparse Identification of Nonlinear Dynamics (SINDy)

Recently, Sparse Identification of Nonlinear Dynamical systems (SINDy) ([Brunton et al., 2016](#)) has emerged as a widely-adopted data-driven method for nonlinear system identification. In many physical systems, the dynamics can be parameterized by a small number of nonlinear function terms, making the governing equations naturally sparse in the space of candidate nonlinear functions. The key idea in SINDy is to identify a sparse set of active terms from the candidate nonlinear function space by transforming the system identification problem into a sparse regression problem. Specifically, for a dynamical system for the state $x(t)$

$$\dot{x}(t) = f(x(t)), \quad (54)$$

the first step is to construct a library of candidate functions $\Theta(x) = [\theta_1(x), \dots, \theta_p(x)]$, where p is the number of candidates. The next step is to collect trajectory data of length M , defined as $X \triangleq [x(t_1), x(t_2), \dots, x(t_M)]^\top \in \mathbb{R}^{M \times n}$, $\Theta(X) \triangleq [\theta_1(X), \dots, \theta_p(X)] \in \mathbb{R}^{M \times np}$, and $\dot{X}(t) \triangleq [\dot{x}(t_1), \dot{x}(t_2), \dots, \dot{x}(t_M)]^\top \in \mathbb{R}^{M \times n}$. The autonomous dynamics (54) can then be modeled in terms of the candidate functions as

$$\dot{X}(t) \approx \Theta(X(t))\Xi, \quad (55)$$

where $\Xi = (\xi_1, \xi_2, \dots, \xi_n)$, and each ξ_k , $k \in \{1, 2, \dots, n\}$ is a sparse vector of coefficients that indicate the active terms. Sparsity is promoted by solving the following optimization problem

$$\min_{\Xi} \frac{1}{2} \|\dot{X} - \Theta(X)\Xi\|^2 + \lambda R(\Xi), \quad (56)$$

where $\lambda > 0$ and $R(\cdot)$ is a regularization term that promotes sparsity. The standard choices for R include the l_0 norm or

the l_1 norm, which is the convex relaxation of the l_0 norm. To solve the sparse regression problem, algorithms such as sequential thresholded least squares (STLSQ) (Brunton et al., 2016), LASSO (O’Brien, 2016), and the sparse relaxed regularized regression (SR3) (Champion et al., 2020) have been developed. There are also several variants that extend SINDy to other control-relevant settings. For example, implicit-SINDy (Mangan et al., 2016) is designed for rational dynamics, while integral-SINDy (Schaeffer and McCalla, 2017) deals with noise robustness using integrated rather than differentiated data. Further, SINDy with control (SINDyc) (Brunton et al., 2016) extends the framework beyond autonomous systems to enable identification with control inputs.

Recent work focuses on embedding prior knowledge to promote physics-informed properties such as Hamiltonian structures (DiPietro et al., 2020; Lee et al., 2022), energy conservation (Holmsen et al., 2023), and stability (Kaptanoglu et al., 2021). Due to the challenges associated with imposing the properties as hard constraints in the SINDy framework, the common practice is to use soft constraints, augmenting the objective function with a penalty term to encourage the desired physical behavior. As a representative example, we consider the ‘trapping SINDy’ framework (Kaptanoglu et al., 2021) that preserves system stability during identification. Trapping SINDy is particularly applicable to fluid and plasma flows with an energy-preserving, quadratic nonlinear structure. Using the standard Lyapunov function $V(x) = \frac{1}{2}\|x\|^2$, a sufficient condition for stability of the dynamics (54) is given by $x^\top f(x) = 0$. Since the vector field $f(x)$ is quadratic, the inner product of $x^\top f(x)$ is cubic polynomial. Therefore, we can eliminate the self-coupled cubic terms such as x_i^3 and impose an antisymmetric structure on cross terms of the form $x_i x_j^2$, so that their contributions are canceled. Such conditions, termed as energy-preserving quadratic nonlinearity constraints, ensure that only quadratic components of $x^\top f(x)$ remain. These conditions can be collectively expressed as a set of linear equality constraints, compactly denoted as $r(\Xi) \triangleq \mathcal{R}vec(\Xi) = 0$, where \mathcal{R} is an appropriate constant matrix and $vec(\Xi)$ is the vectorized form of Ξ . Then, we can obtain a stable nonlinear system model of the form (55) by solving the following optimization problem:

$$\min_{\Xi} \frac{1}{2}\|\dot{\Xi} - \Theta(X)\Xi\|_F^2 + \lambda\|\Xi\|_1 + \alpha\|r(\Xi)\|_2^2, \quad (57)$$

where $\lambda > 0$ and $\alpha > 0$ weight the sparsity of the model and the stability preservation conditions respectively, and can be suitably adjusted to balance accuracy, sparsity, and physically consistent behavior. Several simulation examples illustrating this approach for concrete examples such as the atmospheric oscillator model and the Lorenz system are available in Kaptanoglu et al. (2024).

4.2.4. Port-Hamiltonian Models

Port-Hamiltonian (PH) dynamics have been increasingly used in recent years as a unified formulation for energy-based modeling of systems (Ortega et al., 2001; van der Schaft, 2004; van der Schaft and Jeltsema, 2014; Beattie et al., 2018, 2019; Mehrmann and Unger, 2023). PH systems theory observes

that any physical system can be modeled by energy-storing elements (capacitors, inductors, masses, springs, etc.) and energy-dissipating elements (resistors, dampers, etc.), linked to each other by power-conserving connections, called a Dirac structure. The Dirac structure links flow variables, which quantify the rate of energy transfer (e.g., current, velocity), and effort variables, which quantify the potential for energy transfer (e.g., voltage, force), such that the total power (product of flow and effort variables) is equal to zero.

A standard example of a Dirac structure is the graph of a skew-symmetric map from the effort to the flow variables. PH models used for control have input u representing external effort variables, output y representing external flow variables, and skew-symmetric relationship between the storage, dissipation, and external port variables (see van der Schaft (2024) for details), leading to an input-state-output PH system:

$$\begin{aligned} \dot{x} &= (J(x) - R(x))\nabla H(x) + G(x)u, \\ y &= G^\top(x)\nabla H(x), \end{aligned} \quad (58)$$

where $H(x)$ is the Hamiltonian representing the total energy of the system, $J(x)$ is a skew-symmetric interconnection matrix, $R(x)$ is a symmetric positive semidefinite dissipation matrix, and $G(x)$ is an input gain matrix.

A key property is that any power-conserving interconnection of PH systems is again a PH system. More precisely, if PH systems are interconnected, via their external ports, through a Dirac structure, then we obtain a joint PH system with energy given by the sum of the individual Hamiltonians, energy dissipation relation equal to the direct product of the individual dissipation relations, and Dirac structure given by the composition of the individual Dirac structures.

The increase in stored energy of a PH system is less than or equal to the externally supplied power, which means that the system is passive with respect to the supply rate. PH systems may possess other conserved quantities, primarily determined by their Dirac structures. Conserved quantities which are independent of the Hamiltonian are called Casimir functions $C(x)$. They satisfy $\frac{\partial C}{\partial x}(x)^\top(J(x) - R(x)) = 0$ and can be used to construct candidate Lyapunov functions for the system (Ortega et al., 1999, 2008; Xu et al., 2022).

Various methods have been proposed for identification of PH system models. Branford and Rapisarda (2019) use energy conservation and power flows to identify linear time-varying PH systems from input-output data. They show that minimal state trajectories can be obtained from a rank-revealing factorization of an energy matrix, obtained by integrating the power balance of the effort and flow trajectories. Benner et al. (2020) obtain PH realizations of strictly passive systems from frequency response data using the Loewner approach for model reduction (Mayo and Antoulas, 2007) to enforce a PH structure on the model. Ortega and Yin (2024) propose a structure-preserving learning scheme for single-input single-output linear PH systems with n states. The paper establishes morphisms between controllable and observable linear systems and normal form PH systems. The set of uniquely identifiable PH systems is characterized as a manifold with global Euclidean coordinates and the

parameter complexity for representing such systems is shown to be $O(n)$ instead of $O(n^2)$. Thus, the paper shows interesting connections between controllable and observable canonical forms and the structure-preservation and expressive power properties of the machine learning model.

The benefits of PH system models on learning and adaptive control are reviewed in [Nageshrao et al. \(2016\)](#) with emphasis on speeding up learning via the prior knowledge of the PH structure, obtaining stability or convergence guarantees via the PH model, and interpreting the resulting control laws in the context of physical systems. Model reduction techniques that preserve PH structure as well as stabilization and optimal control of PH systems are discussed in [Mehrmann and Unger \(2023\)](#). Interconnection and damping assignment (IDA) passivity-based control (PBC) ([van der Schaft and Jeltsema, 2014](#)) is a widely used method for stabilizing PH systems using the system input to inject energy and reshape the total energy of the closed-loop system such that its minimum is at a desired equilibrium. [Plaza et al. \(2022\)](#) transform the IDA-PBC method into a supervised learning problem by designing loss functions that capture desirable properties, including prescribed damping, minimum oscillation, assignment of the desired equilibrium, Lyapunov stability, and enforcement of matching conditions ensuring that the desired closed-loop system is obtained. Further examples of applying deep learning methods for identification and control of PH systems are discussed in Sec. 5.2.2.

4.2.5. Gaussian Process Models

Nonlinear system identification can also be approached using Gaussian process (GP) regression ([Rasmussen and Williams, 2006](#)). The book by [Kocijan \(2016\)](#) presents techniques for learning and validating GP dynamics models from measurement data, for embedding prior knowledge into the GP models, and for designing optimal control, model predictive control, and adaptive control based on the GP dynamics models.

A GP is a stochastic process, that is, a collection of random variables indexed by time or space, such that any finite subset of the random variables has a joint Gaussian distribution. This can be viewed as a distribution $\mathcal{GP}(\mu(z), k(z, z'))$ for a function $f(z)$ with mean function $\mu(z) = \mathbb{E}[f(z)]$ and covariance function (or kernel) $k(z, z') = \text{Cov}[f(z), f(z')]$.

Consider a regression problem:

$$y_k = f(z_k) + \epsilon_k, \quad \epsilon_k \sim \mathcal{N}(0, E), \quad (59)$$

where the objective is to approximate the function $f(z)$ given a dataset $\mathcal{D} = \{z_k, y_k\}_k$ of Gaussian noisy measurements with zero mean and covariance E . The GP approach to regression imposes a GP prior distribution on $f(z)$ and computes the posterior of $f(z)$ conditioned on the data \mathcal{D} . The values $f(Z^*) = [f(z_1^*)^\top \cdots f(z_M^*)^\top]^\top$ of the function $f(z)$ at a set of query points Z^* are predicted by using that the observations $Y = [y_1^\top \cdots y_N^\top]^\top$ in the dataset and the query function values $f(Z^*)$ have a joint Gaussian distribution:

$$\begin{bmatrix} Y \\ f(Z^*) \end{bmatrix} \sim \mathcal{N}\left(\begin{bmatrix} \mu(Z) \\ \mu(Z^*) \end{bmatrix}, \begin{bmatrix} k(Z, Z) + I \otimes E & k(Z, Z^*) \\ k(Z^*, Z) & k(Z^*, Z^*) \end{bmatrix}\right), \quad (60)$$

where \otimes is the Kronecker product and Z are the locations where the training observations Y were obtained from. Then, the posterior distribution of $f(Z^*)$ conditioned on the dataset \mathcal{D} (of observations Y and locations Z) is obtained as the conditional distribution from the above joint distribution. Specifically, $f(Z^*) | \mathcal{D}$ has a GP distribution mean function:

$$\mu(Z^*) + k(Z^*, Z)(k(Z, Z) + I \otimes E)^{-1}(Y - \mu(Z)) \quad (61)$$

and kernel:

$$k(Z^*, Z^*) - k(Z^*, Z)(k(Z, Z) + I \otimes E)^{-1}k(Z, Z^*). \quad (62)$$

In system identification ([Särkkä, 2021](#)), GPs are used to form time series predictions (e.g., impulse response or autoregressive models) or directly represent the dynamics model and output model of a state-space representation (3).

[Pillonetto et al. \(2014\)](#) use GP regression to model the impulse response $g(t)$ in (7) of LTI systems. Given input-output data, the impulse response is inferred via the posterior mean of a GP, with hyperparameters (kernel parameters and noise variance) estimated by maximizing the marginal likelihood. To guarantee BIBO stability of the identified model, the kernel should be absolutely integrable, $\int \int |k(t, t')| dt dt' < \infty$, which ensures that the impulse response $g(t)$, estimated by the GP mean, is almost surely integrable. The authors show that commonly used stationary kernels, such as the Gaussian (RBF) or spline kernels, fail to meet this criterion but can be modified via exponential or algebraic decay terms to ensure integrability and, hence, BIBO stability of the impulse response estimates.

A GP model can also be used to learn a state-space model (3) directly using input-output data. [Frigola et al. \(2013, 2014\)](#) model the dynamics f as a sparse GP with inducing points and the output model h as a parametric density (e.g., Gaussian or Poisson), and optimize the model parameters via variational inference. A joint variational distribution is specified over the inducing points, (latent) states, and state transitions and a particular factorization is chosen to make the Evidence Lower Bound (ELBO) computationally efficient. [Eleftheriadis et al. \(2017\)](#) assume that the state posterior has a Markov-structured Gaussian distribution and introduce a bi-directional recurrent neural network to facilitate smoothing of the state posterior over the data sequences and recovery of the variational parameters. In closely related work, [Doerr et al. \(2018\)](#) propose an improved factorization, which captures the true system transitions, and compute the ELBO stochastic gradients analytically via the reparametrization trick. These methods are demonstrated to learn dynamics models of neural activity in rats' hippocampus, of a hydraulic actuator that controls a robot arm, and of a belt-driven pulley with two electric motors.

State-space GP models can also be used to ensure stability. [Berkenkamp et al. \(2016\)](#) introduce a residual GP model to capture uncertainty in a nominal dynamics model and estimate the region of attraction (RoA) of the closed-loop system under a fixed control policy. A Lyapunov function is used to certify a subset of the RoA by verifying that its derivative remains negative with high probability, given the GP uncertainty. The

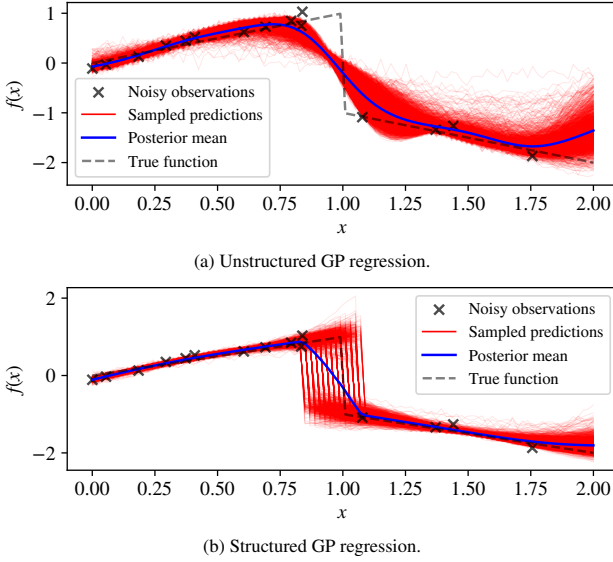


Figure 6: Learning a piecewise-linear dynamics function f via GPJax (Pinder and Dodd, 2022) with structured GP regression (b) is more accurate than with unstructured GP regression (a).

method iteratively expands the certified RoA by actively selecting new states near the boundary, updating the GP model, and recomputing the RoA without leaving the certified safe region. In subsequent work, Berkenkamp et al. (2017) extended the approach to allow modifying the control policy to achieve optimal stabilization performance, captured by a cumulative cost function, while maintaining stability guarantees.

GP regression can be used to approximate an explicit control law for model predictive control (Grancharova et al., 2007; Binder et al., 2019; Hewing et al., 2020). For example, Rose et al. (2023) use a sampling-based scenario approach to provide bounds on the approximation errors and ensure recursive feasibility and input-to-state stability. Beyond model predictive control, recent work (Wang et al., 2018; Castañeda et al., 2021; Long et al., 2022; Dhiman et al., 2023) has extended the types of safety and stability guarantees for controllers synthesized from GP system models by considering worst-case and probabilistic formulations of control Lyapunov function and control barrier function constraints to account for the presence of model uncertainty.

In connection with Sec. 4.2.4, GP regression can be used to learn Lagrangian and port-Hamiltonian system models (58) from state-input data. Evangelisti and Hirche (2022) introduce a physically constrained formulation of GP regression to respect the structure of Lagrangian systems and guarantee energy conservation. This requires extending the GP kernel to symmetric matrix spaces and using Cholesky decomposition to provide probabilistic guarantees that the energy GP has positive-definite quadratic form. Subsequent work by Evangelisti and Hirche (2024) integrates the Lagrangian GP model into covariance-adaptive momentum observers to enable learning-based external force and disturbance estimation. The GP prediction error bounds are used to establish exponential stability guarantees for the observer. Regarding Hamiltonian systems, Beckers

et al. (2022) and Beckers (2023) formulate a joint GP over the Hamiltonian and its partial derivatives and use a specific matrix kernel to guarantee that the GP almost surely generates valid port-Hamiltonian trajectories. As in the deterministic case, the interconnection of two GP port-Hamiltonian systems remains a GP port-Hamiltonian system. The approach is demonstrated to learn the dynamics of an iron ball in the magnetic field of a controlled inductor. The results show that training a GP whose kernel does not capture the port-Hamiltonian system structure requires ten times more samples compared to a GP that does.

Several modern GP libraries designed for large-scale inference with GPU acceleration are available, including GPyTorch (Gardner et al., 2018), GPflow (Matthews et al., 2017), Pyro (Bingham et al., 2019), and GPJax (Pinder and Dodd, 2022). For example, GPJax (Pinder and Dodd, 2022) allows us to learn a dynamics function f from data more accurately by incorporating prior knowledge of the system in a GP regression model in JAX, as shown in Example 4.3.

Example 4.3 (Learning dynamics using GP regression). Consider learning a piecewise-linear system:

$$y = f(x) = \begin{cases} ax, & \text{if } x \leq x_{th}, \\ bx, & \text{if } x > x_{th}, \end{cases} \quad (63)$$

where the ground-truth parameters are $a = 1$, $b = -1$, $x_{th} = 1$. A dataset of 15 pairs (x, y) is generated from the ground-truth dynamics to train standard (unstructured) and structured GP regression models, implemented in GPJax (Pinder and Dodd, 2022). While the unstructured GP model does not assume any prior knowledge of the system, the structured GP model encodes the piecewise-linearity of the dynamics f by replacing the constant mean of an unstructured GP with (63). The unknown parameters a , b and x_{th} in (63) are then trained to fit the data, leading to better prediction accuracy as shown in Fig. 6.

5. Deep Learning-based System Identification

Deep learning for system identification is usually formulated as a supervised learning problem. Recall that in a system identification problem, we are given a dataset $\mathcal{W} = \{(u_{i,k}, y_{i,k})\}_i$ of input-output trajectories from a continuous-time dynamical system. We seek to learn a nonlinear state-space model with dynamics f_θ and output model h_θ , where the model parameters θ is obtained from the unconstrained optimization (14) or the constrained system identification problem (21). For fitting of the deep learning based system ID models, discretely sampled data from the continuous-time system is often assumed. Some methods assume access to not only the input-output trajectories, but also the state trajectories thus $\mathcal{W}^+ = \{(x_{i,k}, u_{i,k}, y_{i,k})\}_i$, which we will discuss in context. We will start with reviewing common model choices for system identification from classic deep learning architectures (e.g., feedforward neural networks, recurrent neural networks) to physics-informed deep learning architectures (e.g., neural ordinary differential equations, recurrent equilibrium networks), and then surveying recent literature on incorporating control-relevant system properties into deep learning models.

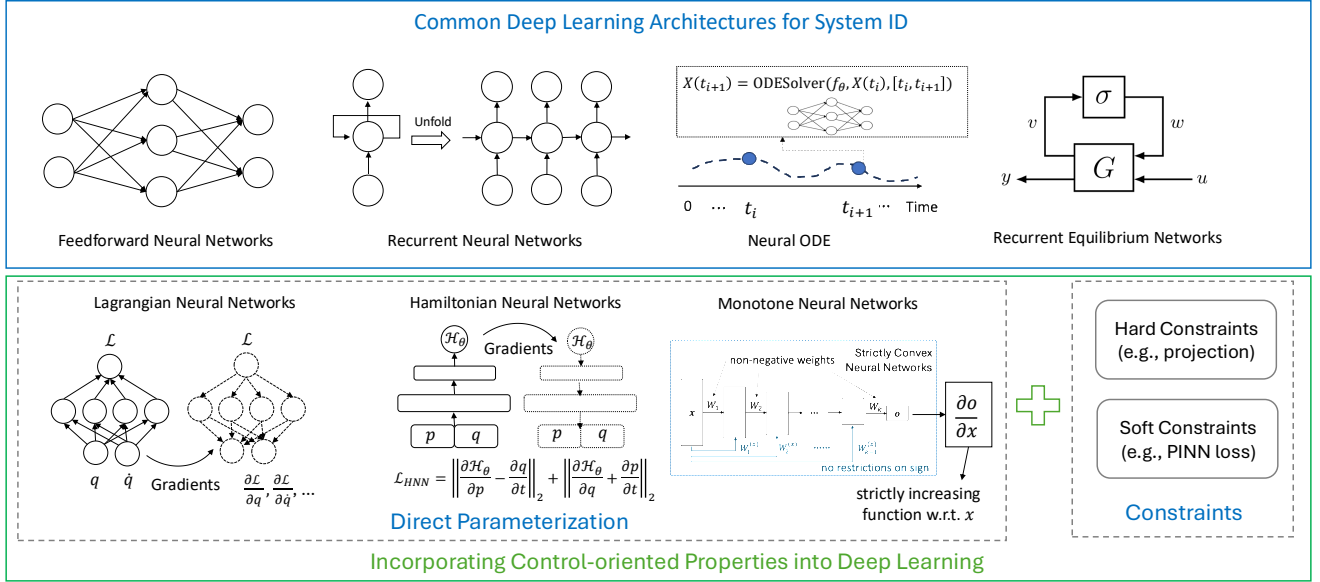


Figure 7: Overview of the deep learning architectures and control-oriented architectures for system identification.

5.1. Deep Learning Architectures for System Identification

5.1.1. Feedforward Neural Networks

One basic model for fitting the functions $\{f_\theta, h_\theta\}$ is via an n -layer feedforward neural network (FNN). The feedforward neural network (FNN) approach assumes access to the true system state $x_{i,k}$ and models the state-transition and output mappings as

$$\begin{aligned}\hat{x}_{i,k+1} &= f_\theta(x_{i,k}, u_{i,k}) := \text{FNN}_1(x_{i,k}, u_{i,k}), \\ \hat{y}_{i,k} &= h_\theta(x_{i,k}, u_{i,k}) := \text{FNN}_2(x_{i,k}, u_{i,k}).\end{aligned}\quad (64)$$

Each FNN consists of $L \in \mathbb{N}^+$ hidden layers that is defined as,

$$\text{FNN}(\xi) := (l_L \circ l_{L-1} \circ \dots \circ l_1)(\xi),$$

where layers l_i start with the input layer $l_0 = \xi$ and continue as

$$l_{i+1}(l_i, \theta_{i+1}) = \sigma(W_{i+1}l_i + b_{i+1}), \quad i = 0, \dots, L-1.$$

σ is a nonlinear activation function, weights W_{i+1} and biases b_{i+1} are parameters in the neural network to be learned, collected into θ_i , and then into $\theta = [\theta_1^\top, \dots, \theta_L^\top]^\top$. It has been shown that, the FNN has universal approximation capability (Hornik et al., 1989), thus is able to model almost all systems with continuous f_θ, h_θ over a compact set. The model parameters f_θ, h_θ are optimized to minimize the error between predictions and the true state $x_{i,k+1}$ and output $y_{i,k}$.

Applications of FNN for system identification have been found in literature since the 90s (Kuschewski et al., 1993; Lu and Basar, 1998). Nagabandi et al. (2018) deploys an FNN to model the robotics dynamics, which is further used for model-based reinforcement learning. Recent applications of FNN for system identification include various robotic and mechanical systems (Gillespie et al., 2018; Pan and Duraisamy, 2018; Shi et al., 2019; Robinson et al., 2022; Ramírez-Chavarría and Schoukens, 2021; Wei and Liu, 2022). However, the formulation provided above requires direct access to the full input-state-output trajectories \mathcal{W}^+ , which may not be available or

observable in many real-world systems. We refer to a recent survey for more recent literature on FNN for system identification (Pillonetto et al., 2023).

5.1.2. Recurrent Neural Networks and Transformers

While FNNs can approximate input-output mappings, they lack an explicit mechanism for handling temporal dependencies, which limits their ability to capture system dynamics over time. Recurrent Neural Networks (RNNs) address this limitation by maintaining a hidden state that evolves over time, making them particularly well-suited for modeling dynamical systems. Specifically, for all $k = 1, \dots, T$, the RNN evolves as

$$\hat{x}_{i,k+1} = f_\theta(\hat{x}_{i,k}, u_{i,k}) := \sigma(W_{hh}\hat{x}_{i,k} + W_{hx}u_{i,k} + b_h), \quad (65a)$$

$$\hat{y}_{i,k} = h_\theta(\hat{x}_{i,k}, u_{i,k}) := \sigma(W_y\hat{x}_{i,k} + b_y), \quad (65b)$$

where σ denotes a nonlinear activation function, and the weight matrices W_{hh}, W_{hx}, W_y and biases b_h, b_y are model parameters to be learned. Compared to FNNs, RNNs introduce a hidden state that evolves over time, enabling the model to infer and maintain internal representations of system dynamics from sequences of input-output data alone. This makes RNNs particularly advantageous for system identification tasks where only input-output trajectories $(u_{i,k}, y_{i,k})$ are available.

To improve the capability of RNNs to capture long-term dependency of system trajectories, features such as Long Short-Term Memory (LSTM) (Hochreiter and Schmidhuber, 1997) and Gated Recurrent Units (GRUs) (Chung et al., 2014) can be adopted. Deep RNNs (Pascanu et al., 2013) further improve RNN for replacing the learnable matrices with deep neural networks. Like FNNs, RNNs have shown to be *universal function approximators* in Sontag (1992); Funahashi and Nakamura (1993). More recent theoretical developments (Hanson and Raiginsky, 2020; Hanson et al., 2021) provide quantitative error

guarantees, specifying the sample size and neurons to reach a desired accuracy.

Given the advanced modeling capabilities of RNNs for dynamical systems, it is not surprising that they are popular choices for system identification and control. Early applications of RNNs and their variants for system identification can be found in [Delgado et al. \(1995\)](#); [Wang and Chen \(2006\)](#); [Wang \(2017\)](#). The identified models can be used for decision making and control ([Pan and Wang, 2011](#)). Notable recent advances include convex RNNs ([Chen et al., 2018b](#)) for system identification, thus leading to a convex model predictive control (MPC) problem with optimality guarantee. For interested readers, we refer to [Bonassi et al. \(2022\)](#) for a recent survey of RNN models for system identification and learning-based control.

As an emerging direction, Transformer networks ([Vaswani et al., 2017](#)) are considered a promising alternative to RNNs for sequence modeling and system identification. [Geneva and Zabaras \(2022\)](#) proposes to apply the self-attention Transformers for physical dynamics modeling, which allows the model to learn longer and more complex temporal dependencies with Koopman-based embedding. For spatiotemporal dynamics, [Han et al. \(2022\)](#) incorporates a graph-based method for the spatial relationships and the Transformer for temporal dynamics. [Park et al. \(2023\)](#) customizes the Transformer for model predictive control, where the Transformers are implemented for multistep-ahead prediction. Besides modeling ODE systems, Transformers have recently emerged as a promising tool for surrogate modeling of partial differential equations (PDEs) ([Li et al., 2023](#)). Because of its good performance, Transformers are widely adopted for different applications such as traffic flow ([Xu et al., 2020; Reza et al., 2022](#)), fluid flow ([Solera-Rico et al., 2024; Hassanian et al., 2023](#)), mechatronic systems ([Ayankoso and Olejnik, 2023](#)), and etc.

5.1.3. Neural Ordinary Differential Equations (Neural ODEs)

One challenge with RNN is that as the trajectory length increases, it requires propagating information over long horizons. Thus, RNNs could lead to high computational cost and difficulties in training. [Chen et al. \(2018a\)](#) introduce neural ODEs that describe the system dynamics as $\dot{\hat{x}}_i(t) = f_\theta(\hat{x}_i(t), u_i(t))$ in the original continuous-time domain,

$$\hat{x}_i(t+1) = \hat{x}_i(t) + \int_{\tau=t}^{t+1} f_\theta(\hat{x}_i(\tau), u_i(\tau)) d\tau, \quad (66a)$$

$$\hat{y}_i(t) = h_\theta(\hat{x}_i(t), u_i(t)), \quad (66b)$$

where f_θ, h_θ are commonly modeled via FNNs. We can view Neural ODEs as introducing the structure of differential equation as a part of prior knowledge about the problem (a.k.a., inductive bias in machine learning). Starting with $\hat{x}_i(t)$ at time t , the state at time $t+1$ is obtained by integrating the neural network f_θ over $[t, t+1]$. The integral in (66a) has to be solved numerically, and can be expensive since the dynamics are modeled as neural networks. Follow-up works ([Quaglino et al., 2020; Kelly et al., 2020; Dupont et al., 2019; Biloš et al., 2021](#)) focus on retaining expressive dynamics at less computational cost. [Zhu et al. \(2021\)](#) proposes neural delay differential

equations, that can be used to learn dynamical systems with delays. [Chen et al. \(2021a\)](#) proposes neural event functions to include discrete events (e.g. switches) in the continuous-time dynamics modeling. To understand the representation capability of Neural ODE, [Ruiz-Balet and Zuazua \(2023\)](#) establishes universal approximation guarantees for ODEs.

For applications, [Quaglino et al. \(2020\)](#) incorporates the spectral element methods with Neural ODEs for fast and accurate system identification, where the dynamics are interpreted as truncated series of Legendre polynomials. To improve generalization, physics-informed design is widely adopted in design of Neural ODEs. For example, [Zhong et al. \(2019\)](#) incorporates the prior knowledge of Hamiltonian dynamics. [Hochlehnert et al. \(2021\)](#) deploys a Central-Difference Lagrange integrator structure for modeling contact dynamics using Neural ODEs. More examples incorporating control-oriented properties are deferred to sections 5.3 and 5.4. Following the benchmark result of ([Rahman et al., 2022](#)), Neural ODEs have shown good performance in system identification, and have been successfully applied in structural identification ([Lai et al., 2021](#)), power systems ([Xiao et al., 2022](#)), robotics ([Huang et al., 2023; Xiao et al., 2023](#)) etc. Another interesting deep learning architecture sharing a similar structure as Neural ODE is the Deep Equilibrium (DEQ) model, which finds a fixed point of a dynamical system corresponding to a neural network ([Bai et al., 2019](#)). [Winston and Kolter \(2020\)](#) extends DEQ by restricting the mapping to be monotone, which guarantees the existence of a unique equilibrium point.

5.1.4. Recurrent Equilibrium Networks

A Recurrent Equilibrium Network (REN) ([Revay et al., 2023](#)) is a flexible model structure that incorporates both a recurrent structure and an equilibrium network. It was introduced to include many established models as special cases, such as FNNs and RNNs. Specifically, REN is given in the following form,

$$\begin{aligned} \hat{x}_{k+1} &= A\hat{x}_k + B_1 w_k + B_2 u_k + b_x, \\ \hat{y}_k &= C_2 \hat{x}_k + D_{21} w_k + D_{22} u_k + b_y, \end{aligned} \quad (67)$$

in which w_k is the solution of an equilibrium network DEQ

$$w_k = \sigma(D_{11}w_k + C_1\hat{x}_k + D_{12}u_k + b_v),$$

A, B, C, D are matrices of appropriate dimension, $b_x \in \mathbb{R}^n, b_y \in \mathbb{R}^p, b_v \in \mathbb{R}^q$ are bias parameters, and σ is a nonlinear activation function. REN models can also be represented as a feedback interconnection of a linear system G (composed of matrices A, B, C, D) and a memoryless nonlinear operator σ , as depicted in Figure 7.

RENs can incorporate built-in guarantees of stability and robustness through either convex or direct parameterization to satisfy sufficient conditions for contractive models and incremental dissipativity. Convex parameterization introduces multipliers to add degrees of freedom, making the model parameters, stability certificate, and multipliers jointly convex. Direct parameterization maps the convex region to a set of free parameters, turning the problem into unconstrained optimization. The

resulting parameters are guaranteed to be well-posed, ensuring the model generates unique state trajectories for any input and initial condition. While RENs model discrete-time dynamics, NodeRENs (Martinelli et al., 2023) extend the framework to continuous-time systems by combining RENs with Neural ODEs. Like RENs, NodeRENs are contractive and dissipative by design and allow training via unconstrained optimization.

5.1.5. Incorporating Control-oriented Properties

As discussed in Section 3.3, there are three common ways of incorporating structures into system identification: *direct parametrization*, *hard constraints*, *soft constraints*. In the next subsections, we will survey deep learning based system identification literature falling under each kind. We start from the direct parametrization with three examples on Lagrangian Neural Networks, Hamiltonian Neural Networks, and Monotone Neural Networks. We then survey ways of incorporating structure as hard constraints and soft constraints, respectively. We end the discussion by comparing hard and soft stability constraints in a learning pendulum dynamics example.

5.2. Direct Parametrization

5.2.1. Lagrangian Neural Networks

Consider the Lagrangian dynamics of a rigid-body system expressed as

$$M(q)\ddot{q} + C(q, \dot{q})\dot{q} + G(q) = \tau, \quad (68)$$

where $q \in \mathbb{R}^n$ represents generalized coordinates, $M(q)$ is the inertia matrix, $C(q, \dot{q})$ is the Coriolis matrix, $G(q)$ denotes conservative forces (e.g., gravity), and τ is the non-conservative control input. To put the Lagrangian dynamics in the standard state-space representation, one could define the state vector $x = (q, \dot{q}) \in \mathbb{R}^{2n}$, and rewrite the dynamics as

$$\begin{aligned} \dot{x}_1 &= x_2, \\ \dot{x}_2 &= M^{-1}(x_1)(\tau - C(x_1, x_2)x_2 - G(x_1)), \end{aligned}$$

so that the overall system dynamics are represented as $\dot{x} = f(x, u)$, consistent with Eq. (3). The system output is modeled as $y = h(x, u)$, where y may represent partial observations such as positions q , velocities \dot{q} , or both.

Instead of directly parameterizing the system dynamics f and output function h as neural network, Roehrl et al. (2020) parametrizes the force term as a neural network $\tau(x, u; \theta)$ with inputs $x = (q, \dot{q})$, control input u , and parameters θ . Given a dataset of trajectories $\mathcal{D} = \{(u_i, y_i)\}_{i=1}^N$, a one-step 4th-order Runge-Kutta method is used to integrate the dynamics and generate predicted trajectories $\hat{\mathcal{D}} = \{(\hat{y}_i)\}_{i=1}^N$. The neural network is trained by minimizing the discrepancy between the observed and predicted outputs, i.e., y_i and \hat{y}_i . Instead of modeling τ as a neural network, Lutter et al. (2018) models $M(q) = L(q)L(q)^\top$ and $G(q)$ as neural networks and represented $C(q, \dot{q})$ in terms of $L(q)$. The approximated inverse dynamics is compared with τ from the dataset to train the models. This approach avoids the need of an ODE solver but requires \ddot{q} in the dataset.

The Lagrangian neural networks in Cranmer et al. (2020) further extend the above methods to general Lagrangian dynamics beyond the rigid-body dynamics in (68). Cranmer et al. (2020) also illustrates that the Lagrangian neural networks can handle systems with disconnected coordinates such as graphs. In terms of controller design based on learned Lagrangian dynamics model, Lutter et al. (2019) designs an energy-based controller for a class of simple under-actuated systems such as Furuta pendulums, cartpoles, and acrobots. In Gupta et al. (2019), the learned Lagrangian dynamics model is used to plan a trajectory using Direct Collocation trajectory Optimization and design a time-varying linear quadratic regulator controller to track the trajectory.

5.2.2. Hamiltonian Neural Networks

Consider the Hamiltonian dynamics of the form,

$$\frac{dq}{dt} = \frac{\partial H}{\partial p}, \frac{dp}{dt} = -\frac{\partial H}{\partial q}, \quad (69)$$

where $q \in \mathbb{R}^n$ and $p \in \mathbb{R}^n$ are the generalized coordinates and momentum of a system. H denotes the total energy of the system, and the Hamilton's equations of motion (69) guarantees that $\frac{dH}{dt} = 0$, i.e. the total energy is conserved along the trajectory. To express the Hamiltonian dynamics in the standard state-space form consistent with Eq. (3), one can define the state vector $x = (q, p) \in \mathbb{R}^{2n}$ and write the dynamics as $\dot{x} = f(x) = J\nabla_x H(x)$. With control inputs, the Hamiltonian dynamics can be modified by an additional forcing term that influences the state evolution by injecting or dissipating energy.

Hamiltonian Neural Networks (HNNs) (Greydanus et al., 2019) parametrize the conserved energy function $\mathcal{H}(q, p; \theta)$ rather than directly learning the system dynamics f . By enforcing the Hamiltonian structure, HNNs provide a principled way to embed hard physical constraints such as energy conservation into the learned model. The training loss of HNN follows

$$c_{HNN}(\theta) = \left\| \frac{dq}{dt} - \frac{\partial \mathcal{H}_\theta}{\partial p} \right\|_2 + \left\| \frac{dp}{dt} + \frac{\partial \mathcal{H}_\theta}{\partial q} \right\|_2,$$

where θ are parameters of the HNN. Bertalan et al. (2019) extends the HNN approach to handle observations of the coordinates q and momentum p from images. The Hamilton's dynamics are modeled using a neural network on a latent space, learned from the observations using an auto-encoder. The auto-encoder and the Hamiltonian dynamics model are trained simultaneously to minimize loss function $c_{HNN}(\theta)$.

Hamiltonian-based models require the second-order derivation of the coordinates q . Chen et al. (2019) explores the use of a leapfrog integrator parameterized by a recurrent neural network to get rid of the need of taking the second-order derivatives. On the same vein, Zhong et al. (2019) uses neural ODEs with Hamiltonian structure to approximate the unknown dynamics. Finzi et al. (2020) shows that it is better, in terms of accuracy and data efficiency, to learn the Lagrangian and Hamiltonian dynamics with Cartesian coordinates with explicit manifold constraints instead of generalized coordinates.

In terms of controller design based on learned Hamiltonian dynamics model, Zhong et al. (2019) designs an energy-shaping regulation controller for fully-actuated systems based on the learned dynamics. Duong and Atanasov (2021) considers first learning Hamiltonian dynamics on $\text{SE}(3)$ manifold (short for Special Euclidean group in three dimensions, describing rigid body transformations combining rotation and translation in 3D space), that encodes Hamiltonian dynamics and the $\text{SE}(3)$ manifold constraints on a neural ODE network. This is suitable for learning the dynamics of single-rigid-body robots such as ground vehicles and quadrotors, where the orientation is often described by a rotation matrix on the $\text{SO}(3)$ manifold (short for Special Orthogonal group in three dimensions, represents all 3×3 rotation matrices that describe rotations in three-dimensional Euclidean space). An energy-based controller is then designed for trajectory tracking tasks for both fully and under-actuated systems such as quadrotors.

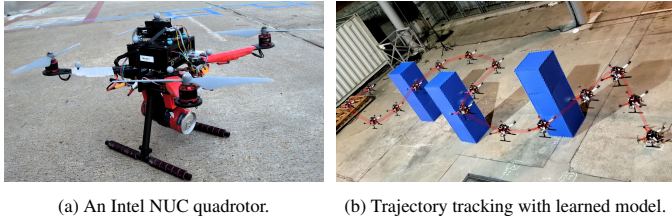


Figure 8: Real experiments with $\text{SE}(3)$ port-Hamiltonian neural ODE network Duong et al. (2024b).

Example 5.1 (Quadrotor Dynamics Identification using Port-Hamiltonian Neural ODE Network). *To illustrate a Hamiltonian neural network for system identification, we provide an example from Duong et al. (2024b) where both Hamiltonian structure and the state manifold constraints are encoded in the neural network architecture. Consider a mobile robot, e.g., a quadrotor, with its generalized coordinate $q = (z, R) \in \text{SE}(3)$ consisting of its position $z \in \mathbb{R}^3$ and orientation $R \in \text{SO}(3)$. Let $\zeta = (v, \omega) \in \mathbb{R}^6$ be the generalized velocity, consisting of the body-frame linear velocity $v \in \mathbb{R}^3$ and the body-frame angular velocity $\omega \in \mathbb{R}^3$. The generalized momentum is defined as $p = \begin{bmatrix} p_v \\ p_\omega \end{bmatrix} = M(q)\zeta \in \mathbb{R}^6$, where $M(q)$ is the generalized mass of the system, p_v is the linear momentum, and p_ω is the angular momentum. The Hamiltonian function is defined as the total energy of the system $H(q, p) = \frac{1}{2}p^\top M^{-1}(q)p + V(q)$ where $T = \frac{1}{2}p^\top M^{-1}(q)p$ is the kinetic energy and $V(q)$ is the potential energy.*

The equations of motions on the $\text{SE}(3)$ manifold are written

in port-Hamiltonian form as:

$$\dot{x} = R \frac{\partial H(q, p)}{\partial p_v}, \quad (70a)$$

$$\dot{R}_i = R_i \times \frac{\partial H(q, p)}{\partial p_\omega}, \quad i = 1, 2, 3 \quad (70b)$$

$$\dot{p}_v = p_v \times \frac{\partial H(q, p)}{\partial p_\omega} - R^\top \frac{\partial H(q, p)}{\partial x} + b_v(q)u \quad (70c)$$

$$\begin{aligned} \dot{p}_\omega = & p_\omega \times \frac{\partial H(q, p)}{\partial p_\omega} + p_v \times \frac{\partial H(q, p)}{\partial p_v} + \\ & \sum_{i=1}^3 R_i \times \frac{\partial H(q, p)}{\partial R_i} + b_\omega(q)u, \end{aligned} \quad (70d)$$

where the input matrix is $B(q) = [b_v(q)^\top \quad b_\omega(q)^\top]^\top$ and the notation \times denotes the cross product of two vectors.

A data set $\mathcal{D} = \{t_{0:N}^{(i)}, q_n^{(i)}, \xi_n^{(i)}, u^{(i)}\}_{i=1}^D$ is collected by applying a constant control input $u^{(i)}$ to the system and sampling the state at times $t_n^{(i)}$ for $n = 0, \dots, N$. Duong et al. (2024b) uses neural networks with parameters θ to approximate the mass $M_\theta^{-1}(q)$, the potential energy $V_\theta(q)$, the dissipation matrix $D_\theta(q, p)$, and the input matrix $B_\theta(q)$, respectively. The model is trained by minimizing a loss function combining errors in orientation, position, and generalized velocity. The orientation error is measured on $\text{SO}(3)$ via the logarithmic map, while position and velocity errors use standard Euclidean norms.

A Crazyflie quadrotor, shown in Fig. 9a, simulated in the physics-based simulator PyBullet (Panerati et al., 2020) is used to verify the approach. The control input $u = [u' \tau^T]^T$ includes a thrust $u' \in \mathbb{R}_{\geq 0}$ and a torque vector $\tau \in \mathbb{R}^3$ generated by the 4 rotors. The quadrotor is controlled from a random starting point to 18 different desired poses using a PID controller (Panerati et al., 2020), providing 18 2.5-second trajectories. The trajectories were used to generate a dataset $\mathcal{D} = \{t_{0:N}^{(i)}, q_n^{(i)}, \xi_n^{(i)}, u^{(i)}\}_{i=1}^D$ with $N = 5$ and $D = 1080$. The $\text{SE}(3)$ port-Hamiltonian ODE network (Duong et al., 2024b) is trained for 500 iterations. The training and test results in Fig. 9 show that the neural networks are able to approximate to the ground-truth values. Fig. 9g and 9h verify that when we roll out the learned dynamics for a long horizon, the law of energy conservation is satisfied via the encoded Hamiltonian structure, and the $\text{SO}(3)$ constraint violation is negligible. The $\text{SE}(3)$ port-Hamiltonian neural ODE networks are also trained with noisy real data collected from a quadrotor (Fig. 8a), and tested with trajectory tracking task (Fig. 8b).

5.2.3. Monotone Neural Networks

Monotone systems have outputs that change in a consistent direction in response to inputs. For a single-input-single-output (SISO) system, there have been papers on SISO monotone neural networks (Sill, 1997; Wehenkel and Louppe, 2019; Liu et al., 2020; Daniels and Velikova, 2010; Sivaraman et al., 2020; Zhang and Zhang, 1999) for learning the dynamical system while preserving the order. For multi-input-multi-output (MIMO) systems, monotonicity has been studied under a collective manner, i.e., $f(\cdot) : \mathbb{R}^n \rightarrow \mathbb{R}^n$, for all $x, x' \in \mathbb{R}^n$,

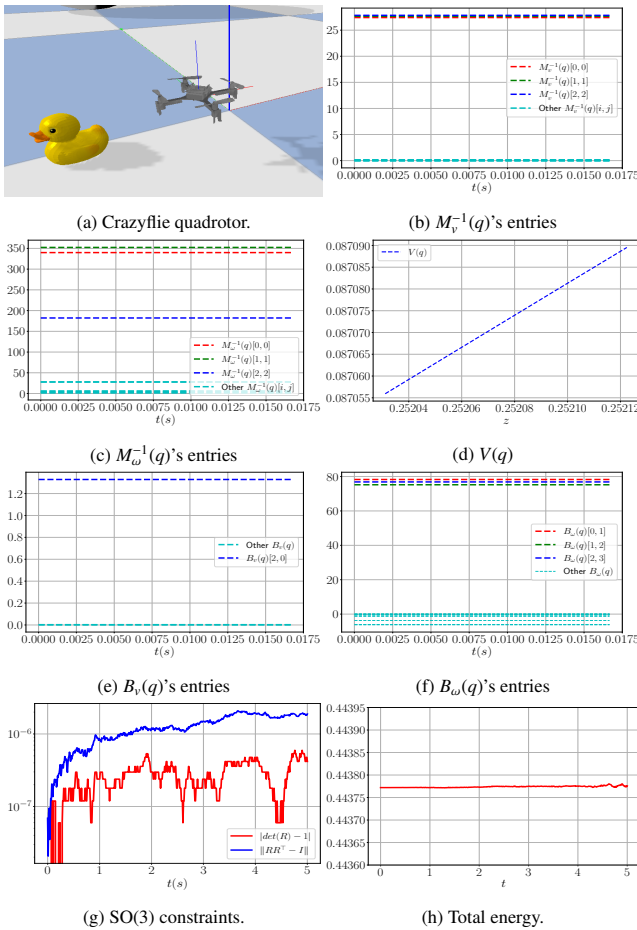


Figure 9: $SE(3)$ port-Hamiltonian neural ODE network on a Crazyflie quadrotor in the PyBullet simulator (Panerati et al., 2020).

$(f(x) - f(x'))^\top (x - x') \geq 0$. In this case, Cui et al. (2024) is inspired by the fact that gradients of convex functions are monotone, and constructs MIMO monotone neural networks (MNN) using gradients of strictly convex neural networks (termed MNN1 in Figure 10). A strictly convex neural network is parameterized as a L -layer FNN with additional residual connection layers that directly pass the input to the hidden layers. With input $l_0 = x$, each layer l_i evolves as,

$$l_{i+1} = \sigma \left(W_{i+1} l_i + W_{i+1}^{(x)} x + b_{i+1} \right), \quad i = 0, \dots, L-1, \quad (71)$$

where $\theta = \{W_{1:L}, W_{1:L}^{(x)}, b_{1:L}\}$ are neural network weights and biases and σ is the non-linear activation function. In order for the neural network output to be strictly convex with respect to the input, all $W_{2:L}$ are required to be *positive*, $W_{1:L}^{(x)}$ could be either positive or negative, and the activation function σ needs to be strictly convex and increasing, such as the softplus activation function Glorot et al. (2011). Such neural network architecture is also known as the input convex neural network (ICNN) Amos et al. (2017) in the literature. Gradient of the strictly convex ICNN output with respect to the network input, i.e., $\frac{\partial \sigma}{\partial x}$ satisfies the monotonicity condition. An illustration of this monotone neural network design is presented in Figure 7.

Wang et al. (2024) introduces another MNN architecture of the form $f(x) = \mu x + m(x)$ where μ is a positive constant (termed MNN2 in Figure 10). $m(x)$ is a feed-through neural network, with connections from each hidden layer to the input and output variables. The feed-through neural network is parameterized to guarantee monotonicity and bi-Lipschitzness via the integral quadratic constraint framework and the Carley transform. MNNs have been applied to monotone system modeling, including power system frequency control (Cui et al., 2024; Feng et al., 2025), power system voltage control (Shi et al., 2022b; Feng et al., 2023), where monotone controller policies are constructed to guarantee closed-loop stability by design.

Example 5.2 (Monotone Neural Network for Power System Model Identification). To illustrate the idea of MNN and standard FNN for monotone system identification, we provide an example for distribution power system identification from Feng et al. (2023). The distribution power network can be represented by a graph $\mathcal{G} = (\mathcal{N}, \mathcal{E})$, where $\mathcal{N} := \{1, 2, 3, \dots, n\}$ represents the node set and \mathcal{E} is the edge set. Each node $i \in \mathcal{N}$ is associated with an active power injection p_i and a reactive power injection q_i . Let V_i be the complex voltage and $v_i = |V_i|^2$ be the squared voltage magnitude. For any node j as a child node of node i , the following equations represent the branch flow model:

$$\begin{aligned} -p_j &= P_{ij} - r_{ij} l_{ij} - \sum_{k:(j,k) \in \mathcal{E}} P_{jk}, \\ -q_j &= Q_{ij} - x_{ij} l_{ij} - \sum_{k:(j,k) \in \mathcal{E}} Q_{jk}, \\ v_j &= v_i - 2(r_{ij} P_{ij} + x_{ij} Q_{ij}) + (r_{ij}^2 + x_{ij}^2) l_{ij}, \quad (i, j) \in \mathcal{E}, \end{aligned}$$

where $l_{ij} = \frac{P_{ij}^2 + Q_{ij}^2}{v_i}$ is the squared current, P_{ij} and Q_{ij} represent the active power and reactive power flow on line (i, j) , and r_{ij}

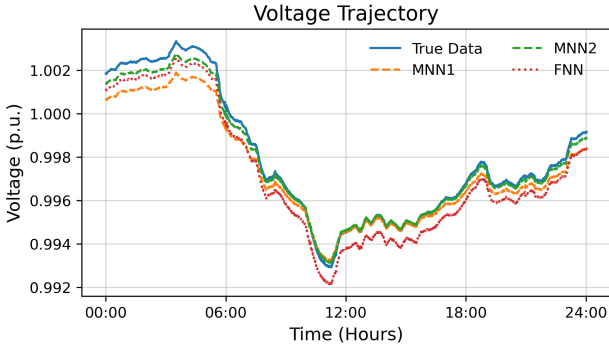


Figure 10: Voltage trajectories of the ground truth using real-world load data, the fit for standard MLP, FTN-based monotone neural network (MNN2), and gradients of input convex neural networks (MNN1) for example 5.2.

and x_{ij} are the line resistance and reactance. With slight violation of notations, we use notations p, q , and v to denote the p_i, q_i, v_i stacked into a vector. The system can be approximated by the following linear equation by dropping high-order terms

$$v = Rp + Xq + v_0 1 = Xq + v^{env},$$

where matrix $R = [R_{ij}]_{n \times n}$, $X = [X_{ij}]_{n \times n}$ are given as follows, $R_{ij} := 2 \sum_{(h,k) \in \mathcal{P}_i \cap \mathcal{P}_j} r_{hk}$, $X_{ij} := 2 \sum_{(h,k) \in \mathcal{P}_i \cap \mathcal{P}_j} x_{hk}$, and $\mathcal{P}_i \subset \mathcal{E}$ is the set of lines on the unique path from bus 0 to bus i . v^{env} is considered as a non-controllable constant. A fact is that for radial distribution systems, R and X are positive definite matrices. As a result, v is monotonically increasing with respect to q following the linearized branch flow model. Similarly, the nonlinear branch flow also exhibits local monotonicity.

All neural networks have two hidden layers, each layer has 100 hidden units. Both trained MNNs (MNN1 and MNN2) achieve MSE values at the scale of e^{-7} ($6.5e^{-7}$ and $3.6e^{-7}$), comparable but slightly worse compared to the FNN's performance ($2.8e^{-7}$). In addition, we observe that training monotone neural networks presents additional challenges relative to standard FNN architecture. Such challenges in training monotone neural networks have also been observed in Mikulincer and Reichman (2022). More broadly, this example illustrates a common tradeoff in control-oriented learning. Incorporating structure into the learning process can provide valuable inductive bias, improving model reliability and interpretability. However, it also limits model expressiveness and can introduce additional optimization challenges. We further discuss such tradeoffs in Section 7.6.

5.3. Hard Constraints

One way to introduce *hard constraints* into learning-based system identification is to first solve the unconstrained system identification problem in (14) and project the solution to the constraint set in (21). On this line, Kolter and Manek (2019) proposes to jointly learn a dynamics model f and Lyapunov function V , both as neural networks, where the dynamics are inherently constrained to be stable. Whenever the learned f does not meet the Lyapunov stability constraints, it is projected

to the following constraint set,

$$\text{Proj}\left(\hat{f}(x), \{f : \nabla V(x)^\top f(x) \leq -\alpha V(x)\}\right) := \hat{f}(x) - \nabla V(x) \frac{\nabla V(x)^\top \hat{f}(x) + \alpha V(x)}{\|\nabla V(x)\|_2^2}. \quad (73)$$

Lawrence et al. (2020) extends Kolter and Manek (2019) to learn discrete-time systems with disturbance $x_{k+1} = f(x_k, w_{k+1})$, where $w_k \in \mathbb{R}^d$ is a stochastic process. A Mixture density networks $p(x_{k+1}|x_k) = \sum_{i=1}^m \pi_i(x_k) \phi_i(x_{k+1}|x_k)$ is proposed to model the dynamics, where each ϕ_i is a kernel function (usually Gaussian), the mean $\hat{\mu}_i(x_i)$ can be parameterized as FNNs and mixing coefficients π_i are also FNNs, which are nonnegative and sum to one. The Lyapunov stability condition is posed to the mean parameters, i.e., $V(\mu_{k+1}) \leq \beta V(\mu_k)$ with $\mu_{k+1} = \sum_{i=1}^m \pi_i(x_k) \hat{\mu}_i(x_k)$. Takeishi and Kawahara (2021) generalizes Kolter and Manek (2019) to learn dynamics models with stable invariant sets rather than an equilibrium point, by modifying the projection step to a set and ensuring invariance on the set. Schlaginhaufen et al. (2021) jointly learn a stable system model (using neural ODEs) and a Lyapunov function for partially observable systems with delays. Min et al. (2023) extends this method to a system with control, by jointly learning the dynamical system, Lyapunov function, and a feedback controller all by neural networks, where the closed-loop stability is guaranteed by projection. Tang et al. (2024) further extends this approach to chaotic systems and learning invariant set.

Dissipativity/passivity extend the concept of Lyapunov stability to input-output dynamical systems by considering “energy” (Brogliato et al., 2007). To incorporate dissipativity as a hard constraint into learned dynamics, Zhong et al. (2020) introduces a deep learning architecture, Dissipative SymODE, that is built on structured Port-Hamiltonian dynamics with energy dissipation matrix for constant inputs. It learns four neural nets, representing the inverse of mass matrix, potential energy, the input matrix, and the dissipation matrix respectively, through NeuralODE. Greydanus and Sosanya (2022), on the other hand, extends Hamiltonian Neural Networks (HNN) (Greydanus et al., 2019) to Dissipative Hamiltonian Neural Networks (D-HNN) by decomposing dynamic systems into dissipative and conserved quantities so that it accommodates the case where the total energy is not conserved. Dragoňa et al. (2021) focuses on general dissipative discrete-time autonomous dynamical systems and enforces dissipativity by formulating a feed-forward neural network as a point-wise affine map and constraining on the corresponding state-dependent affine coefficients. Xu and Sivarajani (2023) proposes a method that learns dissipative dynamical systems using neural models while preserving input-output dissipativity by perturbing the weights of neural networks. Okamoto and Kojima (2024) leverages the Kalman-Yakubovich-Popov (KYP) lemma, which is a necessary and sufficient condition for dissipativity to design a differentiable projection that transforms any dynamics represented by neural networks into dissipative ones and jointly learning the transformed dynamics.

Example 5.3 (Learning Dissipative Dynamics as Hard Constraints). *To demonstrate the idea of learning dissipative dy-*

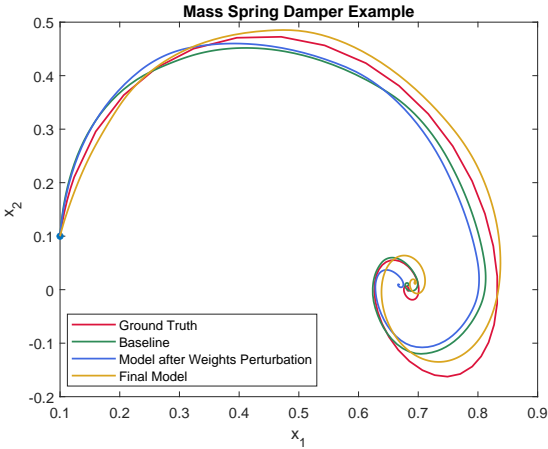


Figure 11: Trajectories of the ground truth, the fit for baseline model, model after weights perturbation and final model for Example 5.3

namics as a hard constraint, we consider a mass-spring-damper system, whose nonlinear dynamics are as follows.

$$m\ddot{x}(t) + c\dot{x}(t) + (kx(t) + \alpha x(t)^3) = u(t),$$

where m is the mass, c is the damping factor, k is the linear stiffness coefficient, and α is a constant that introduces the nonlinearity in the spring. We take $m = 1, c = 1, k = 1, \alpha = 1$ and set state variables to be $x_1 = x$ and $x_2 = \dot{x}$. The state-space model is

$$\begin{bmatrix} \dot{x}_1(t) \\ \dot{x}_2(t) \end{bmatrix} = \begin{bmatrix} x_2(t) \\ -x_2(t) - x_1(t) - x_1(t)^3 \end{bmatrix} + \begin{bmatrix} 0 \\ u(t) \end{bmatrix} \quad (74)$$

We collect step response data with initial point being $[0.1, 0.1]$ and introduce normal distributed noises with mean 0 and standard deviation 0.01. Following the method in Xu and Sivaranjani (2023), we first learn a baseline model, which is a two-layer neural network with LeakyReLU activation function on the hidden layer and with 16 neurons for the hidden layer, and then perturb the weights to enforce dissipativity. At this stage, we obtain a dissipative neural dynamical system with $R = 0$, $S = \frac{1}{2}I$, and $Q = 0$, corresponding to the passive case. For the weight perturbation, we have the results $\lambda_1 = 10, \lambda_2 = 10$, and $\lambda = 27.822$. The distance (Frobenius norm) of weights being moved is 3.2608 and 0.267 for the first and second layer respectively (both weights have 64 entries in total). Then we retrain biases and obtain the final model. We demonstrate the ground truth, the fit for the baseline model, the model after weights perturbation, and the final model in Fig. 11. We observe the final model closely matches the ground truth and retains closeness to the baseline model while guaranteeing incremental dissipativity.

5.4. Soft Constraints

Control-relevant properties can be incorporated into deep learning based system ID approaches as a soft penalty. There have been a large volume of literature on using soft penalty to incorporate the above properties, such as stability, dissipativity, passivity, physics and conservation laws.

A primary example in this category is the physics-informed neural networks (PINNs). PINNs (Raissi et al., 2019) are deep learning models that integrate physical principles into the neural network architecture. Consider we have some prior knowledge about the dynamical system in the form of $P(x, u, y) = 0$. PINNs use both a data-driven loss and a physics-informed loss for learning the system model f_θ and h_θ . The data-driven loss term is defined as in (21),

$$c_{data}(\theta; \mathcal{W}) = \sum_i \int_t \|y_i(t) - \hat{y}_i\|^2$$

and the physics-based loss/regularization term is defined as,

$$c_{physics}(\theta; \mathcal{W}) = \sum_i \int_t P(\hat{x}_i(t), u_i(t), y_i(t))^2.$$

Combining the data-driven and physics-based loss terms forms the total loss function $c(\theta; \mathcal{W}) = c_{data}(\theta; \mathcal{W}) + \lambda c_{physics}(\theta; \mathcal{W})$, where $\lambda c_{physics}(\theta; \mathcal{W}) := r(\theta)$ is the soft regularization term to enforce the physics law. PINNs are trained to minimize $c(\theta; \mathcal{W})$ with respect to parameters θ .

As soft constraints, PINNs can be incorporated into data-driven system identification following two general frameworks: i) By posing a certain structural prior about the system to be identified, we can turn the system identification problem into a parameter identification problem. A simple example is to assume that the system to be identified follows the linear time-invariant system $\dot{x} = Ax + Bu$ and to identify A, B matrices from the data. Richards et al. (2023) extends this idea to learn linear time-varying system models. ii) By posing certain physics laws or/and conservation laws into system identification rather than directly assuming the model parametric forms. A common conservation law that can be used in dynamical system learning is the energy conservation law. A benchmark is available in Zhong et al. (2021) for the design of energy-conserving PINNs that include both Lagrangian neural networks and Hamiltonian neural networks. Until now, PINN-based modeling algorithms have been successfully incorporated in learning Lagrangian mechanics (Roehrl et al., 2020), robotics dynamics (Nicodemus et al., 2022; Liu et al., 2024a), building dynamics (Gokhale et al., 2022), rotor dynamics Liu et al. (2024b), power system dynamics (Huang and Wang, 2023), etc.. PINNs also have achieved great success in modeling dynamical systems governed by PDEs such as fluid mechanics (Mowlavi and Nabi, 2023), see a recent review by Faroughi et al. (2024).

Example 5.4 (PINNs for Building System Identification). To illustrate the idea of PINNs for system identification, we provide an example of a dynamic identification building from Bian et al. (2023). For PINN design, the physics knowledge is incorporated by directly posing a linear resistor-capacitor model structure, where the heat transfer between zone i and zone j is modeled as a resistor coefficient R_{ij} and the heat generation/absorbing within zone i is modeled as a capacitor coefficient C_i . The thermal dynamics in each zone follows,

$$C_i \dot{x}_i = \frac{x_o(t) - x_i(t)}{R_{oi}} + \sum_{j \in N_i} \frac{x_j(t) - x_i(t)}{R_{ji}} + c_p u_i(t)(x_s(t) - x_i(t)) + p_i, \text{ PINN}$$

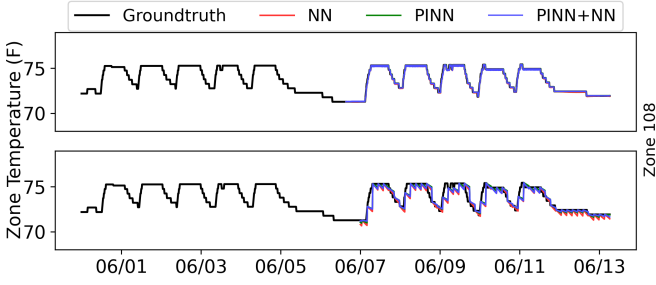


Figure 12: Temperature predictions for 15-minute (top) and 3-hour (bottom) horizons, using one week data for training and the rest for testing.

where $x_i(t)$, $x_o(t)$, $x_s(t)$ are the indoor temperature of zone i , the outdoor temperature, and the temperature of supply air. N_i is the set of rooms that are adjacent to room i , c_p is the specific heat capacity of the air, and p_i is the internal heat gain. $u_i(t)$ denotes the supply air flow rate, which is the control action. Parameters $\{C_i, R_{oi}, R_{ji}, c_p, p_i\}$ are to be identified from data through the PINN training.

In comparison, a standard NN model, as defined in Sec 5.1.1, without prior knowledge can be learned,

$$\dot{x}_i = f_{\theta_i}(x_i(t), u_i(t), x_{N_i}(t), x_o(t), x_s(t)), \quad NN$$

where θ_i are the NN parameters to be learned for zone i .

It is also interesting to consider a combined approach that combines a PINN and a NN,

$$C_i \dot{x}_i = \frac{x_o(t) - x_i(t)}{R_{oi}} + \sum_{j \in N_i} \frac{x_j(t) - x_i(t)}{R_{ji}} + f'_{\theta_i}(x_i(t), u_i(t), x_s(t)), \quad PINN + NN$$

where the learnable parameters are the combination of the NN parameters θ_i and PINN parameters $\{C_i, R_{oi}, R_{ji}\}$.

We train the three models to learn the thermal dynamics of one building zone. Two forecasting horizons are considered: 15 minutes (short-term prediction) and 3 hours (long-term prediction). The training data includes 7-day periods at a 15-minute resolution. Prediction results are presented in Figure 12. For the 15-minute horizon, all methods achieve high accuracy with errors below 0.02 degrees Fahrenheit. For the 3-hour horizon, incorporating physics priors enables the PINN and the combined approach to outperform the standard FNN, with PINN delivering the best test performance across both horizons.

We end this subsection by comparing incorporating control-relevant properties via soft and hard constraints. We consider a case study of learning a stable dynamical system with Lyapunov stability constraint.

Example 5.5 (Soft v.s. Hard Constraints for Learning Stable Pendulum Dynamics). Consider the following stable pendulum dynamics from Kolter and Manek (2019), $\ddot{x} = -b\dot{x} - g \sin x$ where x denotes the angular position, \dot{x} is the angular velocity, and \ddot{x} is the angular acceleration. b is the damping coefficient, and g is the gravity constant.

For incorporating a stability constraint, two neural networks are learned simultaneously: a two-layer NN model f for learning the dynamics, and a neural Lyapunov function V . The neural Lyapunov function is designed as $V(x) = \sigma(g(x) - g(0)) +$

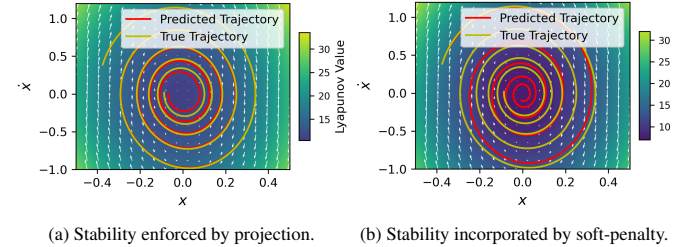


Figure 13: Comparison of hard projection and soft penalty approach for learning stable dynamics with neural dynamics and a neural Lyapunov function.

$\epsilon \|x\|_2^2$, where σ is a smoothed ReLU to make the Lyapunov function continuously differentiable, $g(x)$ is parameterized as an input convex neural network to avoid local optima, and the regularization term ensures strict positive definiteness. To jointly learn the neural dynamics f and the Lyapunov function V , $N = 10^4$ data pairs (x_i, \dot{x}_i) are generated using the true dynamics. We compare two schemes for incorporating the stability constraint.

i) Hard constraint: The loss function for jointly learning f, V is defined as,

$$c_1(f, V) = \sum_i \|\dot{x}_i - \hat{f}(x_i)\|_2,$$

where \hat{f} is defined by the projection in (73) to ensure hard constraint satisfaction of Lyapunov stability.

ii) Soft penalty: The loss function for jointly learning f, V is defined as,

$$c_2(f, V) = \sum_i \sum_i \|\dot{x}_i - f(x_i)\|_2 + \sum_i \lambda \max(0, \Delta V(x_i)),$$

where $f(x_i)$ is the estimated dynamics (without projection), λ is a balancing coefficient, and $\Delta V(x_i) = V(f(x_i)) - V(x_i)$ represents the difference of the Lyapunov energy decay. For stable systems, $\Delta V(x_i) < 0$. Otherwise, it would incur a penalty to guide learning of V, f towards constraint satisfaction. We show the trained Lyapunov function contour (after 2,000 training steps) and predicted trajectories in Figure 13. The background color represents the value of the learned Lyapunov function, with the true dynamics shown in gold and the predicted trajectory in red. Both learned trajectories exhibit stable behavior, while the trajectory with stability enforced by projection achieves higher accuracy. This might be due to the projection provides a stronger prior compared to regulation terms, and the soft penalty adds complexity to the optimization landscape.

5.5. Discussions

Despite the remarkable flexibility of deep learning models for system identification, several fundamental challenges and significant opportunities for future research remain.

One major difficulty lies in imposing hard constraints—such as stability, passivity, or physics knowledge—during training, as these constraints are often nonconvex and make the learning process difficult. This calls for the development of advanced

optimization algorithms that can account for such constraints and guide learning toward meaningful and feasible solutions.

In parallel, there is a growing need to design specialized neural network architectures to achieve a balance between structural constraints and model expressiveness. On the one hand, incorporating structural priors or leveraging physics-inspired parameterizations can help improve generalization and model interpretability. However, as illustrated in Example 5.2, these constraints may also limit model expressiveness and performance, underscoring the trade-off between enforcing physical properties and maintaining flexibility in function approximation. Finally, a promising direction lies in the data-driven *discovery* of system properties. The learned models not only fit the observed trajectories but also uncover underlying system properties—such as conservation laws, stability, controllability, and causal dependencies—that are often difficult to characterize without an exact system model. This aspects will be further discussed in the next section on direct identification and verification of control-relevant properties.

6. Direct Identification and Verification of Control-Relevant Properties

A recently emerging area within control arises from behavioral system theory (Markovsky and Dörfler, 2021), where a representation-free perspective is adopted, and a dynamical system is described through a collection of its input-output trajectories, rather than a transfer function or state-space model. Control-relevant properties like dissipativity can also be extended to this setting, which allows a verification of these properties directly from measured data; this problem has been studied under the broad umbrella of ‘data-driven system analysis’.

Motivated by these developments, the viewpoint in this section is different compared to the previous sections: we are not explicitly interested in identifying a transfer function or state space model for the system. Instead, we aim to verify from a behavioral systems perspective, that is based on measured system trajectories, whether the underlying unknown system satisfies a certain control-theoretic property, or to check whether the set of all systems that could generate the observed data satisfies a control-relevant property like dissipativity. In particular, we are interested in verification methods with rigorous guarantees regarding the verified system property that can be translated to closed-loop settings.

6.1. Control-relevant Properties in the Behavioral Framework

In this section, we review the direct verification of dissipativity (Maupong et al., 2017; Romer et al., 2019a) and more general input-output properties (Koch et al., 2021) for LTI systems from data based on Willems’ fundamental lemma (Willems et al., 2005a) as described in Section 2.1. Since the fundamental lemma characterizes finite horizon trajectories of systems, Maupong et al. (2017) introduce the notion of L -dissipativity.

Definition 6.1 (L -dissipativity). *The discrete-time LTI system (12) is L -dissipative with respect to the supply rate $s(u, y) =$*

$$\begin{aligned} \begin{bmatrix} u \\ y \end{bmatrix}^\top \Pi \begin{bmatrix} u \\ y \end{bmatrix} &\text{ if} \\ \sum_{k=0}^{L-1} \begin{bmatrix} u_k \\ y_k \end{bmatrix}^\top \Pi \begin{bmatrix} u_k \\ y_k \end{bmatrix} &\geq 0, \end{aligned} \quad (75)$$

for all input-output trajectories $\{u_k, y_k\}_{k=0}^{L-1}$ of (12) with initial condition $x_0 = 0$.

Note that the dissipativity in Definition 6.1 is given in an input-output setting, and thus does not include a storage function. For the relationship of this notion to the classical definition of dissipativity in a state-space and input-output setting, we refer to Hill and Moylan (1980).

The key idea to verify L -dissipativity from a single measured trajectory is to parameterize all trajectories of length L of LTI system (12) with $x_0 = 0$, as required in condition (75), by the fundamental lemma (13). By the resulting condition on the parameter α together with the application of Finsler’s lemma, Romer et al. (2019a, (Theorem 2)) provides a computationally appealing linear matrix inequality (LMI) to check whether an LTI system is L -dissipative based on a single measured trajectory. Extensions of this result include data-driven dissipativity verification for LPV systems (Verhoek et al., 2024) using the fundamental lemma for LPV systems (Verhoek et al., 2021b). Furthermore, for linear systems, Koch et al. (2021) investigates the determination of optimal input-output properties characterized by time domain IQCs.

Inspired by the fundamental lemma, De Persis and Tesi (2020) establishes a direct data-driven closed-loop characterization of an LTI system, which builds the basis for a data-driven state-feedback design. Furthermore, this result has led to direct data-driven state-feedback design for polynomial systems (Guo et al., 2022), for Lur’e-type systems (Luppi et al., 2022), for LPV systems (Verhoek et al., 2022), and for nonlinear systems via LPV embedding (Verhoek et al., 2023a) and via nonlinearity cancellation (De Persis et al., 2022). Moreover, the fundamental lemma is suitable for data-driven simulation and output matching control (Markovsky and Rapisarda, 2008), data-driven predictive control with guarantees for LTI systems (Coulson et al., 2019; Berberich et al., 2021), LPV systems (Verhoek et al., 2021a), feedback linearizable systems (Alsatti et al., 2022), bilinear systems (Yuan and Cortés, 2022), nonlinear systems (Berberich et al., 2022a), and system level synthesis (Xue and Matni, 2021).

We conclude that the application of Willems’ fundamental lemma enables a simple and direct verification of dissipativity and related system properties from a single input-output trajectory. However, the analysis via the fundamental lemma calls for noise-free measurements, is restricted to finite horizon, and an extension to general nonlinear systems is unknown.

6.2. Set-Membership Approaches

Set-membership approaches (Fogel, 1979) aim to determine the set of all systems that could generate the observed data. Since this feasible system set contains the underlying system, analyzing all systems within this set yields guarantees for the true system even if it cannot be identified due to, e.g., noisy

data. Set theoretic methods for control, set membership based identification, and broadly, identification under uncertainty and identification for robust control, have a long history (see books such as [Blanchini et al. \(2008\)](#); [Milanese et al. \(2013\)](#); [Chen and Gu \(2003\)](#) and surveys such as [Mäkilä et al. \(1995\)](#); [Milanese and Vicino \(1991\)](#)). Given the wide scope of set membership approaches, we do not consider general set membership based system identification and control here; rather, we focus our attention on set membership approaches for direct identification of control-relevant properties like dissipativity, stability, and monotonicity.

For the ease of presentation, we focus on unknown LTI systems and refer afterwards to possible extensions in various directions. Consider the discrete-time LTI system

$$x_{k+1} = A^* x_k + B^* u_k, \quad (76)$$

with state $x_k \in \mathbb{R}^{n_x}$ and input $u_k \in \mathbb{R}^{n_u}$. To infer on the unknown system matrices A^* and B^* , we assume input-state samples $\{x_k, u_k\}_{k=0}^{N-1}$ are given with $x_{k+1} = A^* x_k + B^* u_k + d_k, k = 0, \dots, N-2$. The unknown disturbance vector d_k can incorporate process noise, nonlinear dynamics, or effects from inexact state measurements. We suppose that the disturbance is bounded $\|d_k\|_2 \leq \epsilon, k = 0, \dots, N-2$, with known bound $\epsilon > 0$. Note that the samples can also stem from multiple trajectories.

Under the given data and the pointwise-in-time noise characterization, we can infer on the set of system matrices

$$\Sigma = \left\{ [A \ B] : \left\| x_{k+1} - [A \ B] \begin{bmatrix} x_k \\ u_k \end{bmatrix} \right\|_2 \leq \epsilon, i = 0, \dots, N-2 \right\} \quad (77)$$

consistent with the data. Note that the true matrices $[A^* \ B^*]$ are contained within Σ as they satisfy $\left\| x_{k+1} - [A^* \ B^*] \begin{bmatrix} x_k \\ u_k \end{bmatrix} \right\|_2 \leq \epsilon, i = 0, \dots, N-2$. While the set membership (77) could directly be exploited to verify dissipativity following [Berberich et al. \(2022b\)](#) or [Martin and Allgöwer \(2021b\)](#), we will consider here an ellipsoidal outer approximation of (77) given by

$$\tilde{\Sigma} = \left\{ [A \ B] : \left[\begin{bmatrix} I \\ [A \ B] \end{bmatrix} \right]^\top \Delta \left[\begin{bmatrix} I \\ [A \ B] \end{bmatrix} \right] \leq 0 \right\} \supseteq \Sigma, \quad (78)$$

as proposed in [Martin and Allgöwer \(2022a\)](#), Proposition 1). The computation of matrix Δ boils down to an SDP with an LMI constraint because Σ corresponds to an intersection of $N-1$ quadratic constraints ([Boyd et al., 1994](#)). Thereby, $\tilde{\Sigma}$ is described by a single quadratic matrix inequality. However, this adds an additional conservatism due to a non-tight description of Σ . Since the set of feasible system matrices is characterized by the quadratic uncertainty description (78), we can analyze the set of linear systems with system matrices (A, B) where

$$x_{k+1} = Ax_k + Bu_k, \quad [A \ B] \in \tilde{\Sigma}, \quad (79)$$

using modern robust control techniques. For that purpose, we equivalently write (79) as a linear fractional representation ([Scherer and Weiland, 2000](#))

$$\begin{bmatrix} x_{k+1} \\ q_k \end{bmatrix} = \begin{bmatrix} 0 & 0 & I \\ I & 0 & 0 \\ 0 & I & 0 \end{bmatrix} \begin{bmatrix} x_k \\ u_k \\ w_k \end{bmatrix} \quad (80)$$

with uncertainty $w_k = [A \ B] q_k$ satisfying the quadratic constraint

$$\begin{bmatrix} q_k \\ w_k \end{bmatrix}^\top \Delta \begin{bmatrix} q_k \\ w_k \end{bmatrix} \leq 0.$$

Now, all systems of (79) are (Q, S, R) -dissipative for the storage function $V(x) = x^\top Xx, X \geq 0$, on $\mathcal{X} \times \mathcal{U} = \mathbb{R}^{n_x+n_u}$ if

$$w^\top Xw - x^\top Xx - \begin{bmatrix} y \\ u \end{bmatrix}^\top \begin{bmatrix} Q & S \\ S^\top & R \end{bmatrix} \begin{bmatrix} y \\ u \end{bmatrix} \leq 0, \quad \forall w : \begin{bmatrix} q \\ w \end{bmatrix}^\top \Delta \begin{bmatrix} q \\ w \end{bmatrix} \leq 0. \quad (81)$$

The infinitely many constraints (81) are implied by

$$w^\top Xw - x^\top Xx - \begin{bmatrix} y \\ u \end{bmatrix}^\top \begin{bmatrix} Q & S \\ S^\top & R \end{bmatrix} \begin{bmatrix} y \\ u \end{bmatrix} - \alpha \begin{bmatrix} q \\ w \end{bmatrix}^\top \Delta \begin{bmatrix} q \\ w \end{bmatrix} \leq 0,$$

for any $\alpha \geq 0$. This technique is well-known in robust control as the S-procedure ([Boyd et al., 1994](#)). With $q = \begin{bmatrix} x \\ u \end{bmatrix}$ and $y = Cx + Du$, we can write equivalently

$$\underbrace{\begin{bmatrix} x \\ u \\ w \end{bmatrix}^\top \phi^\top \begin{array}{c|cc|cc|c} -X & 0 & 0 & 0 & 0 \\ 0 & X & 0 & 0 & 0 \\ 0 & 0 & -Q & -S & 0 \\ 0 & 0 & -S^\top & -R & 0 \\ 0 & 0 & 0 & 0 & -\alpha \Delta \end{array} \phi \begin{bmatrix} x \\ u \\ w \end{bmatrix}}_{=\Omega} \leq 0, \quad (82)$$

with

$$\phi = \begin{bmatrix} I & 0 & 0 \\ 0 & 0 & I \\ C & D & 0 \\ 0 & I & 0 \\ I & 0 & 0 \\ 0 & I & 0 \\ 0 & 0 & I \end{bmatrix}.$$

Therefore, if there exist a matrix $X \geq 0$ and a scalar $\alpha \geq 0$ such that $\Omega \leq 0$, then all systems within the set membership (77), including the true system (76), are dissipative. Note that Ω is linear with respect to X and α . Thus, suitable values can be efficiently found by standard LMI solvers ([Löfberg, 2004](#)). Similar results can be found in [Koch et al. \(2022\)](#) exploiting the LMI-based robust control framework of [Scherer and Weiland \(2000\)](#). Moreover, [van Waarde et al. \(2022\)](#) exploits a matrix S-lemma to verify dissipativity for the feasible system set (79).

In contrast to the behavioral approach in Section 6.1, the set-membership approach enables dissipativity determination from noisy data and over an arbitrary time horizon, as required for the application of feedback laws ([Khalil, 2002](#)). Set membership approaches have also been extended to various model classes beyond LTI systems and control-relevant properties like stability and monotonicity as discussed in the sequel.

Polynomial dynamics: For systems with polynomial dynamics, common in applications such as fluid mechanics ([Chernyshenko et al., 2014](#)) and robotics ([Majumdar et al., 2013](#)), the dynamics can be expressed as $x_{k+1} = Fz(x_k, u_k)$ with unknown coefficient matrix F and a known vector of monomials $z(x_k, u_k)$. Dissipativity can then be verified using sum-of-squares relaxations, leading to an SDP formulation ([Martin](#)

and Allgöwer, 2021b). More generally, input-output properties such as integral quadratic constraints (IQCs) can also be verified using this representation (Martin and Allgöwer, 2022a).

General nonlinear dynamics: While linear and polynomial systems directly lead to a set membership suitable for an analysis by SDPs, general nonlinear systems yield non-convex optimization problems, even in the model-based case. To circumvent the non-convexity and to provide guarantees for the verification of system properties, the nonlinear system behavior can be embedded into a system representation suitable for an analysis using SDPs as summarized in the survey Martin et al. (2023). For example, dissipativity has been verified using Taylor-based approximations (Martin and Allgöwer, 2022b), piecewise polynomial models (Martin and Allgöwer, 2021a), or embedding into linear parameter-varying (LPV) representations (Miller and Sznaier, 2023; Verhoeck et al., 2023a).

General control-relevant properties: Set-membership based identification has also been extended to learn systems that are known to satisfy control-relevant properties. For example, works such as Cerone et al. (2011); Lauricella and Fagiano (2020); Lauricella (2020); Tobenkin et al. (2013) develop set membership approaches explicitly incorporating a priori information on system stability in an error-in-variable (EIV) framework. Set-membership based identification for monotone dynamical systems has also been considered in the literature (Makdesi et al., 2023). In fact, exploiting a priori knowledge on monotonicity or dissipativity of the system has also been shown to improve the accuracy and data efficiency of set-membership approaches (Ramdani et al., 2006; Berberich et al., 2022b).

Summarizing, the set-membership perspective combined with modern robust control techniques establishes a flexible framework for verifying system properties for linear and nonlinear systems from noisy data with guarantees. Related to this approach, the data-informativity framework (Van Waarde et al., 2023) provides conditions on when the collected samples are informative to infer system properties as controllability or stabilizability. We now present an example to demonstrate direct data-driven verification of dissipativity from noisy data using set-membership approaches.

Example 6.2. We consider a mass-spring-damper system $m\ddot{y}(t) + d\dot{y}(t) + Ky(t) = u(t)$ with position of the mass $y(t)$, external force $u(t)$, mass $m = 1 \text{ kg}$, damping coefficient $d = 1 \frac{\text{kg}}{\text{s}}$, and stiffness $K = 1 \frac{\text{kg}}{\text{s}^2}$. The continuous-time system is discretized in time with time step $T = 0.5 \text{ s}$ and the Euler method, which yields the discrete-time state-space representation

$$\begin{aligned} x_{k+1} &= \begin{bmatrix} 1 & T \\ -\frac{KT}{m} & -\frac{dT}{m} + 1 \end{bmatrix} x_k + \begin{bmatrix} 0 \\ T \end{bmatrix} u_k, \quad t \in \mathbb{N}, \\ y_k &= \begin{bmatrix} 1 & 0 \end{bmatrix} x_k. \end{aligned}$$

We assume that the system order $n_x = 2$ is known but the system matrices are completely unknown. To infer on the unknown system dynamics, the mass-spring-damper system is simulated over $N - 1$ time steps for initial condition zero, input $u_k = \cos(0.05k)$, and randomly drawn process noise $\|d_k\|_2 \leq \epsilon$ with various but known $\epsilon > 0$. Thereby, noisy state-input data $\{x_k, u_k\}_{k=0}^{N-1}$ are available to derive the set membership (77).

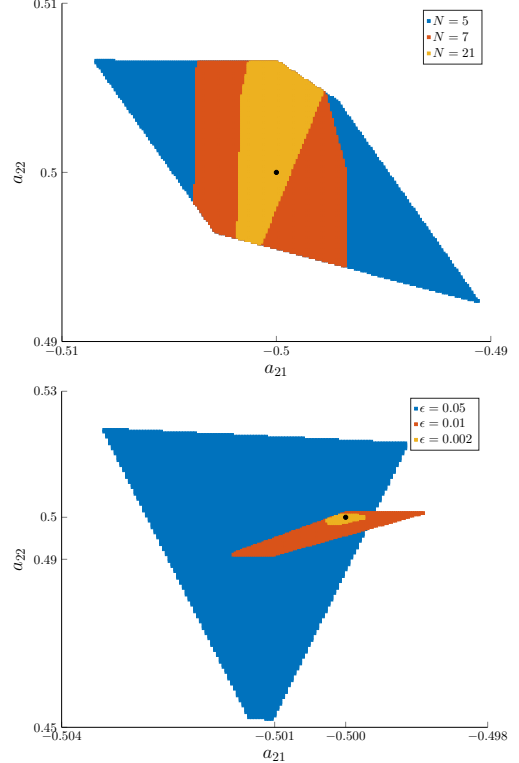


Figure 14: Projected set membership (83) for $\epsilon = 0.005$ and different data length N (top) and (83) for $N = 21$ and different noise bounds ϵ (bottom). True coefficients are depicted by a black dot.

Figure 14 illustrates the projected set membership

$$\left\{ a_{21}, a_{22} \in \mathbb{R} : \left\| \begin{bmatrix} x_{k+1} - \begin{bmatrix} 1 & T \\ a_{21} & a_{22} \end{bmatrix} x_k - \begin{bmatrix} 0 \\ T \end{bmatrix} u_k \end{bmatrix} \right\|_2 \leq \epsilon, \quad k = 0, \dots, N - 2 \right\}. \quad (83)$$

As expected, the true coefficients $a_{21}^* = -0.5$ and $a_{22}^* = 0.5$ are always elements of the set membership. The top figure illustrates that (83) decreases for an increasing amount of samples N . In particular, additional samples never increase the set, i.e., the set membership for $N = 21$ is a subset of the set membership for $N = 5$ and $N = 7$. Based on Martin and Allgöwer (2022a), (77) even converges to a singleton containing only the true coefficient matrices for $N \rightarrow \infty$ and persistently exciting data. The bottom figure illustrates (83) when the simulated trajectory is affected by differently large noise. Since the process noise d_k influences the trajectory, the set memberships are not necessarily subsets of each other.

For dissipativity verification, we first apply Proposition 1 of Martin and Allgöwer (2022a) to obtain ellipsoidal outer approximations of (77) while minimizing the volume of the ellipses. Subsequently, we search for a matrix $X \geq 0$ and a scalar $\alpha \geq 0$ such that $\Omega \leq 0$ from (82). In this numerical example, we examine on the one hand the \mathcal{L}_2 -gain from the input u to the position y . Thus, we consider (Q, S, R) -dissipativity with $Q = -1, S = 0$, and $R = \gamma^2, \gamma > 0$, where γ corresponds to an upper bound on the \mathcal{L}_2 -gain. Hence, we additionally minimize

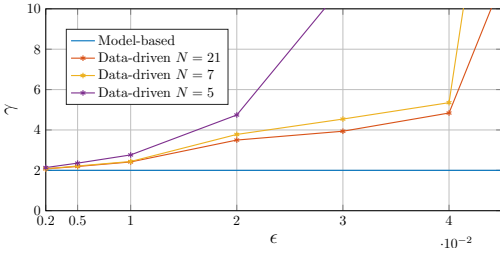


Figure 15: Data-driven inference on the \mathcal{L}_2 -gain.

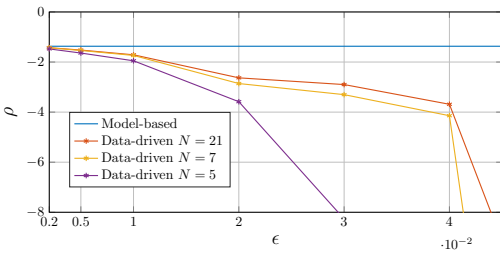


Figure 16: Data-driven inference on the input-feedforward passivity parameter.

over $\gamma > 0$. Moreover, we investigate input-feedforward passivity, which corresponds to the maximal ρ such that the system is (Q, S, R) -dissipativity with $Q = 0$, $S = 0.5$, and $R = \rho$. The resulting SDPs with LMI constraint are solved in MATLAB using YALMIP ([Löfberg, 2004](#)) and the SDP solver MOSEK ([MOSEK ApS, 2025](#)).

Figure 15 and Figure 16 compare the inference on the \mathcal{L}_2 -gain and input-feedforward passivity parameter, respectively, obtained from the true system and from data for various data lengths N and different large noise ϵ . Since the obtained inferences are guaranteed system properties, we only obtain larger values than the true \mathcal{L}_2 -gain and smaller values than the true input-feedforward passivity parameter. As expected, the determined bounds are more accurate for a larger set of data and smaller noise. Indeed, the data-driven inferences correspond almost to the true \mathcal{L}_2 -gain and passivity parameter for very small noise and even for a small amount of samples. Furthermore, since the data-driven inferences do not significantly improve from $N = 7$ compared to $N = 21$, we can conclude that the data $\{x_k, u_k\}_{k=8}^{21}$ is not informative for the (Q, S, R) -dissipativity verification. To further improve the obtained bounds, one could consider a more exiting input or experiments with different initial conditions.

6.3. Online Schemes

The behavioral and the set-membership approach suppose given trajectories, that is, both are offline methods according to [Hou and Wang \(2013\)](#). In contrast, online methods strive to improve the data-driven inference by iteratively performing experiments if the system or a simulation is available for further experiments. Thus, online schemes provide in each iteration an input trajectory that can be applied to refine the data-driven inference on the system property.

For discrete-time LTI SISO systems with $u_k = y_k = 0$ for

$k \leq 0$, a finite output sequence can be computed by

$$\underbrace{\begin{bmatrix} y_1 \\ y_2 \\ y_3 \\ \vdots \\ y_L \end{bmatrix}}_{=y} = \underbrace{\begin{bmatrix} g_0 & 0 & 0 & \cdots & 0 \\ g_1 & g_0 & 0 & \cdots & 0 \\ g_2 & g_1 & g_0 & \cdots & 0 \\ \vdots & \vdots & & \ddots & \vdots \\ g_{L-1} & g_{L-2} & \cdots & g_1 & g_0 \end{bmatrix}}_{=G} \underbrace{\begin{bmatrix} u_1 \\ u_2 \\ u_3 \\ \vdots \\ u_L \end{bmatrix}}_{=u},$$

with impulse response g_0, \dots, g_{L-1} . Thus, the \mathcal{L}_2 -gain over a finite time horizon L is given by

$$\min_{u \in \mathbb{R}^L \setminus \{0\}} \frac{y^\top y}{u^\top u} = \min_{u \in \mathbb{R}^L \setminus \{0\}} \frac{u^\top G^\top Gu}{u^\top u} = \min_{u \in \mathbb{R}^L \setminus \{0\}} J(u). \quad (84)$$

To solve this optimization problem for unknown G , [Wahlberg et al. \(2010\)](#) shows that the gradient of $J(u)$ can be obtained by evaluating the system response for two specific input sequences. Thus, a power iteration can be applied to solve (84) without knowledge of G . In [Romer et al. \(2021\)](#), this idea is unified as a framework of iterative sampling schemes for determining the operator gain, passivity, and conic relations of LTI systems. Such approaches have also been extended to finding lower order surrogate models [Martin et al. \(2020\)](#) for linear systems while establishing finite horizon system properties. Works such as [Wu et al. \(2013\)](#); [Welikala et al. \(2022\)](#); [Tanemura and Azuma \(2019\)](#) further focus on estimating stability properties such as \mathcal{L}_2 gain and various passivity indices (e.g., input feed-forward and output feedback), and lower bounds on gain and phase margins ([Isoshima et al., 2023](#)) from data. There are also schemes to improve the efficiency, convergence speed, number of required experiments, and the robustness of data-driven estimation of properties such as passivity and dissipativity ([Tanemura and Azuma, 2018; Iijima et al., 2020](#)).

To handle noisy data and nonlinear systems, and to obtain finite data guarantees, [Romer et al. \(2019b\)](#) solves, among others, the \mathcal{L}_2 -gain optimization problem (84) by Gaussian process optimization. By modelling $J(u)$ as Gaussian process, the worst-case input with respect to the system property is identified and subsequently applied to the system. Then the Gaussian process model can be updated by the new input-output sample. To achieve an iterative scheme for nonlinear systems, noisy data, and deterministic guarantees, [Martin and Allgöwer \(2020\)](#) considers the Lipschitz approximation of [Callies \(2014\)](#) for the input-output mapping of a dynamical system. This approximation can intrinsically be used to obtain an upper bound on the \mathcal{L}_2 -gain. Subsequently, the worst-case input can be identified and applied in order to refine the model and the inference on the \mathcal{L}_2 -gain. Summarizing, the presented schemes provide an iterative experiment design to refine data-driven inference of control-relevant properties. However, only finite horizon guarantees can be provided and the number of samples for a meaningful inference is larger than that required for the behavioral and set-membership approach.

6.4. Input Design

We conclude this section by making some remarks on the challenges associated with the input design within the behavioral framework. In this setting, [De Persis and Tesi \(2021\)](#)

and [Alsatti et al. \(2023\)](#) present ideas for the design of inputs to ensure persistently exciting input-output sequences for locally identifying nonlinear systems and for certain classes of nonlinear systems, respectively. While these works determine one experiment to identify the system, multiple experiments are typically necessary for learning an uncertain nonlinear dynamics. In Section 6.3, we also reviewed schemes for verifying control-relevant properties by iteratively performing experiments. These schemes provide an input sequence in each iteration step to refine the data-driven inference. However, these iterations typically converge rather slowly, requiring a large amount of experiments. Thus, the application of these iterative schemes is time consuming and the suggested input sequences may not obey any safety conditions, limiting their practical application. To reduce the size of the set membership (77) by additional experiments, one could consider state-input pairs which generate informative constraints on (77). Here the challenge is to identify these pairs and to steer the system safely to the corresponding state. Moreover, while this procedure would reduce the conservatism of the set membership, it is not guaranteed to refine the inference on the system property. Given these challenges, input design for direct data-driven identification and control-relevant property verification in the behavioral setting is an important consideration that merits investigation.

7. Future Directions

As we have outlined earlier, there is an impressive array of work that has now appeared, and continues to be done, utilizing the recent developments from learning to extend and complement classical system identification algorithms. Nevertheless, there remain rich problems that are unsolved in this area. In the following, rather than focusing on specific challenges on the various directions surveyed in the paper, we outline some major open directions that have not been explored much in the literature so far, yet represent important problems of great practical and theoretical interest.

7.1. Networked System Identification

Another major open question is the identification of networked systems, where imposing interconnection structure on the learned system matrices in addition to control-oriented and physics properties is a challenge. Many systems of practical interest are networked sub-systems that are dynamically coupled. Thus, for instance, it will be of interest when learning a model for a transportation network to preserve the structure of arterial roads and traffic intersections. Similarly, for a chemical reaction network, it may be of interest to learn the reaction rates while preserving the structure of the reactants and products.

A simple model of these interconnections for a linear system can be imposing certain elements of the system matrices A and B to be zero. Unfortunately, even for simple linear systems, identifying the system matrices typically yields a full matrix with scant regard to the desired structure. It is not clear that just setting the specified elements in the learned system matrices to be zero is necessarily the best solution. There has been

some initial work [Fattah et al. \(2019\)](#) on imposing a sparsity pattern on the learned system matrices; however, that work requires special assumptions on the matrices which may be difficult to check. Similarly, for special interconnection structures (i.e., those satisfying the so-called partially nested information pattern), some works [Ye et al. \(2022b,a\)](#) have shown that imposing sparsity constraints may not be important for learning optimal control laws; however, once again, it is not clear how generalizable these results are. The general problem of *imposing interconnection structure* during networked system identification remains open and an important avenue for future work.

Further, several networked systems like chemical reaction networks, power grids, and traffic flow networks satisfy control-relevant properties like monotonicity that can be exploited for scalable control synthesis [Sivarjanji et al. \(2017\)](#). There have been some recent developments in this direction in [Revay et al. \(2021\)](#), where an identification for large-scale networked systems with monotonicity guarantees is proposed. However, network identification preserving both the graph structure and various control-relevant properties is still an open problem.

7.2. Network Identification

A related problem is the identification of network structure itself from the data. In other words, consider an interconnected system as before, but now the interconnection structure is unknown and needs to be estimated from the data along with the parameters of the nodes describing the dynamical subsystems and edges describing the interconnections. This problem naturally arises in a variety of settings, with a concrete example being the identification of the structure of infrastructure systems such as the distribution grid in power systems or transportation network flows. There are classical fields such as network tomography ([Vardi, 1996](#); [Coates et al., 2002](#)) that address such a problem, although typically under simplifications such as absent or known node dynamics. From the domain of data science, a powerful idea that has been used in fields such as identification of gene regulatory networks is that if the observations from different nodes could be treated purely as a data series, one could associate statistical closeness among the series (as measured using quantities such as mutual information) with a weighted edge between the nodes ([Villaverde et al., 2014](#)). Extensions such as considering directed mutual information have been proposed to include directed edges that represent which node affects the other one.

Recent developments in causal inference ([Pearl, 2010](#)) have also aimed to consider similar problems of identifying causal networks whereby random variables representing data series at nodes affect each other causally. Granger causality ([Granger, 2001](#)) based methods have emerged as particularly powerful when the nodes represent random processes, as in the general framework considered in this paper. However, Granger causality based approaches necessitate presence of delays in the dynamic dependencies. New techniques have been proposed for the case when the nodes represent linear time-invariant subsystems ([Veedu et al., 2023](#)). However, it is fair to say that the general problem when the node dynamics can be non-linear, edges

may have dynamics, and partial information about the network structure may be available, remains largely open.

7.3. Switched and Time-varying Systems

Our discussion so far has assumed that both the node dynamics and the interconnection structure are time-invariant. For the general case when these quantities can be arbitrarily time-varying, it is difficult to collect enough data to perform any identification. However, for the case when there is some additional structure on the time-variation, it may be possible to obtain useful identification algorithms. A popular and practically important case is when the node dynamics can be modeled as switched (or more generally, hybrid) system. Switched systems, where the system switches between a set of individual modes that may be linear or non-linear, have proven to be immensely useful in modeling many situations of practical interest such as power grid operation (Feng et al., 2025; Ochoa et al., 2023), robotics (Tomlin et al., 2002; Grizzle et al., 2014), etc.. There is a large theory for modeling, analysis, and control of such systems available, with further classification into classes such as state-dependent or state-independent switching, deterministic or stochastic switching, autonomous or controlled switching, and so on.

The easiest extension of the methods we considered in this paper to switched system identification is if the active mode is known at any time and each mode is identified separately. Even in this case, if there is some additional information available about how the dynamics in each mode are related (e.g., the dynamics of temperature increase when a heater is on v/s decrease when a heater is off have many common parameters), one may envisage utilizing data from one mode to identify the dynamics of other modes. More generally, if the mode is unknown, then the identification problem is even more difficult since it involves simultaneous identification of a discrete variable (i.e., which mode is active) and the continuous dynamics. Relevant classical fields here include change point detection (Fu et al., 2024) and hidden Markov models (Smyth, 1994) and many numerical algorithms have been proposed to identify the dynamics of the switched systems (Lauer and Bloch, 2018). However, the fundamental difficulty of the optimization problem here constrains the performance and analysis of these algorithms except under some specific conditions. For instance, if the switching signal is not being controlled, and some of the modes of the system are unstable, the problem largely remains open (Shi et al., 2022a).

If additionally, as we argued in the paper, we aim to preserve physics-relevant properties during identification, an additional step that needs to be solved is to define the properties of interest. As an example, extension of properties such as dissipativity and passivity to switched systems requires care since the modes that are not active may gain energy (Zhao and Hill, 2008). The core intuition is the same as in classic results on stability of switched autonomous systems – it is easy to construct examples where a system that switches among individually stable modes is unstable. There is existing work on defining dissipativity to switched systems keeping this subtlety in mind (Lavaei and Zamani, 2022; McCourt and Antsaklis, 2012;

Li et al., 2016; Zhao and Hill, 2007; Haddad et al., 2006; Agarwal et al., 2016; Wang et al., 2013; Xia et al., 2016; Sivarajani et al., 2018; Zhao and Gupta, 2016). However, these works tend to require multiple storage functions and become computationally complex. There is little, if any work, on utilizing these definitions during identification of the system and further using them for control. Given the generality and importance of switched and time-varying systems in practical applications, control-informed system identification for these systems is an important direction for future work.

7.4. Experiment Design

Experiment design, broadly pertaining to the design of input sequences, data filtering, and sampling approaches are central to system identification. The design of input sequences for identification is particularly critical. Ideally, the input sequence must yield rich and meaningful data that excite all modes. On the other hand, the collection of data samples for system identification may be expensive, especially in online settings. Typically, the goal is to balance these tradeoffs.

This problem has been extensively studied in classical system identification, including closed-loop identification for control (see works such as (Goodwin, 1977; Hjalmarsson, 2005; Gevers and Ljung, 1986) for a survey of this area) and the persistent excitation conditions (Narendra and Annaswamy, 1987; Willems et al., 2005b; Markovsky et al., 2023). Input design for ML-based system identification is especially critical, since learning algorithms (such as neural network training) often require massive amounts of data, which is difficult to acquire in control applications. However, this area has received limited consideration in learning-based identification. A key open question is how to optimize input design while simultaneously ensuring that the learned model satisfies control-relevant properties. Imposing such properties places nontrivial structural constraints on the feasible excitation signals, thus altering the underlying geometry of the optimal experiment design problem. Further, imposing control-theoretic constraints may require balancing information gain against performance degradation or violations of control-relevant properties during data collection. Therefore, developing principled methods for experiment design while imposing control-relevant properties, particularly in online or data-limited regimes, is a critical direction.

7.5. Machine Learning vs Data-driven System Representations

We discussed the emerging paradigm of data-driven representations for control in Section 6, including approaches to provide guaranteed inferences on control-theoretic properties even in presence of noise. However, the system representations for nonlinear systems are tailored towards system analysis and control design using LMI techniques. Therefore, the nonlinearity of the system can not precisely be incorporated into a data-driven system representation, thus yielding conservative results that may only hold locally. On the other hand, models from machine learning are flexible and can explain complex nonlinear phenomena. However, the obtained system representations are usually strongly nonlinear, and are hence difficult to exploit

for system analysis and control. Thus, closing the gap between data-driven system representations tailored for control and machine learning approximations can be an interesting direction for future research. Thereby, the benefits of both worlds could be fused into a new class of surrogate models. Initial works in this direction include, for instance, [Hu et al. \(2023\)](#) and [Fiedler et al. \(2021\)](#). Related to merging these two worlds, it is important to note that data-driven control lacks standardized datasets and benchmarks as is common in the machine learning community, which makes meaningful comparison of different frameworks challenging. Developing such benchmarks and meaningful control-relevant use cases will be important to enable rapid advances in this area.

7.6. Tradeoffs in Control-Oriented System Identification

A central challenge in both classical and learning-based system identification is the tradeoff between control-relevant constraints and model expressivity. On one hand, physics-based priors and control-relevant constraints provide useful inductive biases that can reduce sample complexity, yield tractable formulations for learning-based identification, aid identifiability in problems with scarce data, and enable safe and interpretable closed-loop control. On the other hand, hard constraints or rigid model parameterizations can introduce model bias that limits the ability to capture complex real-world dynamics and generalize to unseen data, especially when the true system deviates from nominal operating conditions or exhibits non-ideal behavior, potentially undermining the very advantages that make data-driven models attractive in control applications. This merits a re-examination of classical considerations such as the closely related bias-variance tradeoff and the impact of structure and constraints on generalizability in the context of learning-based and data-driven models ([Pillonetto et al., 2025](#)). A key direction for future research is to establish universal approximation theorems for structured model classes that satisfy control-theoretic constraints. Such results would formalize the representational capacity of control-relevant models and guide the design of models and architectures that are both expressive and guaranteed to satisfy physics or control properties of interest.

Acknowledgments

The work of Y. Shi and J. Feng was supported by NSF grant ECCS-2442689, DOE grant DE-SC0025495, and a Schmidt Sciences AI2050 Early Career Fellowship. The work of J. Feng was also supported by the UC-National Laboratory In-Residence Graduate Fellowship L24GF7923. The work of Y. Xu, S. Sivarajani, and V. Gupta was supported in part by the Air Force Office of Scientific Research under Grant FA9550-23-1-0492. The work of V. Gupta was partially supported under ARO grant W911NF2310111 and ONR grant N000142312604. Y. Xu was also partially supported by the Purdue University College of Engineering Seed Funding for High Impact Papers, Books, and Monographs. The work of N. Atanasov and T. Duong was supported by NSF grants CCF-2112665 (TILOS) and CCF-2402689 (ExpandAI). The work of

F. Allgöwer was funded by the Deutsche Forschungsgemeinschaft (DFG, German Research Foundation) under Germany's Excellence Strategy – EXC 2075 – 390740016 and within grant AL 316/15-1 – 468094890. T. Martin thanks the Graduate Academy of the SC SimTech for its support.

References

- Agarwal, E., McCourt, M.J., Antsaklis, P.J., 2016. Dissipativity of hybrid systems: Feedback interconnections and networks, in: 2016 American Control Conference (ACC), IEEE. pp. 6060–6065.
- Agarwal, E., Sivarajani, S., Gupta, V., Antsaklis, P., 2019. Sequential synthesis of distributed controllers for cascade interconnected systems, in: 2019 American Control Conference (ACC), IEEE. pp. 5816–5821.
- Agarwal, E., Sivarajani, S., Gupta, V., Antsaklis, P., 2020. Compositional verification of passivity for cascade interconnected nonlinear systems, in: 2020 28th Mediterranean Conference on Control and Automation (MED), IEEE. pp. 319–324.
- Agarwal, E., Sivarajani, S., Gupta, V., Antsaklis, P.J., 2021. Distributed synthesis of local controllers for networked systems with arbitrary interconnection topologies. *IEEE Transactions on Automatic Control* 66.
- Alsatti, M., Lopez, V.G., Berberich, J., Allgöwer, F., Müller, M.A., 2022. Practical exponential stability of a robust data-driven nonlinear predictive control scheme. *arXiv preprint arXiv: 2204.01150v2*.
- Alsatti, M., Lopez, V.G., Müller, M.A., 2023. On the design of persistently exciting inputs for data-driven control of linear and nonlinear systems. *IEEE Control Systems Letters* 7, 2629–2634.
- Althoff, M., Frehse, G., Girard, A., 2021. Set propagation techniques for reachability analysis. *Annual Review of Control, Robotics, and Autonomous Systems* 4, 369–395.
- Amos, B., Xu, L., Kolter, J.Z., 2017. Input convex neural networks, in: International conference on machine learning, PMLR. pp. 146–155.
- Angeli, D., 2021. Monotone systems in biology, in: Encyclopedia of systems and control. Springer, pp. 1320–1327.
- Angeli, D., Sontag, E.D., 2003. Monotone control systems. *IEEE Transactions on automatic control* 48, 1684–1698.
- Antsaklis, P.J., Goodwine, B., Gupta, V., McCourt, M.J., Wang, Y., Wu, P., Xia, M., Yu, H., Zhu, F., 2013. Control of cyberphysical systems using passivity and dissipativity based methods. *European Journal of Control* 19, 379–388.

- Arcak, M., 2022. Compositional design and verification of large-scale systems using dissipativity theory: Determining stability and performance from subsystem properties and interconnection structures. *IEEE Control Systems Magazine* 42, 51–62.
- Arcak, M., Meissen, C., Packard, A., 2016. Networks of dissipative systems: compositional certification of stability, performance, and safety. Springer.
- Ayankoso, S., Olejnik, P., 2023. Time-series machine learning techniques for modeling and identification of mechatronic systems with friction: A review and real application. *Electronics* 12.
- Bai, S., Kolter, J.Z., Koltun, V., 2019. Deep equilibrium models. *Advances in neural information processing systems* 32.
- Bao, J., Lee, P.L., 2007. Process control: the passive systems approach. Springer Science & Business Media.
- Beattie, C., Mehrmann, V., Xu, H., Zwart, H., 2018. Linear port-Hamiltonian descriptor systems. *Mathematics of Control, Signals, and Systems* 30.
- Beattie, C.A., Mehrmann, V., Van Dooren, P., 2019. Robust port-Hamiltonian representations of passive systems. *Automatica* 100, 182–186.
- Beckers, T., 2023. Data-driven Bayesian Control of Port-Hamiltonian Systems, in: *IEEE Conference on Decision and Control (CDC)*.
- Beckers, T., Seidman, J., Perdikaris, P., Pappas, G.J., 2022. Gaussian Process Port-Hamiltonian Systems: Bayesian Learning with Physics Prior, in: *IEEE Conference on Decision and Control (CDC)*, pp. 1447–1453.
- Benner, P., Goyal, P., Van Dooren, P., 2020. Identification of port-Hamiltonian systems from frequency response data. *Systems and Control Letters* 143, 104741.
- Berberich, J., Köhler, J., Müller, M.A., Allgöwer, F., 2021. Data-driven model predictive control with stability and robustness guarantees. *IEEE Transactions on Automatic Control* 66, 1702–1717.
- Berberich, J., Köhler, J., Müller, M.A., Allgöwer, F., 2022a. Linear tracking mpc for nonlinear systems—part ii: The data-driven case. *IEEE Trans. Automat. Control* 67, 4406–4421.
- Berberich, J., Scherer, C.W., Allgöwer, F., 2022b. Combining prior knowledge and data for robust controller design. *IEEE Transactions on Automatic Control* 68, 4618–4633.
- Berkenkamp, F., Moriconi, R., Schoellig, A.P., Krause, A., 2016. Safe learning of regions of attraction for uncertain, nonlinear systems with gaussian processes, in: *IEEE Conference on Decision and Control (CDC)*, pp. 4661–4666.
- Berkenkamp, F., Turchetta, M., Schoellig, A., Krause, A., 2017. Safe model-based reinforcement learning with stability guarantees, in: *Advances in Neural Information Processing Systems (NeurIPS)*.
- Bertalan, T., Dietrich, F., Mezić, I., Kevrekidis, I.G., 2019. On learning Hamiltonian systems from data. *Chaos: An Interdisciplinary Journal of Nonlinear Science* 29.
- Bevanda, P., Beier, M., Kerz, S., Lederer, A., Sosnowski, S., Hirche, S., 2022. Diffeomorphically learning stable koopman operators. *IEEE Control Systems Letters* 6, 3427–3432.
- Bevanda, P., Sosnowski, S., Hirche, S., 2021. Koopman operator dynamical models: Learning, analysis and control. *Annual Reviews in Control* 52, 197–212.
- Bian, Y., Fu, X., Liu, B., Rachala, R., Gupta, R.K., Shi, Y., 2023. Bear-data: Analysis and applications of an open multizone building dataset, in: *Proceedings of the 10th ACM International Conference on Systems for Energy-Efficient Buildings, Cities, and Transportation*, pp. 240–243.
- Biloš, M., Sommer, J., Rangapuram, S.S., Januschowski, T., Günemann, S., 2021. Neural flows: Efficient alternative to neural odes. *Advances in Neural Information Processing Systems* 34, 21325–21337.
- Binder, M., Darivianakis, G., Eichler, A., Lygeros, J., 2019. Approximate explicit model predictive controller using Gaussian processes, in: *IEEE Conference on Decision and Control (CDC)*, pp. 841–846.
- Bingham, E., Chen, J.P., Jankowiak, M., Obermeyer, F., Pradhan, N., Karaletsos, T., Singh, R., Szerlip, P.A., Horsfall, P., Goodman, N.D., 2019. Pyro: Deep universal probabilistic programming. *J. Mach. Learn. Res.* 20, 28:1–28:6.
- Blanchini, F., Miani, S., et al., 2008. Set-theoretic methods in control. volume 78. Springer.
- Bonassi, F., Farina, M., Xie, J., Scattolini, R., 2022. On recurrent neural networks for learning-based control: Recent results and ideas for future developments. *Journal of Process Control* 114, 92–104.
- Boyd, S., Ghaoui, L.E., Feron, E., Balakrishnan, V., 1994. *Linear Matrix Inequalities in System and Control Theory*. SIAM, Philadelphia.
- Bradde, T., Grivet-Talocia, S., Calafio, G.C., Proskurnikov, A.V., Mahmood, Z., Daniel, L., 2020. Bounded input dissipativity of linearized circuit models. *IEEE Transactions on Circuits and Systems I: Regular Papers* 67, 2064–2077.
- Branford, E., Rapisarda, P., 2019. From Dirac structure to state model: identification of linear time-varying port-Hamiltonian systems, in: *IEEE Conference on Decision and Control (CDC)*, pp. 2666–2671.

- Brauer, F., Castillo-Chavez, C., Castillo-Chavez, C., 2012. Mathematical models in population biology and epidemiology. volume 2. Springer.
- Brogliato, B., Lozano, R., Maschke, B., Egeland, O., et al., 2007. Dissipative systems analysis and control. Theory and Applications 2, 2–5.
- Brunton, S.L., Proctor, J.L., Kutz, J.N., 2016. Discovering governing equations from data by sparse identification of nonlinear dynamical systems. Proceedings of the national academy of sciences 113, 3932–3937.
- Calliess, J.P., 2014. Conservative decision-making and inference in uncertain dynamical systems. PhD thesis, University of Oxford.
- Castañeda, F., Choi, J.J., Zhang, B., Tomlin, C.J., Sreenath, K., 2021. Pointwise feasibility of Gaussian process-based safety-critical control under model uncertainty, in: IEEE Conference on Decision and Control (CDC), pp. 6762–6769.
- Cerone, V., Piga, D., Regruto, D., 2011. Enforcing stability constraints in set-membership identification of linear dynamic systems. Automatica 47, 2488–2494.
- Champion, K., Zheng, P., Aravkin, A.Y., Brunton, S.L., Kutz, J.N., 2020. A unified sparse optimization framework to learn parsimonious physics-informed models from data. IEEE Access 8, 169259–169271.
- Chen, H., Fang, J., 2003. Enforcing bounded realness of s parameter through trace parameterization, in: Electrical Performance of Electrical Packaging (IEEE Cat. No. 03TH8710), IEEE. pp. 291–294.
- Chen, J., Gu, G., 2003. Control oriented system identification: An h approach. New York .
- Chen, R.T., Rubanova, Y., Bettencourt, J., Duvenaud, D.K., 2018a. Neural ordinary differential equations. Advances in neural information processing systems 31.
- Chen, R.T.Q., Amos, B., Nickel, M., 2021a. Learning neural event functions for ordinary differential equations, in: International Conference on Learning Representations.
- Chen, Y., Shi, Y., Zhang, B., 2018b. Optimal control via neural networks: A convex approach, in: International Conference on Learning Representations.
- Chen, Z., Liu, Y., Sun, H., 2021b. Physics-informed learning of governing equations from scarce data. Nature Communications 12.
- Chen, Z., Zhang, J., Arjovsky, M., Bottou, L., 2019. Symplectic recurrent neural networks. International Conference on Learning Representations (ICLR) .
- Chernyshenko, S.I., Goulart, P., Huang, D., Papachristodoulou, A., 2014. Polynomial sum of squares in fluid dynamics: a review with a look ahead. Philosophical Transactions of the Royal Society A 372, 20130350.
- Chou, C.T., Maciejowski, J.M., 1997. System identification using balanced parametrizations. IEEE transactions on automatic control 42, 956–974.
- Chung, J., Gulcehre, C., Cho, K., Bengio, Y., 2014. Empirical evaluation of gated recurrent neural networks on sequence modeling. arXiv preprint arXiv:1412.3555 .
- Coates, A., Hero III, A.O., Nowak, R., Yu, B., 2002. Internet tomography. IEEE Signal processing magazine 19, 47–65.
- Coelho, C.P., Phillips, J., Silveira, L.M., 2004. A convex programming approach for generating guaranteed passive approximations to tabulated frequency-data. IEEE Transactions on Computer-Aided Design of Integrated Circuits and Systems 23, 293–301.
- Coogan, S., 2019. A contractive approach to separable lyapunov functions for monotone systems. Automatica 106, 349–357.
- Coogan, S., Arcak, M., 2015. A compartmental model for traffic networks and its dynamical behavior. IEEE Transactions on Automatic Control 60, 2698–2703.
- Coulson, J., Lygeros, J., Dörfler, F., 2019. Data-enabled predictive control: In the shallows of the deepc, in: European Control Conference (ECC), pp. 307–312.
- Cranmer, M., Greydanus, S., Hoyer, S., Battaglia, P., Spergel, D., Ho, S., 2020. Lagrangian neural networks. arXiv preprint arXiv:2003.04630 .
- Cui, W., Jiang, Y., Zhang, B., Shi, Y., 2024. Structured neural-pi control with end-to-end stability and output tracking guarantees. Advances in Neural Information Processing Systems 36.
- Cuomo, S., Cola, V.S.D., Giampaolo, F., Rozza, G., Raissi, M., Piccialli, F., 2022. Scientific machine learning through physics-informed neural networks: Where we are and what's next. Journal of Scientific Computing 92.
- Daniels, H., Velikova, M., 2010. Monotone and partially monotone neural networks. IEEE Transactions on Neural Networks 21, 906–917.
- De Persis, C., Rotulo, M., Tesi, P., 2022. Learning controllers from data via approximate nonlinearity cancellation. IEEE Trans. Automat. Control .
- De Persis, C., Tesi, P., 2020. Formulas for data-driven control: Stabilization, optimality and robustness. IEEE Trans. Automat. Control 65, 909–924.
- De Persis, C., Tesi, P., 2021. Designing experiments for data-driven control of nonlinear systems, in: Proc. Symposium on Mathematical Theory of Networks and Systems, p. 285–290.
- Delgado, A., Kambhampati, C., Warwick, K., 1995. Dynamic recurrent neural network for system identification and control. IEE Proceedings-Control Theory and Applications 142, 307–314.

- Dhiman, V., Khojasteh, M.J., Franceschetti, M., Atanasov, N., 2023. Control Barriers in Bayesian Learning of System Dynamics. *IEEE Transactions on Automatic Control (TAC)* 68, 214–229.
- DiPietro, D., Xiong, S., Zhu, B., 2020. Sparse symplectically integrated neural networks. *Advances in Neural Information Processing Systems* 33, 6074–6085.
- Dirr, G., Ito, H., Rantzer, A., Rüffer, B., 2015. Separable lyapunov functions for monotone systems: Constructions and limitations. *Discrete Contin. Dyn. Syst. Ser. B* 20, 2497–2526.
- Doerr, A., Daniel, C., Schiegg, M., Duy, N.T., Schaal, S., Toussaint, M., Sebastian, T., 2018. Probabilistic recurrent state-space models, in: International Conference on Machine Learning (ICML), pp. 1280–1289.
- Drgona, J., Nghiem, T.X., Beckers, T., Fazlyab, M., Mallada, E., Jones, C., Vrabie, D., Brunton, S.L., Findeisen, R., 2025. Safe physics-informed machine learning for dynamics and control. *arXiv preprint arXiv:2504.12952* .
- Drgoňa, J., Tuor, A.R., Chandan, V., Vrabie, D.L., 2021. Physics-constrained deep learning of multi-zone building thermal dynamics. *Energy and Buildings* 243, 110992.
- Dumitrescu, B., 2002. Parameterization of positive-real transfer functions with fixed poles. *IEEE Transactions on Circuits and Systems I: Fundamental Theory and Applications* 49, 523–526.
- Duong, T., Altawaitan, A., Stanley, J., Atanasov, N., 2024a. Port-Hamiltonian neural ODE networks on Lie groups for robot dynamics learning and control. *IEEE Transactions on Robotics* 40, 3695–3715.
- Duong, T., Altawaitan, A., Stanley, J., Atanasov, N., 2024b. Port-hamiltonian neural ODE networks on Lie groups for robot dynamics learning and control. *IEEE Transactions on Robotics* 40, 3695–3715.
- Duong, T., Atanasov, N., 2021. Hamiltonian-based neural ode networks on the se (3) manifold for dynamics learning and control. *arXiv preprint arXiv:2106.12782* .
- Dupont, E., Doucet, A., Teh, Y.W., 2019. Augmented neural odes. *Advances in neural information processing systems* 32.
- Eleftheriadis, S., Nicholson, T., Deisenroth, M., Hensman, J., 2017. Identification of gaussian process state space models, in: Advances in Neural Information Processing Systems (NeurIPS).
- Evangelisti, G., Hirche, S., 2022. Physically consistent learning of conservative Lagrangian systems with Gaussian processes, in: IEEE Conference on Decision and Control (CDC), pp. 4078–4085.
- Evangelisti, G., Hirche, S., 2024. Data-driven momentum observers with physically consistent gaussian processes. *IEEE Transactions on Robotics* 40, 1938–1951.
- Fan, F., Yi, B., Rye, D., Shi, G., Manchester, I.R., 2022. Learning stable koopman embeddings, in: 2022 American Control Conference (ACC), IEEE. pp. 2742–2747.
- Fan, F., Yi, B., Rye, D., Shi, G., Manchester, I.R., 2024. Learning stable koopman embeddings for identification and control. *arXiv preprint arXiv:2401.08153* .
- Faroughi, S.A., Pawar, N.M., Fernandes, C., Raissi, M., Das, S., Kalantari, N.K., Kourosh Mahjour, S., 2024. Physics-guided, physics-informed, and physics-encoded neural networks and operators in scientific computing: Fluid and solid mechanics. *Journal of Computing and Information Science in Engineering* 24, 040802.
- Fattah, S., Matni, N., Sojoudi, S., 2019. Learning sparse dynamical systems from a single sample trajectory, in: 2019 IEEE 58th Conference on Decision and Control (CDC), IEEE. pp. 2682–2689.
- Feng, J., Cui, W., Cortés, J., Shi, Y., 2025. Online event-triggered switching for frequency control in power grids with variable inertia. *IEEE Transactions on Power Systems* 40, 3347–3360.
- Feng, J., Shi, Y., Qu, G., Low, S.H., Anandkumar, A., Wierman, A., 2023. Stability constrained reinforcement learning for decentralized real-time voltage control. *IEEE Transactions on Control of Network Systems* , 1–12.
- Fiedler, C., Scherer, C., Trimpe, S., 2021. Learning-enhanced robust controller synthesis with rigorous statistical and control-theoretic guarantees, in: Proc. 60th Conf. Decision and Control (CDC), pp. 5122–5129.
- Finzi, M., Wang, K.A., Wilson, A.G., 2020. Simplifying Hamiltonian and Lagrangian neural networks via explicit constraints, in: Advances in Neural Information Processing Systems (NeurIPS).
- Fogel, E., 1979. System identification via membership set constraints with energy constrained noise. *IEEE Transactions on Automatic Control* 24, 752–758.
- Forbes, J.R., 2011. Extensions of input-output stability theory and the control of aerospace systems. University of Toronto.
- Forni, F., Sepulchre, R., van der Schaft, A.J., 2013. On differential passivity of physical systems, in: Proc. 52nd IEEE Conference on Decision and Control (CDC), pp. 6580–6585.
- Frigola, R., Chen, Y., Rasmussen, C.E., 2014. Variational gaussian process state-space models, in: Advances in Neural Information Processing Systems (NeurIPS).

- Frigola, R., Lindsten, F., Schön, T.B., Rasmussen, C.E., 2013. Bayesian inference and learning in Gaussian process state-space models with particle MCMC, in: Advances in Neural Information Processing Systems (NeurIPS).
- Fu, X., Fan, K., Zozmann, H., Schüller, L., Calabrese, J.M., 2024. Simultaneous identification of changepoints and model parameters in switching dynamical systems. bioRxiv , 2024–01.
- Funahashi, K.i., Nakamura, Y., 1993. Approximation of dynamical systems by continuous time recurrent neural networks. *Neural networks* 6, 801–806.
- Gaby, N., Zhang, F., Ye, X., 2022. Lyapunov-Net: A deep neural network architecture for Lyapunov function approximation, in: IEEE Conference on Decision and Control (CDC), pp. 2091–2096.
- Gardner, J.R., Pleiss, G., Bindel, D., Weinberger, K.Q., Wilson, A.G., 2018. GPY Torch: Blackbox matrix-matrix Gaussian process inference with GPU acceleration, in: Advances in Neural Information Processing Systems (NeurIPS).
- Geneva, N., Zabarasz, N., 2022. Transformers for modeling physical systems. *Neural Networks* 146, 272–289.
- Gevers, M., 2005. Identification for control: From the early achievements to the revival of experiment design. *European journal of control* 11, 335–352.
- Gevers, M., Ljung, L., 1986. Optimal experiment designs with respect to the intended model application. *Automatica* 22, 543–554.
- Gillespie, M.T., Best, C.M., Townsend, E.C., Wingate, D., Killpack, M.D., 2018. Learning nonlinear dynamic models of soft robots for model predictive control with neural networks, in: 2018 IEEE International Conference on Soft Robotics (RoboSoft), IEEE. pp. 39–45.
- Glorot, X., Bordes, A., Bengio, Y., 2011. Deep sparse rectifier neural networks, in: Proceedings of the fourteenth international conference on artificial intelligence and statistics, JMLR Workshop and Conference Proceedings. pp. 315–323.
- Goethals, I., Van Gestel, T., Suykens, J., Van Dooren, P., De Moor, B., 2003. Identifying positive real models in subspace identification by using regularization. *IFAC Proceedings Volumes* 36, 1369–1373.
- Gokhale, G., Claessens, B., Develder, C., 2022. Physics informed neural networks for control oriented thermal modeling of buildings. *Applied Energy* 314, 118852.
- Golubitsky, M., Stewart, I., 2002. The symmetry perspective: from equilibrium to chaos in phase space and physical space. volume 200. Springer.
- Goodwin, G.C., 1977. Dynamic system identification: experiment design and data analysis. *Mathematics in science and engineering* 136.
- Grancharova, A., Kocjan, J., Johansen, T.A., 2007. Explicit stochastic nonlinear predictive control based on Gaussian process models, in: European Control Conference (ECC), pp. 2340–2347.
- Granger, C., 2001. Investigating causal relations by econometric models and cross-spectral methods, in: Essays in econometrics: collected papers of Clive WJ Granger, pp. 31–47.
- Greiner, W., Müller, B., 2012. Quantum mechanics: symmetries. Springer Science & Business Media.
- Greydanus, S., Dzamba, M., Yosinski, J., 2019. Hamiltonian neural networks, in: Advances in Neural Information Processing Systems.
- Greydanus, S., Sosanya, A., 2022. Dissipative hamiltonian neural networks: Learning dissipative and conservative dynamics separately. arXiv preprint arXiv:2201.10085 .
- Grivet-Talocia, S., 2004. Passivity enforcement via perturbation of hamiltonian matrices. *IEEE Transactions on Circuits and Systems I: Regular Papers* 51, 1755–1769.
- Grivet-Talocia, S., Gustavsen, B., 2015. Passive macromodeling: Theory and applications. John Wiley & Sons.
- Grivet-Talocia, S., Ubolli, A., 2006. On the generation of large passive macromodels for complex interconnect structures. *IEEE transactions on advanced packaging* 29, 39–54.
- Grizzle, J.W., Chevallereau, C., Sinnet, R.W., Ames, A.D., 2014. Models, feedback control, and open problems of 3d bipedal robotic walking. *Automatica* 50, 1955–1988.
- Guo, M., De Persis, C., Tesi, P., 2022. Data-driven stabilization of nonlinear polynomial systems with noisy data. *IEEE Trans. Automat. Control* 67, 4210–4217.
- Gupta, J.K., Menda, K., Manchester, Z., Kochenderfer, M.J., 2019. A general framework for structured learning of mechanical systems. arXiv preprint arXiv:1902.08705 .
- Gustavsen, B., 2007. Computer code for passivity enforcement of rational macromodels by residue perturbation. *IEEE Transactions on Advanced Packaging* 30, 209–215.
- Gustavsen, B., 2008. Passivity enforcement of rational models via modal perturbation. *IEEE Transactions on Power Delivery* 23, 768–775.
- Gustavsen, B., Semlyen, A., 1999. Rational approximation of frequency domain responses by vector fitting. *IEEE Transactions on power delivery* 14, 1052–1061.
- Gustavsen, B., Semlyen, A., 2001. Enforcing passivity for admittance matrices approximated by rational functions. *IEEE transactions on power systems* 16, 97–104.
- Haddad, W.M., Chellaboina, V., Hui, Q., 2010. Nonnegative and compartmental dynamical systems. Princeton University Press.

- Haddad, W.M., Chellaboina, V., Nersesov, S.G., 2006. Impulsive and hybrid dynamical systems: stability, dissipativity, and control. Princeton University Press.
- Han, X., Gao, H., Pfaff, T., Wang, J.X., Liu, L., 2022. Predicting physics in mesh-reduced space with temporal attention, in: International Conference on Learning Representations.
- Hanson, J., Raginsky, M., 2020. Universal simulation of stable dynamical systems by recurrent neural nets, in: Learning for Dynamics and Control, PMLR. pp. 384–392.
- Hanson, J., Raginsky, M., Sontag, E., 2021. Learning recurrent neural net models of nonlinear systems, in: Learning for Dynamics and Control, PMLR. pp. 425–435.
- Hao, W., Huang, B., Pan, W., Wu, D., Mou, S., 2024. Deep koopman learning of nonlinear time-varying systems. *Automatica* 159, 111372.
- Hara, K., Inoue, M., Sebe, N., 2020. Learning koopman operator under dissipativity constraints. *IFAC-PapersOnLine* 53, 1169–1174.
- Haseli, M., Cortés, J., 2023. Modeling nonlinear control systems via koopman control family: Universal forms and subspace invariance proximity. arXiv preprint arXiv:2307.15368 .
- Hassanian, R., Myneni, H., Helgadóttir, A., Riedel, M., 2023. Deciphering the dynamics of distorted turbulent flows: Lagrangian particle tracking and chaos prediction through transformer-based deep learning models. *Physics of Fluids* 35.
- Hatanaka, T., Chopra, N., Fujita, M., Spong, M.W., 2015. Passivity-based control and estimation in networked robotics. Springer.
- Hewing, L., Kabzan, J., Zeilinger, M.N., 2020. Cautious model predictive control using Gaussian process regression. *IEEE Transactions on Control Systems Technology* 28, 2736–2743.
- Hill, D.J., Moylan, P., 1980. Dissipative dynamical systems: Basic input-output and state properties. *Journal of The Franklin Institute-engineering and Applied Mathematics* 309, 327–357.
- Hines, G.H., Arcak, M., Packard, A.K., 2011. Equilibrium-independent passivity: A new definition and numerical certification. *Automatica* 47, 1949–1956.
- Hirsch, M., Smith, H., 2005. Monotone dynamical systems. *Handbook of Differential Equations: Ordinary Differential Equations* 2, 239.
- Hjalmarsson, H., 2005. From experiment design to closed-loop control. *Automatica* 41, 393–438.
- Hoagg, J.B., Lacy, S.L., Erwin, R.S., Bernstein, D.S., 2004. First-order-hold sampling of positive real systems and subspace identification of positive real models, in: Proceedings of the 2004 American control conference, IEEE. pp. 861–866.
- Hochlehnert, A., Terenin, A., Sæmundsson, S., Deisenroth, M., 2021. Learning contact dynamics using physically structured neural networks, in: International Conference on Artificial Intelligence and Statistics, PMLR. pp. 2152–2160.
- Hochreiter, S., Schmidhuber, J., 1997. Long short-term memory. *Neural computation* 9, 1735–1780.
- Holm, D., 2008. Geometric Mechanics. World Scientific Publishing Company.
- Holmsen, S., Eidnes, S., Riemer-Sørensen, S., 2023. Pseudo-hamiltonian system identification. arXiv preprint arXiv:2305.06920 .
- Hornik, K., Stinchcombe, M., White, H., 1989. Multilayer feedforward networks are universal approximators. *Neural networks* 2, 359–366.
- Hou, Z.S., Wang, Z., 2013. From model-based control to data-driven control: Survey, classification and perspective. *Information Sciences* 235, 3–35.
- Hu, Z., De Persis, C., Tesi, P., 2023. Learning controllers from data via kernel-based interpolation , 8509–8514.
- Huang, B., Ma, X., Vaidya, U., 2018. Feedback stabilization using koopman operator, in: 2018 IEEE Conference on Decision and Control (CDC), IEEE. pp. 6434–6439.
- Huang, B., Wang, J., 2023. Applications of physics-informed neural networks in power systems - a review. *IEEE Transactions on Power Systems* 38, 572–588.
- Huang, Y., Rodriguez, I.D.J., Zhang, H., Shi, Y., Yue, Y., 2023. Fi-ode: Certified and robust forward invariance in neural odes. arXivorg .
- Iijima, K., Tanemura, M., Azuma, S.i., Chida, Y., 2020. Reduction in the amount of data for data-driven passivity estimation, in: 2020 IEEE Conference on Control Technology and Applications (CCTA), IEEE. pp. 134–139.
- Isoshima, K., Tanemura, M., Chida, Y., 2023. Data-driven estimation of the lower bounds of gain and phase margins. *Automatica* 153, 111008.
- Jena, A., Huang, T., Sivarajanji, S., Kalathil, D., Xie, L., 2021. Distributed learning-based stability assessment for large scale networks of dissipative systems, in: 2021 60th IEEE Conference on Decision and Control (CDC), IEEE. pp. 1509–1514.
- Kaptanoglu, A.A., Callaham, J.L., Aravkin, A., Hansen, C.J., Brunton, S.L., 2021. Promoting global stability in data-driven models of quadratic nonlinear dynamics. *Physical Review Fluids* 6, 094401.

- Kaptanoglu, A.A., Silva, B.T., Brunton, S.L., Kutz, J.N., 2024. Pysindy example: Trapping sindy for lorenz model. URL: https://pysindy.readthedocs.io/en/stable/examples/8_trapping_sindy_paper_examples/example.html. accessed: 2024-04-15.
- Karniadakis, G., Kevrekidis, I., Lu, L., Perdikaris, P., Wang, S., Li, Y., 2021. Physics-informed machine learning. *Nature Reviews Physics* 3, 422–440.
- Kelly, J., Bettencourt, J., Johnson, M.J., Duvenaud, D.K., 2020. Learning differential equations that are easy to solve. *Advances in Neural Information Processing Systems* 33, 4370–4380.
- Khalil, H.K., 2002. Nonlinear Systems (3rd ed.). Prentice Hall.
- Koch, A., Berberich, J., Allgöwer, F., 2022. Provably robust verification of dissipativity properties from data. *IEEE Transactions on Automatic Control* 67, 4248–4255.
- Koch, A., Berberich, J., Köhler, J., Allgöwer, F., 2021. Determining optimal input-output properties: A data-driven approach. *Automatica* 134, 109906.
- Kocijan, J., 2016. Modelling and control of dynamic systems using Gaussian process models. Springer.
- Kolter, J.Z., Manek, G., 2019. Learning stable deep dynamics models. *Advances in neural information processing systems* 32.
- Korda, M., Mezić, I., 2018. Linear predictors for nonlinear dynamical systems: Koopman operator meets model predictive control. *Automatica* 93, 149–160.
- Kottenstette, N., Antsaklis, P.J., 2010. Relationships between positive real, passive dissipative, & positive systems, in: *Proceedings of the 2010 American control conference*, IEEE. pp. 409–416.
- Kuschewski, J.G., Hui, S., Zak, S.H., 1993. Application of feedforward neural networks to dynamical system identification and control. *IEEE transactions on control systems technology* 1, 37–49.
- Lacy, S.L., Bernstein, D.S., 2003. Subspace identification with guaranteed stability using constrained optimization. *IEEE Transactions on automatic control* 48, 1259–1263.
- Lai, Z., Mylonas, C., Nagarajaiah, S., Chatzi, E., 2021. Structural identification with physics-informed neural ordinary differential equations. *Journal of Sound and Vibration* 508, 116196.
- Lauer, F., Bloch, G., 2018. Hybrid system identification: Theory and algorithms for learning switching models. volume 478. Springer.
- Lauricella, M., 2020. Set membership identification and filtering of linear systems with guaranteed accuracy .
- Lauricella, M., Fagiano, L., 2020. Set membership identification of linear systems with guaranteed simulation accuracy. *IEEE Transactions on Automatic Control* 65, 5189–5204.
- Lavaei, A., Zamani, M., 2022. From dissipativity theory to compositional synthesis of large-scale stochastic switched systems. *IEEE Transactions on Automatic Control* 67, 4422–4437.
- Lawrence, N., Loewen, P., Forbes, M., Backstrom, J., Gopaluni, B., 2020. Almost surely stable deep dynamics. *Advances in Neural Information Processing Systems* 33, 18942–18953.
- Lechner, M., Hasani, R., Rus, D., Grosu, R., 2020. Gershgorin loss stabilizes the recurrent neural network compartment of an end-to-end robot learning scheme, in: *2020 IEEE International Conference on Robotics and Automation (ICRA)*, IEEE. pp. 5446–5452.
- Lee, K., Trask, N., Stinis, P., 2022. Structure-preserving sparse identification of nonlinear dynamics for data-driven modeling, in: *Mathematical and Scientific Machine Learning, PMLR*. pp. 65–80.
- Leenheer, P.D., Angeli, D., Sontag, E.D., 2007. Monotone chemical reaction networks. *Journal of mathematical chemistry* 41, 295–314.
- Li, J., Zhao, J., Chen, C., 2016. Dissipativity and feedback passivation for switched discrete-time nonlinear systems. *Systems & Control Letters* 87, 47–55.
- Li, Z., Shu, D., Barati Farimani, A., 2023. Scalable transformer for pde surrogate modeling, in: *Advances in Neural Information Processing Systems*, Curran Associates, Inc.. pp. 28010–28039.
- Liu, J., Borja, P., Della Santina, C., 2024a. Physics-informed neural networks to model and control robots: A theoretical and experimental investigation. *Advanced Intelligent Systems* 6, 2300385.
- Liu, X., Cheng, W., Xing, J., Chen, X., Zhao, Z., Zhang, R., Huang, Q., Lu, J., Zhou, H., Zheng, W.X., Pan, W., 2024b. Physics-informed neural network for system identification of rotors. *IFAC-PapersOnLine* 58, 307–312. 20th IFAC Symposium on System Identification SYSID 2024.
- Liu, X., Han, X., Zhang, N., Liu, Q., 2020. Certified monotonic neural networks. *Advances in Neural Information Processing Systems* 33, 15427–15438.
- Ljung, L., 2010. Perspectives on system identification. *Annual Reviews in Control* 34, 1–12.
- Ljung, L., Andersson, C., Tiels, K., Schön, T.B., 2020. Deep learning and system identification. *IFAC-PapersOnLine* 53, 1175–1181.
- Ljung, L., et al., 1987. Theory for the user. *System identification* .

- Löfberg, J., 2004. Yalmip: A toolbox for modeling and optimization in matlab, in: IEEE International Conference on Robotics and Automation, pp. 284–289.
- Long, K., Dhiman, V., Leok, M., Cortés, J., Atanasov, N., 2022. Safe control synthesis with uncertain dynamics and constraints. *IEEE Robotics and Automation Letters* 7, 7295–7302.
- Lopez, V.G., Müller, M.A., 2022. On a continuous-time version of willems’ lemma, in: 2022 IEEE 61st conference on decision and control (CDC), IEEE. pp. 2759–2764.
- Lovisari, E., Como, G., Savla, K., 2014. Stability of monotone dynamical flow networks, in: 53rd IEEE Conference on Decision and Control, IEEE. pp. 2384–2389.
- Lu, S., Basar, T., 1998. Robust nonlinear system identification using neural-network models. *IEEE Transactions on Neural Networks* 9, 407–429.
- Luppi, A., De Persis, C., Tesi, P., 2022. On data-driven stabilization of systems with nonlinearities satisfying quadratic constraints. *Systems & Control Lett.* 163, 105206.
- Lurie, A.I., 2002. Analytical Mechanics. Springer Science & Business Media.
- Lutter, M., Listmann, K., Peters, J., 2019. Deep Lagrangian Networks for end-to-end learning of energy-based control for under-actuated systems, in: IEEE/RSJ International Conference on Intelligent Robots and Systems (IROS).
- Lutter, M., Ritter, C., Peters, J., 2018. Deep Lagrangian networks: using physics as model prior for deep learning, in: International Conference on Learning Representations (ICLR).
- Mabrok, M.A., Aksikas, I., Meskin, N., 2023. Koopman operator approximation under negative imaginary constraints. *IEEE Control Systems Letters* 7, 2767–2772.
- Mabrok, M.A., Kallapur, A.G., Petersen, I.R., Lanzon, A., 2011. Enforcing a system model to be negative imaginary via perturbation of hamiltonian matrices, in: 2011 50th IEEE Conference on Decision and Control and European Control Conference, IEEE. pp. 3748–3752.
- Maciejowski, J.M., 1995. Guaranteed stability with subspace methods. *Systems & Control Letters* 26, 153–156.
- Majumdar, A., Ahmadi, A.A., Tedrake, R., 2013. Control design along trajectories with sums of squares programming, in: Proc. IEEE International Conference on Robotics and Automation, pp. 4054–4061.
- Makdesi, A., Girard, A., Fribourg, L., 2023. Data-driven models of monotone systems. *IEEE Transactions on Automatic Control* 69, 5294–5309.
- Mäkilä, P.M., Partington, J.R., Gustafsson, T.K., 1995. Worst-case control-relevant identification. *Automatica* 31, 1799–1819.
- Manchester, I.R., Tobenkin, M.M., Megretski, A., 2012. Stable nonlinear system identification: Convexity, model class, and consistency. *IFAC Proceedings Volumes* 45, 328–333.
- Mangan, N.M., Brunton, S.L., Proctor, J.L., Kutz, J.N., 2016. Inferring biological networks by sparse identification of nonlinear dynamics. *IEEE Transactions on Molecular, Biological, and Multi-Scale Communications* 2, 52–63.
- Markovsky, I., 2014. Low-rank approximation: Algorithms, implementation, applications. Springer.
- Markovsky, I., Dörfler, F., 2021. Behavioral systems theory in data-driven analysis, signal processing, and control. *Annual Reviews in Control* 52, 42–64.
- Markovsky, I., Prieto-Araujo, E., Dörfler, F., 2023. On the persistency of excitation. *Automatica* 147, 110657.
- Markovsky, I., Rapisarda, P., 2008. Data-driven simulation and control. *International Journal of Control* 81, 1946–1959.
- Marquez, H., Damaren, C., 1995. On the design of strictly positive real transfer functions. *IEEE Transactions on Circuits and Systems I: Fundamental Theory and Applications* 42, 214–218.
- Marsden, J., Ratiu, T., 2013. Introduction to Mechanics and Symmetry: A Basic Exposition of Classical Mechanical Systems. Springer Science & Business Media.
- Martin, T., Allgöwer, F., 2020. Iterative data-driven inference of nonlinearity measures via successive graph approximation, in: Proc. 59th Conference on Decision and Control (CDC), pp. 4760–4765.
- Martin, T., Allgöwer, F., 2021a. Data-driven system analysis of nonlinear systems using polynomial approximation. arXiv preprint arXiv: 2108.11298 .
- Martin, T., Allgöwer, F., 2021b. Dissipativity verification with guarantees for polynomial systems from noisy input-state data. *IEEE Control Systems Letters* 5, 1399–1404.
- Martin, T., Allgöwer, F., 2022a. Data-driven inference on optimal input-output properties of polynomial systems with focus on nonlinearity measures. *IEEE Transactions on Automatic Control* 68, 2832–2847.
- Martin, T., Allgöwer, F., 2022b. Determining dissipativity for nonlinear systems from noisy data using Taylor polynomial approximation, in: Proc. American Control Conference (ACC), pp. 1432–1437.
- Martin, T., Koch, A., Allgöwer, F., 2020. Data-driven surrogate models for LTI systems via saddle-point dynamics, in: Proc. 21st IFAC World Congress, pp. 953–958.
- Martin, T., Schön, T.B., Allgöwer, F., 2023. Guarantees for data-driven control of nonlinear systems using semidefinite programming: A survey. *Annual Reviews in Control* .

- Martinelli, D., Galimberti, C.L., Manchester, I.R., Furieri, L., Ferrari-Trecate, G., 2023. Unconstrained parametrization of dissipative and contracting neural ordinary differential equations, in: 2023 62nd IEEE Conference on Decision and Control (CDC), IEEE. pp. 3043–3048.
- Matthews, A.G.d.G., van der Wilk, M., Nickson, T., Fujii, K., Boukouvalas, A., León-Villagrá, P., Ghahramani, Z., Hensman, J., 2017. GPflow: A Gaussian process library using TensorFlow. *Journal of Machine Learning Research* 18.
- Maupong, T.M., Mayo-Maldonado, J.C., Rapisarda, P., 2017. On Lyapunov functions and data-driven dissipativity, in: Proc. 20th IFAC World Congress, pp. 7783–7788.
- Mauroy, A., Goncalves, J., 2016. Linear identification of non-linear systems: A lifting technique based on the koopman operator, in: 2016 IEEE 55th Conference on Decision and Control (CDC), IEEE. pp. 6500–6505.
- Mayo, A., Antoulas, A., 2007. A framework for the solution of the generalized realization problem. *Linear Algebra and its Applications* 425, 634–662.
- McCourt, M.J., Antsaklis, P.J., 2012. Stability of interconnected switched systems using qsr dissipativity with multiple supply rates, in: 2012 American Control Conference (ACC), IEEE. pp. 4564–4569.
- Megretski, A., 2008. Convex optimization in robust identification of nonlinear feedback, in: 2008 47th IEEE Conference on Decision and Control, IEEE. pp. 1370–1374.
- Megretski, A., Rantzer, A., 1997. System analysis via integral quadratic constraints. *IEEE Transactions on Automatic Control* 42, 819–830.
- Mehrmann, V., Unger, B., 2023. Control of port-hamiltonian differential-algebraic systems and applications. *Acta Numerica* 32, 395–515.
- Mikulincer, D., Reichman, D., 2022. Size and depth of monotone neural networks: interpolation and approximation. *Advances in Neural Information Processing Systems* 35, 5522–5534.
- Milanese, M., Norton, J., Piet-Lahanier, H., Walter, É., 2013. Bounding approaches to system identification. Springer Science & Business Media.
- Milanese, M., Vicino, A., 1991. Optimal estimation theory for dynamic systems with set membership uncertainty: An overview. *Automatica* 27, 997–1009.
- Miller, J., Sznajer, M., 2023. Data-driven gain scheduling control of linear parameter-varying systems using quadratic matrix inequalities. *IEEE Control Systems Letters* 7, 835–840.
- Miller, S.T., Lindner, J.F., Choudhary, A., Sinha, S., Ditto, W.L., 2020. The scaling of physics-informed machine learning with data and dimensions. *Chaos, Solitons & Fractals: X* 5, 100046.
- Min, Y., Richards, S.M., Azizan, N., 2023. Data-driven control with inherent lyapunov stability, in: 2023 62nd IEEE Conference on Decision and Control (CDC), IEEE. pp. 6032–6037.
- Mitjans, M., Wu, L., Tron, R., 2024. Learning deep koopman operators with convex stability constraints. arXiv preprint arXiv:2404.15978 .
- MOSEK ApS, 2025. MOSEK optimization suite. <https://www.mosek.com/>.
- Mowlavi, S., Nabi, S., 2023. Optimal control of pdes using physics-informed neural networks. *Journal of Computational Physics* 473, 111731.
- Nagabandi, A., Kahn, G., Fearing, R.S., Levine, S., 2018. Neural network dynamics for model-based deep reinforcement learning with model-free fine-tuning, in: 2018 IEEE international conference on robotics and automation (ICRA), IEEE. pp. 7559–7566.
- Nageshrao, S.P., Lopes, G.A.D., Jeltsema, D., Babuška, R., 2016. Port-Hamiltonian systems in adaptive and learning control: A survey. *IEEE Transactions on Automatic Control* 61, 1223–1238.
- Narendra, K.S., Annaswamy, A.M., 1987. Persistent excitation in adaptive systems. *International Journal of Control* 45, 127–160.
- Nghiem, T.X., Drgoňa, J., Jones, C., Nagy, Z., Schwan, R., Dey, B., Chakrabarty, A., Di Cairano, S., Paulson, J.A., Caron, A., et al., 2023. Physics-informed machine learning for modeling and control of dynamical systems. arXiv preprint arXiv:2306.13867 .
- Nicodemus, J., Kneifl, J., Fehr, J., Unger, B., 2022. Physics-informed neural networks-based model predictive control for multi-link manipulators. *IFAC-PapersOnLine* 55, 331–336. 10th Vienna International Conference on Mathematical Modelling MATHMOD 2022.
- Noether, E., 1983. Invariante variationsprobleme, in: Gesammelte Abhandlungen-Collected Papers. Springer, pp. 231–239.
- O'Brien, C.M., 2016. Statistical learning with sparsity: the lasso and generalizations .
- Ochoa, D.E., Galarza-Jimenez, F., Wilches-Bernal, F., Schoenwald, D.A., Poveda, J.I., 2023. Control systems for low-inertia power grids: A survey on virtual power plants. *IEEE Access* 11, 20560–20581.
- Okamoto, Y., Kojima, R., 2024. Learning deep dissipative dynamics. arXiv preprint arXiv:2408.11479 .
- Opdenacker, P.C., Jonckheere, E.A., 1988. A contraction mapping preserving balanced reduction scheme and its infinity norm error bounds. *IEEE Transactions on Circuits and Systems* 35, 184–189.

- Ortega, J.P., Yin, D., 2024. Learnability of linear port-Hamiltonian systems. *Journal of Machine Learning Research* 25, 1–56.
- Ortega, R., Perez, J.A.L., Nicklasson, P.J., Sira-Ramirez, H.J., 2013. Passivity-based control of Euler-Lagrange systems: mechanical, electrical and electromechanical applications. Springer Science & Business Media.
- Ortega, R., van der Schaft, A., Castanos, F., Astolfi, A., 2008. Control by interconnection and standard passivity-based control of port-Hamiltonian systems. *IEEE Transactions on Automatic Control* 53, 2527–2542.
- Ortega, R., van der Schaft, A., Maschke, B., Escobar, G., 1999. Energy-shaping of port-controlled Hamiltonian systems by interconnection, in: *IEEE Conference on Decision and Control (CDC)*, pp. 1646–1651.
- Ortega, R., Van Der Schaft, A.J., Mareels, I., Maschke, B., 2001. Putting energy back in control. *IEEE Control Systems Magazine* 21, 18–33.
- Pan, S., Duraisamy, K., 2018. Long-time predictive modeling of nonlinear dynamical systems using neural networks. *Complexity* 2018, 4801012.
- Pan, Y., Wang, J., 2011. Model predictive control of unknown nonlinear dynamical systems based on recurrent neural networks. *IEEE Transactions on Industrial Electronics* 59, 3089–3101.
- Panerati, J., Zheng, H., Zhou, S., Xu, J., Prorok, A., Schöllig, A., 2020. Learning to Fly: a PyBullet Gym Environment to Learn the Control of Multiple Nano-quadcopters. <https://github.com/utiasDSL/gym-pybullet-drones>.
- Park, J., Babaei, M.R., Munoz, S.A., Venkat, A.N., Hedengren, J.D., 2023. Simultaneous multistep transformer architecture for model predictive control. *Computers & Chemical Engineering* 178, 108396.
- Pascanu, R., Gulcehre, C., Cho, K., Bengio, Y., 2013. How to construct deep recurrent neural networks. *arXiv preprint arXiv:1312.6026*.
- Pearl, J., 2010. Causal inference. *Causality: objectives and assessment*, 39–58.
- Peternell, K., 1995. Identification of linear dynamic systems by subspace and realization-based algorithms. na.
- Pillonetto, G., Aravkin, A., Gedon, D., Ljung, L., Ribeiro, A.H., Schön, T.B., 2023. Deep networks for system identification: a survey. *arXiv preprint arXiv:2301.12832*.
- Pillonetto, G., Aravkin, A., Gedon, D., Ljung, L., Ribeiro, A.H., Schön, T.B., 2025. Deep networks for system identification: a survey. *Automatica* 171, 111907.
- Pillonetto, G., Dinuzzo, F., Chen, T., De Nicolao, G., Ljung, L., 2014. Kernel methods in system identification, machine learning and function estimation: A survey. *Automatica* 50, 657–682.
- Pinder, T., Dodd, D., 2022. GPJax: A Gaussian process framework in JAX. *Journal of Open Source Software* 7, 4455.
- Pintelon, R., Schoukens, J., 2012. System identification: a frequency domain approach. John Wiley & Sons.
- Plaza, S.S.E., Reyes-Baez, R., Jayawardhana, B., 2022. Total energy shaping with neural interconnection and damping assignment - passivity based control, in: *Learning for Dynamics and Control Conference (L4DC)*, pp. 520–531.
- Prakash, N.P.S., Chen, Z., Horowitz, R., 2022. Data-driven strictly positive real system identification with prior system knowledge, in: *2022 American Control Conference (ACC)*, IEEE, pp. 3949–3954.
- Quaglino, A., Gallieri, M., Masci, J., Koutník, J., 2020. Snode: Spectral discretization of neural odes for system identification, in: *International Conference on Learning Representations*.
- Rahman, A., Dragoňa, J., Tuor, A., Strube, J., 2022. Neural ordinary differential equations for nonlinear system identification, in: *2022 American Control Conference (ACC)*, pp. 3979–3984.
- Raissi, M., Perdikaris, P., Karniadakis, G.E., 2019. Physics-informed neural networks: A deep learning framework for solving forward and inverse problems involving nonlinear partial differential equations. *Journal of Computational physics* 378, 686–707.
- Ramdani, N., Meslem, N., Raissi, T., Candau, Y., 2006. Set-membership identification of continuous-time systems. *IFAC Proceedings Volumes* 39, 446–451.
- Ramírez-Chavarría, R.G., Schoukens, M., 2021. Nonlinear finite impulse response estimation using regularized neural networks. *IFAC-PapersOnLine* 54, 174–179. 19th IFAC Symposium on System Identification SYSID 2021.
- Rantzer, A., Bernhardsson, B., 2014. Control of convex-monotone systems, in: *53rd IEEE Conference on Decision and Control*, IEEE, pp. 2378–2383.
- Rasmussen, C.E., Williams, C.K.I., 2006. *Gaussian Processes for Machine Learning*. The MIT Press.
- Revay, M., Umenberger, J., Manchester, I.R., 2021. Distributed identification of contracting and/or monotone network dynamics. *IEEE Transactions on Automatic Control* 67, 3410–3425.
- Revay, M., Wang, R., Manchester, I.R., 2023. Recurrent equilibrium networks: Flexible dynamic models with guaranteed stability and robustness. *IEEE Transactions on Automatic Control*.

- Reza, S., Ferreira, M.C., Machado, J., Tavares, J.M.R., 2022. A multi-head attention-based transformer model for traffic flow forecasting with a comparative analysis to recurrent neural networks. *Expert Systems with Applications* 202, 117275.
- Richards, S.M., Slotine, J.J., Azizan, N., Pavone, M., 2023. Learning control-oriented dynamical structure from data, in: International Conference on Machine Learning, PMLR. pp. 29051–29062.
- Robinson, H., Pawar, S., Rasheed, A., San, O., 2022. Physics guided neural networks for modelling of non-linear dynamics. *Neural Networks* 154, 333–345.
- Roehrl, M.A., Runkler, T.A., Brandstetter, V., Tokic, M., Obermayer, S., 2020. Modeling system dynamics with physics-informed neural networks based on lagrangian mechanics. *IFAC-PapersOnLine* 53, 9195–9200.
- Romer, A., Berberich, J., Köhler, J., Allgöwer, F., 2019a. One-shot verification of dissipativity properties from input-output data. *IEEE Control Systems Letters* 3, 709–714.
- Romer, A., Montenbruck, J.M., Allgöwer, F., 2021. Sampling strategies for data-driven inference of input–output system properties. *IEEE Transactions on Automatic Control* 66, 1144–1159.
- Romer, A., Trimpe, S., Allgöwer, F., 2019b. Data-driven inference of passivity properties via gaussian process optimization, in: Proc. European Control Conf. (ECC), p. 29–35.
- Roorda, B., Heij, C., 1995. Global total least squares modeling of multivariable time series. *IEEE Transactions on Automatic Control* 40, 50–63.
- Rose, A., Pfefferkorn, M., Nguyen, H.H., Findeisen, R., 2023. Learning a Gaussian process approximation of a model predictive controller with guarantees, in: IEEE Conference on Decision and Control (CDC), pp. 4094–4099.
- Rowley, C.W., Mezić, I., Bagheri, S., Schlatter, P., Henningson, D.S., 2009. Spectral analysis of nonlinear flows. *Journal of fluid mechanics* 641, 115–127.
- Ruiz-Balet, D., Zuazua, E., 2023. Neural ode control for classification, approximation, and transport. *SIAM Review* 65, 735–773.
- Saraswat, D., Achar, R., Nakhla, M.S., 2004. A fast algorithm and practical considerations for passive macromodeling of measured/simulated data. *IEEE Transactions on Advanced Packaging* 27, 57–70.
- Saraswat, D., Achar, R., Nakhla, M.S., 2005. Global passivity enforcement algorithm for macromodels of interconnect subnetworks characterized by tabulated data. *IEEE Transactions on Very Large Scale Integration (VLSI) Systems* 13, 819–832.
- Särkkä, S., 2021. Use of gaussian processes in system identification, in: Encyclopedia of Systems and Control. Springer, pp. 2393–2402.
- Schaeffer, H., McCalla, S.G., 2017. Sparse model selection via integral terms. *Physical Review E* 96, 023302.
- van der Schaft, A., 2024. Port-hamiltonian nonlinear systems. arXiv preprint: 2412.19673 .
- van der Schaft, A., Jeltsema, D., 2014. Now Publishers.
- van der Schaft, A.J., 2004. Port-Hamiltonian systems: network modeling and control of nonlinear physical systems, in: Advanced dynamics and control of structures and machines. Springer, pp. 127–167.
- van der Schaft, A.J., 2013. On differential passivity. IFAC Proceedings Volumes 46, 21–25.
- Scherer, C.W., Weiland, S., 2000. Linear matrix inequalities in control, Lecture Notes (Compilation: 2015). <https://www.imng.uni-stuttgart.de/mst/files/LectureNotes.pdf>.
- Schlaginhaufen, A., Wenk, P., Krause, A., Dorfler, F., 2021. Learning stable deep dynamics models for partially observed or delayed dynamical systems. *Advances in Neural Information Processing Systems* 34, 11870–11882.
- Schön, T.B., Wills, A., Ninness, B., 2011. System identification of nonlinear state-space models. *Automatica* 47, 39–49.
- Schoukens, M., Tiels, K., 2017. Identification of block-oriented nonlinear systems starting from linear approximations: A survey. *Automatica* 85, 272–292.
- Shali, B.M., van Waarde, H.J., 2024. Towards a representer theorem for identification of passive systems. arXiv preprint arXiv:2404.08297 .
- Shi, G., Shi, X., O’Connell, M., Yu, R., Azizzadenesheli, K., Anandkumar, A., Yue, Y., Chung, S.J., 2019. Neural lander: Stable drone landing control using learned dynamics, in: 2019 International Conference on Robotics and Automation (ICRA), pp. 9784–9790.
- Shi, S., Mazhar, O., De Schutter, B., 2022a. Finite-sample analysis of identification of switched linear systems with arbitrary or restricted switching. *IEEE Control Systems Letters* 7, 121–126.
- Shi, Y., Qu, G., Low, S., Anandkumar, A., Wierman, A., 2022b. Stability constrained reinforcement learning for real-time voltage control, in: 2022 American Control Conference (ACC), IEEE. pp. 2715–2721.
- Shiromoto, H.S., Revay, M., Manchester, I.R., 2018. Distributed nonlinear control design using separable control contraction metrics. *IEEE Transactions on Control of Network Systems* 6, 1281–1290.

- Sill, J., 1997. Monotonic networks, in: Proceedings of the 10th International Conference on Neural Information Processing Systems, pp. 661–667.
- Simpson-Porco, J.W., 2018. Equilibrium-independent dissipativity with quadratic supply rates. *IEEE Transactions on Automatic Control* 64, 1440–1455.
- Sivaraman, A., Farnadi, G., Millstein, T., Van den Broeck, G., 2020. Counterexample-guided learning of monotonic neural networks. *Advances in Neural Information Processing Systems* 33, 11936–11948.
- Sivarajani, S., Agarwal, E., Gupta, V., 2022. Data-driven identification of dissipative linear models for nonlinear systems. *IEEE Transactions on Automatic Control* 67, 4978–4985.
- Sivarajani, S., Agarwal, E., Gupta, V., Antsaklis, P., Xie, L., 2020a. Distributed mixed voltage angle and frequency droop control of microgrid interconnections with loss of distribution-pmu measurements. *IEEE Open Access Journal of Power and Energy* 8, 45–56.
- Sivarajani, S., Agarwal, E., Xie, L., Gupta, V., Antsaklis, P., 2020b. Mixed voltage angle and frequency droop control for transient stability of interconnected microgrids with loss of pmu measurements, in: 2020 American Control Conference (ACC), IEEE. pp. 2382–2387.
- Sivarajani, S., Forbes, J.R., Seiler, P., Gupta, V., 2018. Conic-sector-based analysis and control synthesis for linear parameter varying systems. *IEEE Control systems letters* 2, 224–229.
- Sivarajani, S., Sadraddini, S., Gupta, V., Belta, C., 2017. Distributed control policies for localization of large disturbances in urban traffic networks, in: 2017 American Control Conference (ACC), IEEE. pp. 3542–3547.
- Sjöberg, J., Zhang, Q., Ljung, L., Benveniste, A., Delyon, B., Glorennec, P.Y., Hjalmarsson, H., Juditsky, A., 1995. Nonlinear black-box modeling in system identification: a unified overview. *Automatica* 31, 1691–1724.
- Smith, H.L., 2017. Monotone dynamical systems: reflections on new advances & applications. *Discrete Contin. Dyn. Syst* 37, 485–504.
- Smyth, P., 1994. Hidden markov models for fault detection in dynamic systems. *Pattern recognition* 27, 149–164.
- Solera-Rico, A., Sanmiguel Vila, C., Gómez-López, M., Wang, Y., Almarshjary, A., Dawson, S.T., Vinuesa, R., 2024. β -variational autoencoders and transformers for reduced-order modelling of fluid flows. *Nature Communications* 15, 1361.
- Son, H., Jang, J.W., Han, W.J., Hwang, H.J., 2023. Sobolev training for physics-informed neural networks. *Communications in Mathematical Sciences* 21, 1679–1705.
- Sontag, E.D., 1992. Neural nets as systems models and controllers, in: Proc. Seventh Yale Workshop on Adaptive and Learning Systems.
- Strässer, R., Schaller, M., Worthmann, K., Berberich, J., Allgöwer, F., 2025. Koopman-based feedback design with stability guarantees. *IEEE Transactions on Automatic Control* 70, 355–370.
- Takeishi, N., Kawahara, Y., 2021. Learning dynamics models with stable invariant sets, in: Proceedings of the AAAI Conference on Artificial Intelligence, pp. 9782–9790.
- Tanemura, M., Azuma, S.i., 2018. Efficient data-driven estimation of passivity properties. *IEEE Control Systems Letters* 3, 398–403.
- Tanemura, M., Azuma, S.i., 2019. Closed-loop data-driven estimation on passivity property, in: 2019 IEEE Conference on Control Technology and Applications (CCTA), IEEE. pp. 630–634.
- Tang, S., Sapsis, T., Azizan, N., 2024. Learning chaotic dynamics with embedded dissipativity. arXiv preprint arXiv:2410.00976 .
- Tobenkin, M.M., Manchester, I.R., Megretski, A., 2013. Stable nonlinear identification from noisy repeated experiments via convex optimization, in: 2013 American Control Conference, IEEE. pp. 3936–3941.
- Tobenkin, M.M., Manchester, I.R., Wang, J., Megretski, A., Tedrake, R., 2010. Convex optimization in identification of stable non-linear state space models, in: 49th IEEE Conference on Decision and Control (CDC), IEEE. pp. 7232–7237.
- Tomlin, C., Pappas, G.J., Sastry, S., 2002. Conflict resolution for air traffic management: A study in multiagent hybrid systems. *IEEE Transactions on automatic control* 43, 509–521.
- Umenberger, J., Manchester, I.R., 2018. Specialized interior-point algorithm for stable nonlinear system identification. *IEEE Transactions on Automatic Control* 64, 2442–2456.
- Vaccaro, R.J., Vukina, T., 1993. A solution to the positivity problem in the state-space approach to modeling vector-valued time series. *Journal of Economic Dynamics and Control* 17, 401–421.
- Van Der Schaft, A., Jeltsema, D., 2014. Port-Hamiltonian systems theory: An introductory overview. *Foundations and Trends in Systems and Control* .
- Van Gestel, T., Suykens, J.A., Van Dooren, P., De Moor, B., 2001. Identification of stable models in subspace identification by using regularization. *IEEE Transactions on Automatic control* 46, 1416–1420.
- Van Overschee, P., De Moor, B., 1996. Subspace identification for linear systems: Theory–Implementation–Applications. Springer.

- Van Overschee, P., De Moor, B., 2012. Subspace identification for linear systems: Theory—Implementation—Applications. Springer Science & Business Media.
- Van Waarde, H.J., Eising, J., Camlibel, M.K., Trentelman, H.L., 2023. The informativity approach: To data-driven analysis and control. *IEEE Control Systems Magazine* 43, 32–66.
- Vardi, Y., 1996. Network tomography: Estimating source-destination traffic intensities from link data. *Journal of the American statistical association* 91, 365–377.
- Vaswani, A., Shazeer, N., Parmar, N., Uszkoreit, J., Jones, L., Gomez, A.N., Kaiser, Ł., Polosukhin, I., 2017. Attention is all you need. *Advances in neural information processing systems* 30.
- Veedu, M.S., Melbourne, J., Salapaka, M.V., 2023. Causal structure recovery of linear dynamical systems: An fft based approach. arXiv preprint arXiv:2309.02571 .
- Verhaegen, M., Verdult, V., 2007. Filtering and system identification: a least squares approach. Cambridge university press.
- Verhoek, C., Abbas, H.S., Tóth, R., 2023a. Direct data-driven lpv control of nonlinear systems: An experimental result. *IFAC-PapersOnLine* 56, 2263–2268. 22nd IFAC World Congress.
- Verhoek, C., Abbas, H.S., Tóth, R., Haesaert, S., 2021a. Data-driven predictive control for linear parameter-varying systems, in: Proc. 4th IFAC Workshop on LPV Systems, pp. 101–108.
- Verhoek, C., Berberich, J., Haesaert, S., Allgöwer, F., Tóth, R., 2024. Data-driven dissipativity analysis of linear parameter-varying systems. *IEEE Transactions on Automatic Control* 69, 8603–8616.
- Verhoek, C., Koelewijn, P.J.W., Tóth, R., 2023b. Convex incremental dissipativity analysis of nonlinear systems. *Automatica* 150, 110859.
- Verhoek, C., Tóth, R., Abbas, H.S., 2022. Direct data-driven state-feedback control of linear parameter-varying systems. arXiv preprint arXiv: 2211.17182 .
- Verhoek, C., Tóth, R., Haesaert, S., Koch, A., 2021b. Fundamental lemma for data-driven analysis of linear parameter-varying systems, in: Proc. 60th Conference on Decision and Control (CDC), pp. 5040–5046.
- Vidyasagar, M., 1979. New passivity-type criteria for large-scale interconnected systems. *IEEE Transactions on Automatic Control* 24, 575–579.
- Villaverde, A.F., Ross, J., Morán, F., Banga, J.R., 2014. Mider: network inference with mutual information distance and entropy reduction. *PloS one* 9, e96732.
- van Waarde, H.J., Camlibel, M.K., Rapisarda, P., Trentelman, H.L., 2022. Data-driven dissipativity analysis: application of the matrix S-lemma. *IEEE Control Systems Magazine* 42, 140–149.
- van Waarde, H.J., Camlibel, M.K., Trentelman, H.L., 2025. Data-Based Linear Systems and Control Theory. First ed., Kindle Direct Publishing. URL: <https://henkvanwaarde.github.io/dblsct>.
- Wahlberg, B., Syberg, M.B., Hjalmarsson, H., 2010. Non-parametric methods for \mathcal{L}_2 -gain estimation using iterative experiments. *Automatica* 46, 1376–1381.
- Wang, J.S., Chen, Y.P., 2006. A fully automated recurrent neural network for unknown dynamic system identification and control. *IEEE Transactions on Circuits and Systems I: Regular Papers* 53, 1363–1372.
- Wang, L., Theodorou, E.A., Egerstedt, M., 2018. Safe learning of quadrotor dynamics using barrier certificates, in: IEEE International Conference Robotics and Automation (ICRA), pp. 2460–2465.
- Wang, R., Dvijotham, K.D., Manchester, I., 2024. Monotone, bi-lipschitz, and polyak-łojasiewicz networks, in: Forty-first International Conference on Machine Learning.
- Wang, R., Walters, R., Yu, R., 2020. Incorporating symmetry into deep dynamics models for improved generalization, in: International Conference on Learning Representations.
- Wang, R., Yu, R., 2021. Physics-Guided Deep Learning for Dynamical Systems: A survey. arXiv 2107.01272.
- Wang, Y., 2017. A new concept using lstm neural networks for dynamic system identification, in: 2017 American Control Conference (ACC), pp. 5324–5329.
- Wang, Y., Gupta, V., Antsaklis, P.J., 2013. On passivity of a class of discrete-time switched nonlinear systems. *IEEE Transactions on Automatic Control* 59, 692–702.
- Wang, Y., Zhang, Z., Koh, C.K., Pang, G.K., Wong, N., 2010. Peds: Passivity enforcement for descriptor systems via hamiltonian-symplectic matrix pencil perturbation, in: 2010 IEEE/ACM International Conference on Computer-Aided Design (ICCAD), IEEE. pp. 800–807.
- Wehenkel, A., Louppe, G., 2019. Unconstrained monotonic neural networks. *Advances in neural information processing systems* 32.
- Wei, T., Liu, C., 2022. Safe control with neural network dynamic models, in: Learning for Dynamics and Control Conference, PMLR. pp. 739–750.
- Welikala, S., Lin, H., Antsaklis, P.J., 2022. On-line estimation of stability and passivity metrics, in: 2022 IEEE 61st Conference on Decision and Control (CDC), IEEE. pp. 267–272.

- Willard, J., Jia, X., Xu, S., Steinbach, M., Kumar, V., 2020. Integrating physics-based modeling with machine learning: A survey. arXiv preprint arXiv:2003.04919 .
- Willems, J.C., 1986a. From time series to linear system – part i. finite dimensional linear time invariant systems. *Automatica* 22, 561–580.
- Willems, J.C., 1986b. From time series to linear system—part ii. exact modelling. *Automatica* 22, 675–694.
- Willems, J.C., 1987. From time series to linear system – part iii: Approximate modelling. *Automatica* 23, 87–115.
- Willems, J.C., Rapisarda, P., Markovsky, I., De Moor, B.L., 2005a. A note on persistency of excitation. *Systems & Control Letters* 54, 325–329.
- Willems, J.C., Rapisarda, P., Markovsky, I., De Moor, B.L., 2005b. A note on persistency of excitation. *Systems & Control Letters* 54, 325–329.
- Williams, M.O., Kevrekidis, I.G., Rowley, C.W., 2015. A data-driven approximation of the koopman operator: Extending dynamic mode decomposition. *Journal of Nonlinear Science* 25, 1307–1346.
- Winston, E., Kolter, J.Z., 2020. Monotone operator equilibrium networks. *Advances in neural information processing systems* 33, 10718–10728.
- Wu, P., McCourt, M.J., Antsaklis, P.J., 2013. Experimentally determining passivity indices: Theory and simulation. *ISIS* , 002.
- Xia, M., Antsaklis, P.J., Gupta, V., Zhu, F., 2016. Passivity and dissipativity analysis of a system and its approximation. *IEEE Transactions on Automatic Control* 62, 620–635.
- Xiao, T., Chen, Y., Huang, S., He, T., Guan, H., 2022. Feasibility study of neural ode and dae modules for power system dynamic component modeling. *IEEE Transactions on Power Systems* 38, 2666–2678.
- Xiao, W., Wang, T.H., Hasani, R., Lechner, M., Ban, Y., Gan, C., Rus, D., 2023. On the forward invariance of neural odes, in: International conference on machine learning, PMLR. pp. 38100–38124.
- Xu, L., Zakwan, M., Ferrari-Trecate, G., 2022. Neural energy casimir control for port-hamiltonian systems, in: IEEE Conference on Decision and Control (CDC), pp. 4053–4058.
- Xu, M., Dai, W., Liu, C., Gao, X., Lin, W., Qi, G.J., Xiong, H., 2020. Spatial-temporal transformer networks for traffic flow forecasting. arXiv preprint arXiv:2001.02908 .
- Xu, Y., Sivarajani, S., 2023. Learning dissipative neural dynamical systems. *IEEE Control Systems Letters* 7, 3531–3536.
- Xue, A., Matni, N., 2021. Data-driven system level synthesis, in: Proc. of Machine Learning Research, p. 1–12.
- Ye, L., Chi, M., Gupta, V., 2022a. Regret bounds for learning decentralized linear quadratic regulator with partially nested information structure. arXiv preprint arXiv:2210.08886 .
- Ye, L., Zhu, H., Gupta, V., 2022b. On the sample complexity of decentralized linear quadratic regulator with partially nested information structure. *IEEE Transactions on Automatic Control* 68, 4841–4856.
- Yeung, E., Kundu, S., Hodas, N., 2019. Learning deep neural network representations for koopman operators of nonlinear dynamical systems, in: 2019 American Control Conference (ACC), IEEE. pp. 4832–4839.
- Yu, R., Wang, R., 2024. Learning dynamical systems from data: An introduction to physics-guided deep learning. *Proceedings of the National Academy of Sciences* 121, e2311808121.
- Yuan, Z., Cortés, J., 2022. Data-driven optimal control of bilinear systems. *IEEE Control Systems Letters* 6, 2479–2484.
- Zhang, H., Zhang, Z., 1999. Feedforward networks with monotone constraints, in: IJCNN'99. International Joint Conference on Neural Networks. Proceedings (Cat. No. 99CH36339), IEEE. pp. 1820–1823.
- Zhao, J., Hill, D.J., 2007. Dissipativity based stability of switched systems with state-dependent switchings, in: 2007 46th IEEE Conference on Decision and Control, IEEE. pp. 4027–4032.
- Zhao, J., Hill, D.J., 2008. Dissipativity theory for switched systems. *IEEE Transactions on Automatic Control* 53, 941–953.
- Zhao, Y., Gupta, V., 2016. Feedback passivation of discrete-time systems under communication constraints. *IEEE Transactions on Automatic Control* 61, 3521–3526.
- Zhong, Y.D., Dey, B., Chakraborty, A., 2019. Symplectic ODE-Net: learning Hamiltonian dynamics with control, in: International Conference on Learning Representations (ICLR).
- Zhong, Y.D., Dey, B., Chakraborty, A., 2020. Dissipative symoden: Encoding hamiltonian dynamics with dissipation and control into deep learning. arXiv preprint arXiv:2002.08860 .
- Zhong, Y.D., Dey, B., Chakraborty, A., 2021. Benchmarking energy-conserving neural networks for learning dynamics from data, in: Learning for dynamics and control, PMLR. pp. 1218–1229.
- Zhu, Q., Guo, Y., Lin, W., 2021. Neural delay differential equations.
- Zinage, V., Bakolas, E., 2023. Neural koopman lyapunov control. *Neurocomputing* 527, 174–183.